UNIVERSITY OF SOUTHAMPTON
Faculty of Engineering and Applied Science
Department of Electronics and Computer Science

Teletraffic Performance of Microcellular Networks

by

Matthew Ho Yin Au
B.Eng.

A Doctoral Thesis submitted in partial fulfilment of the requirements for the award of Doctor of Philosophy at the University of Southampton

September 1997

Supervisor: Professor Raymond Steele
B.Sc., Ph.D., D.Sc., CEng., FEng., FIEE, SMIEEE

This thesis is dedicated to my parents and brothers

Contents

UNIVERSITY OF SOUTHAMPTON

ABSTRACT

FACULTY OF ENGINEERING AND APPLIED SCIENCE
DEPARTMENT OF ELECTRONICS AND COMPUTER SCIENCE

Doctor of Philosophy

TELETRAFFIC PERFORMANCE OF MICROCELLULAR NETWORKS

by

Matthew Ho Yin Au

The teletraffic performance of street microcellular networks in a rectilinear urban city is studied. The microcellular base station (BS) antennas are installed at a height below the urban skyline, producing irregular shape cells that are dependent on buildings of city block size. There are 144 buildings in our rectilinear city arranged in a 12 by 12 matrix. Each building has a cross sectional area of 100 by 100 metres, the roads between the buildings are 20 metres wide, with the BSs located at each road intersection. The mobile stations (MSs) are assumed to be housed in vehicles travelling at constant speed. The MSs are arranged to have a probability of 0.8 to continue travelling in the same direction at road junctions, and a probability of 0.1 of either turning left or right. To avoid edge effects, the city is arranged to wrap around from the East-most edge to the West-most edge, and from the North-most edge to the South-most edge, which means that a MS that leaves the network on say the East side will reappear at the same North level from the West side.

Two handover (HO) priority schemes, the HO guard channel scheme and the HO queueing scheme, are studied for a system that adopts a fixed channel assignment (FCA) strategy. Both schemes are designed to reduce the probability of a call being forced to terminate, P_F, in exchange for an increase in the probability of a new call being blocked, P_B. For the HO guard channel scheme with eight channels per BS, then the effect of reserving one channel exclusively for HO, is for P_F to decrease from 16.7% to 14.2%, but for P_B to increase from 2% to 5.8%. For the HO queueing scheme P_F is decreased from 8.3% to 4.5%, but P_B is increased from 1.1%

to 1.7% compared to when queueing is not employed. Both HO priority schemes fail to achieve the desire level of P_F for our microcellular network when the HO rates are high. We utilise the overlapped radio coverage between two adjacent cells by proposing two BS selection algorithms which we call the BS load equalisation (BSLE) and the re-arrangement upon blocking (RAUB) algorithms. The BSLE and the RAUB systems improve the channel utilisation by 32% and 68%, respectively, over the standard directed retry algorithm.

To combat unpredictable teletraffic demands and the high cost of network infrastructure, a system of moving BSs (MBSs) is proposed. The advantage of mounting BSs on vehicles, such as buses, is that there is less fixed infrastructure, and the MBSs tend to be trapped in dense traffic and thereby are in a good position to relieve temporary teletraffic hot spots. Normal fixed BSs (FBSs) are also positioned to provide the basic service. A system that adopts a dynamic channel assignment (DCA) strategy is studied for the deployment of this MBS system. In addition, two network access schemes, the standard access scheme and the power escalation access (PEA) scheme, are proposed. The effects of introducing road traffic congestion in the central part of the city on these two schemes are addressed. In the congested zone, the system adopting the PEA scheme decreases P_B from 43% to 2.7%, while P_F is decreased from 38% to 6% when 144 MBSs and 144 FBSs are deployed compared to when only 144 FBSs are deployed. In the non-congested zone, P_B is reduced from 0.87% to 0.2%, while P_F is reduced from 6.8% to 2%.

Our results are obtained from a computer simulation program specifically developed for this research. The simulation program has a graphical user interface (UI), allowing the status of the simulated system to be monitored visually in real time. Armed with this simulator, and with supporting theory, we have proposed new methods for improving the teletraffic performance of microcellular networks.

Acknowledgements

I would like to take this opportunity to thank my mother for her love and continuous support throughout the years. I would also like to express my sincere gratitude to my supervisor, Professor Raymond Steele, for his guidance and the share of his vision on the subject as well as life in general. A special thank you to Dr. Mostafa Nofal for his assistance in the derivation of the mathematical model.

I am grateful to all the colleagues and staff in the Communication Research Group in the Department of Electronics and Computer Science, in particular, to Dr. Lajos Hanzo for his encouragement and constructive discussions. I would also like to thank Derek Chandler, who helped me to produce the radio coverage maps, and other colleagues at Multiple Access Communications Ltd.

List of Abbreviations

AGCH	Access Grant Channel.
AMPS	Advanced Mobile Phone Service.
BCCH	Broadcast Control Channel.
BCO	Borrowing with Channel Ordering.
BS	Base Station.
BSC	Base Station Controller.
BSIC	Base Station Identity Code.
BSLE	Base Station Load Equalisation.
CCH	Control Channel.
CDMA	Code Division Multiple Access.
CI	Cell Identity.
D-AMPS	Digital Advanced Mobile Phone Service.
DCA	Dynamic Channel Allocation.
DCS-1800	Digital Communication System at 1800.
DS	Direct Sequence.
FBS	Fixed Base Station.
FCA	Fixed Channel Allocation.
FCCH	Frequency Correction Channel.
FDD	Frequency Division Duplex.
FDMA	Frequency Division Multiple Access.
FEC	Forward Error Correction.
GOS	Grade Of Service.
GSM	Global System for Mobile communications.
GUI	Graphical User Interface.
HCA	Hybrid Channel Assignment.
HLR	Home Location Register.
HO	Handover.
ISDN	Integrated Services Digital Network.
LOS	Line Of Sight.
MA	Multiple Access.
MBS	Moving Base Station.
MCC	Mobile Country Code.
MNC	Mobile Network Code.

MS	Mobile Station.
MSC	Mobile Switching Centre.
NMT	Nordic Mobile Telephone.
OOS	Out Of Sight.
PDF	Probability Density Function.
PEA	Power Escalation Access.
PN	Pseudo-random Noise.
PSTN	Public Switch Telephone Network.
RACH	Random Access Channel.
RAUB	Re-Arrangement Upon Blocking.
SCH	Synchronisation Channel.
SIR	Signal to Interference Radio.
TACS	Total Access Communications System.
TCH	Traffic Channel.
TDMA	Time Division Multiple Access.
UI	User Interface.
VLR	Visitor Location Register.

List of Principal Symbols

A_c	Carried traffic per cell.
A_{CT}	Total carried traffic.
A_{cn}	Carried traffic per overlapping region.
B	Channel bandwidth.
C	Number of cells per cluster.
D	Reuse distance.
d_1	The distance from the transmitter to the corner.
d_2	The distance from the corner to the receiver.
δ	Level-2 inter-handover hysteresis threshold factor.
ϵ	Ratio of the cell area to the city area.
η	Spectral efficiency.
h_b	Base station antenna height.
h_m	Mobile station antenna height.
L	Distance from the centre of cross shaped cell to its border.
λ	Radio wavelength.
λ_a	New call arrival rate in the non-overlapping region.
λ_b	New call arrival rate in the overlapping region.
λ_h	Handover rate.
λ_n	Total new call arrival rate per cell.
λ_{nu}	New call arrival rate per user.
M	Total number of users present in the city.
M_u	Number of users per cell.
μ_a	Average departure rate of new calls in the non-overlapping area.
μ_b	Average departure rate of new calls in the overlapping area.
μ_c	Call departure rate.
μ_h	Average departure rate of previously handed over mobile stations.
N	Total number of channels per base station.
N_h	Number of handover exclusive channels.
PL_{los}	Line of sight pathloss.
PL_{oos}	Out of sight pathloss.

P_F	Forced termination probability.
P_h	Probability that a handover call requires another handover.
P_{B0}	Call congestion probability of a base station.
P_{Bav}	Average new call blocking probability.
P_{fh}	Probability that a handover attempt fails.
ϕ	Ratio of the handover area to the overlapping area.
R	Cell radius.
R_b	Breakpoint distance in the pathloss model.
$\mathrm{Rx}_{\mathrm{min}}$	Minimum receiver threshold.
$\mathrm{Rx}_{\mathrm{opt}}$	Optimum received power level.
r	The distance between the transmitter and the receiver.
ρ	Channel utilisation.
S	Cell area.
S_T	Network radio coverage area.
$\mathrm{SIR}_{\mathrm{min}}$	Minimum acceptable signal to interference ratio.
T_c	Mean call duration.
T_{Ha}	Channel holding time of new calls in the non-overlapping area.
T_{Hb}	Channel holding time of new calls in the overlapping area.
T_{Hh}	Channel holding time of previously handed over mobile stations.
T_{ch}	Average channel holding time.
$\mathrm{Tx}_{\mathrm{max}}$	Maximum transmission power.
v	Speed of a vehicle.
W	Length of the overlapping radio coverage area.
ζ	Ratio of the non-overlapping area to the overlapping area.

Chapter 1

Introduction

1.1 Background

This thesis is concerned with the teletraffic performance of street microcells in cellular mobile radio systems. Mobile radio systems use radio channels to connect the mobile stations (MSs) with the base stations (BSs) [1]. These radio links between the BSs and their MSs provide for user mobility. The back-haul network, or the fixed cellular infrastructure is organised in different ways depending on each particular cellular system [2]. Typically BSs are controlled by base station controllers (BSCs) who in turn connect to mobile switching centres (MSCs). There are gateway MSCs that interconnect to other networks. There are also numerous data bases, such as home location registers (HLRs) and visitor location registers (VLRs), plus a system of operational management control. Interconnection of the infrastructure is usually accomplished by leasing lines from fixed wire carriers. We are not concerned here with the cellular network infrastructure, although we often refer to the network control.

Let us return to the basics, and the important role of a BS. A BS can serve one or more MSs. The radio coverage provided by a BS is called a cell. The shape and size of a cell depends on the terrain where the BS is located and on the transmission power of the BS. Consequently radio cells have irregular shapes. In order to compare results, most researchers model a cell as having a hexagonal shape. This shape is chosen because of its ease in mathematical

analysis, although it cannot be physically realised.

The cells are tessellated over the service area to achieve seamless coverage. As radio bandwidth is a scarce resource, the radio channels must be reused to achieve higher capacities [3]. Cells are grouped to form clusters. The radio channels are partitioned into sets and assigned to each cell in the cluster. These radio channels are then reused in other clusters. Figure 1.1 shows a seven-cell cluster reuse pattern. Cells that are labelled with the same number use the same channel set, and they cause cochannel interference to each other. Consequently the cluster size must be chosen to meet the system's minimum level of signal-to-interference ratio (SIR).

Equation 1.1 relates the *re-use distance* (D) and the distance from the cell centre to its apex (R) to the *cluster size* (C) for hexagonal cells [4]. The cluster size is the number of BSs that utilise the complete set of channels and is given by

$$C = \frac{1}{3} * \left(\frac{D}{R}\right)^2 . \tag{1.1}$$

Both R and D are marked on Figure 1.1. Notice that D is the distance between the centre of any two cells in adjacent clusters that have the same cell number.

Spectral efficiency in cellular radio may be defined as

$$\eta = \frac{A_{CT}}{S_T W} \qquad Erlangs/Hz/m^2 \tag{1.2}$$

where A_{CT} is the total traffic carried by the network, in Erlangs, S_T is the total area covered by the network, and W is the allocated bandwidth.

It can be shown that [5]:

$$\eta = \frac{\rho}{SCB} \tag{1.3}$$

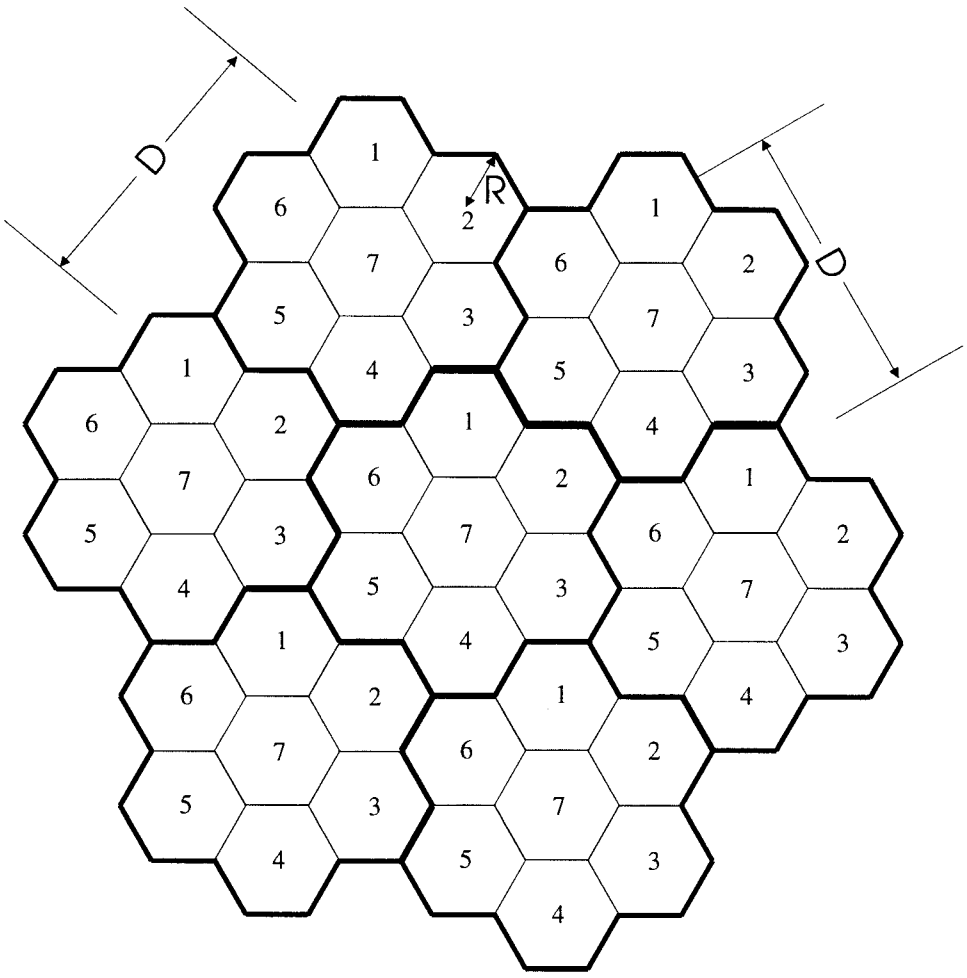

Figure 1.1: A seven-cell cluster

where ρ is the utilisation of each BS channel, S is the cell area, C is the number of cells per cluster and B is the bandwidth of each channel. The smaller the area of the cell, the greater the spectral efficiency.

Cells are categorised according to their sizes. Picocells covering up to a few metres are used for indoor communications, microcells covering from 10 to 400 m are used for dense outdoor urban areas [6], macrocells covering 1 to 5 km are used for suburban areas or overlaying the street microcells in urban areas [7, 8, 9], large cells covering 5 to 35 km for rural areas and satellite cells formed by spot beams covering over 50 km for global communications.

First generation analogue cellular radio systems, e.g. Nordic mobile telephone (NMT), Advanced mobile phone service (AMPS), Total access communications system (TACS), etc, use large cells and macrocells. Second generation systems, e.g. Global system of mobile telecommunications (GSM), Digital communication system at 1800 MHz (DCS 1800), D-AMPS (Interim Standard 54, IS-54), Qualcomm CDMA (IS-95), etc, currently deploying microcells in some dense urban areas. Apart from achieving high capacities, smaller cells also prolong the battery life of the handheld mobiles as the transmission power is significantly reduced.

The BS antennas in street microcells are located below the urban skyline [10]. The surrounding buildings act as electromagnetic shields, significantly reducing the received signal levels. Consequently the shapes of the microcells depend significantly on the topologies of the buildings.

Figure 1.2 shows a pathloss plot of a macrocell whose dipole antenna was mounted on top of a building at 43 metres above sea level. The macrocell being on top of a tall building can oversee most of the city. The pathloss plot was produced by NP-Workplace [11], a radio cell planning tool, from Multiple Access Communications Ltd. Another pathloss plot was also generated for four microcells residing in the same city as shown in Figure 1.3. The antennas of the microcells are mounted at 3 metres above the street level and are below the urban skyline. A close-up of three of these microcells is shown in Figure 1.4. All pathloss predictions are generated for a receiver height of 2 metres. The radical differences in cell shapes between the microcells and the macrocell are apparent in these plots. While irregular shaped roads result in irregular shaped microcells, rectilinear roads yield regular shaped microcells. It is customary to use rectilinear roads for microcellular analysis in the same way that hexagonal cells are used for analysing macrocellular

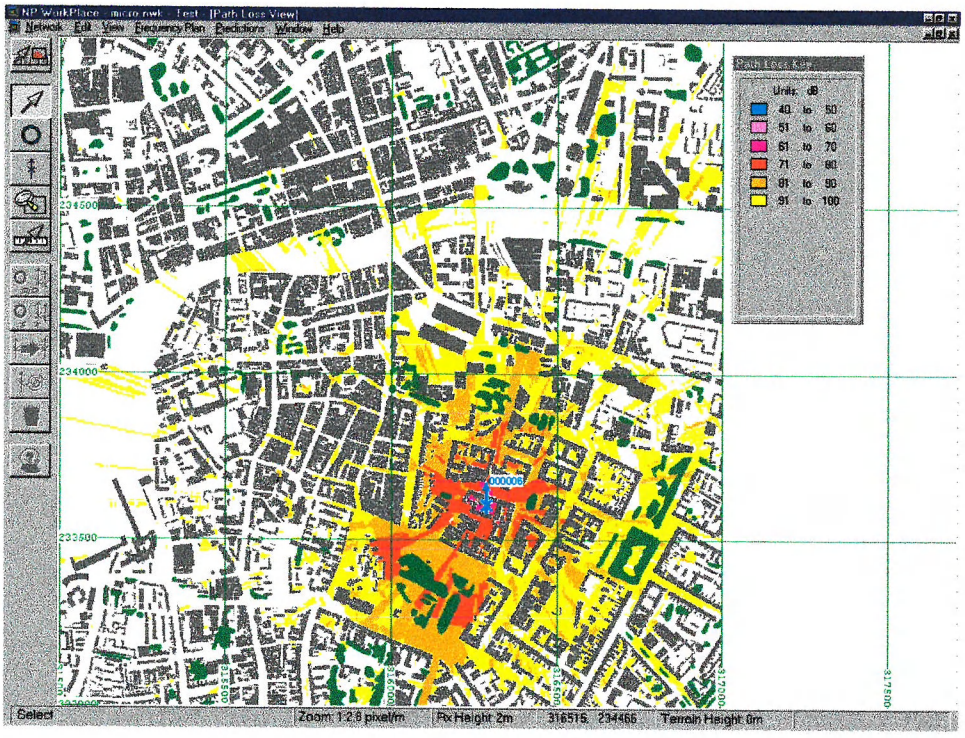

Figure 1.2: Pathloss prediction of a macrocellular BS mounted on top of a tall building. The grey areas are buildings, the white areas are open spaces and the green areas are vegetation.

networks. Accordingly this thesis adopts the rectilinear Manhattan model with roads running in both horizontal and vertical directions as shown in Figure 1.5.

In mobile radio systems users can move from one cell to another during their calls. Consequently a procedure known as *handover* (HO) is needed to switch an ongoing call from one BS to another. When smaller cells are used, the number of HOs is increased. This requires the HO procedure to have small signalling overheads and fast algorithms. In a street microcellular network, a user turning round a corner and becoming out-of-sight (OOS) of its serving BS would immediately experience approximately 20 dB loss in received signal strength. This sudden drop in received signal strength may fall below the receiver threshold and result in a dropped call if the HO procedure cannot take place promptly.

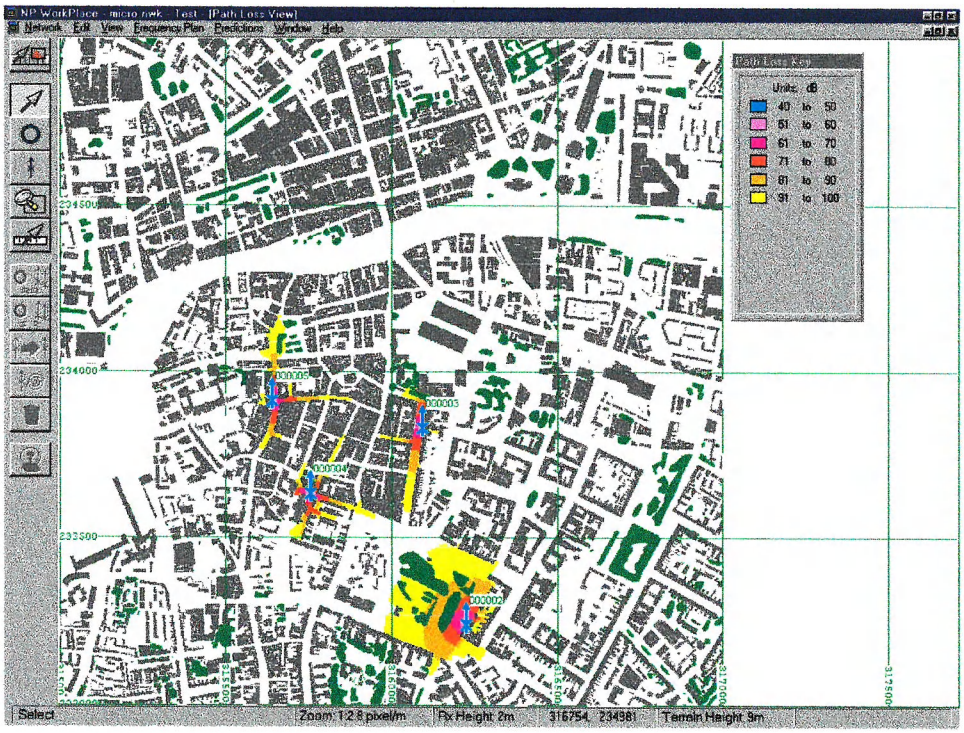

Figure 1.3: Pathloss predictions of four microcellular BSs mounted below the urban skyline. The grey areas are buildings, the white areas are open spaces and the green areas are vegetation.

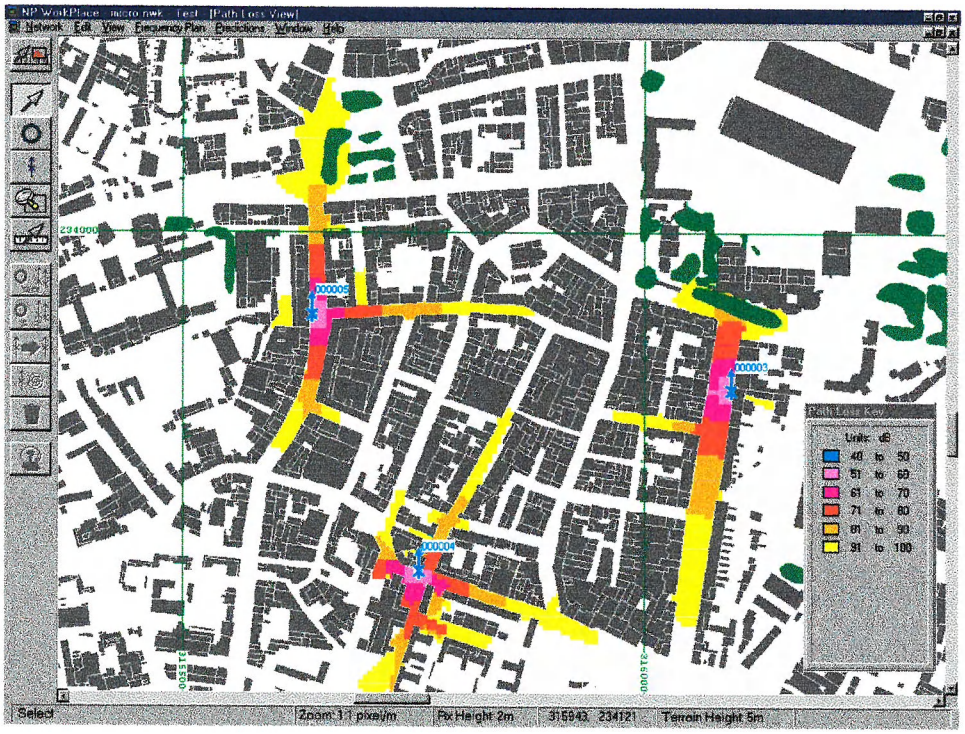

Figure 1.4: Close-up of the pathloss plot of the microcells. The grey areas are buildings, the white areas are open spaces and the green areas are vegetation.

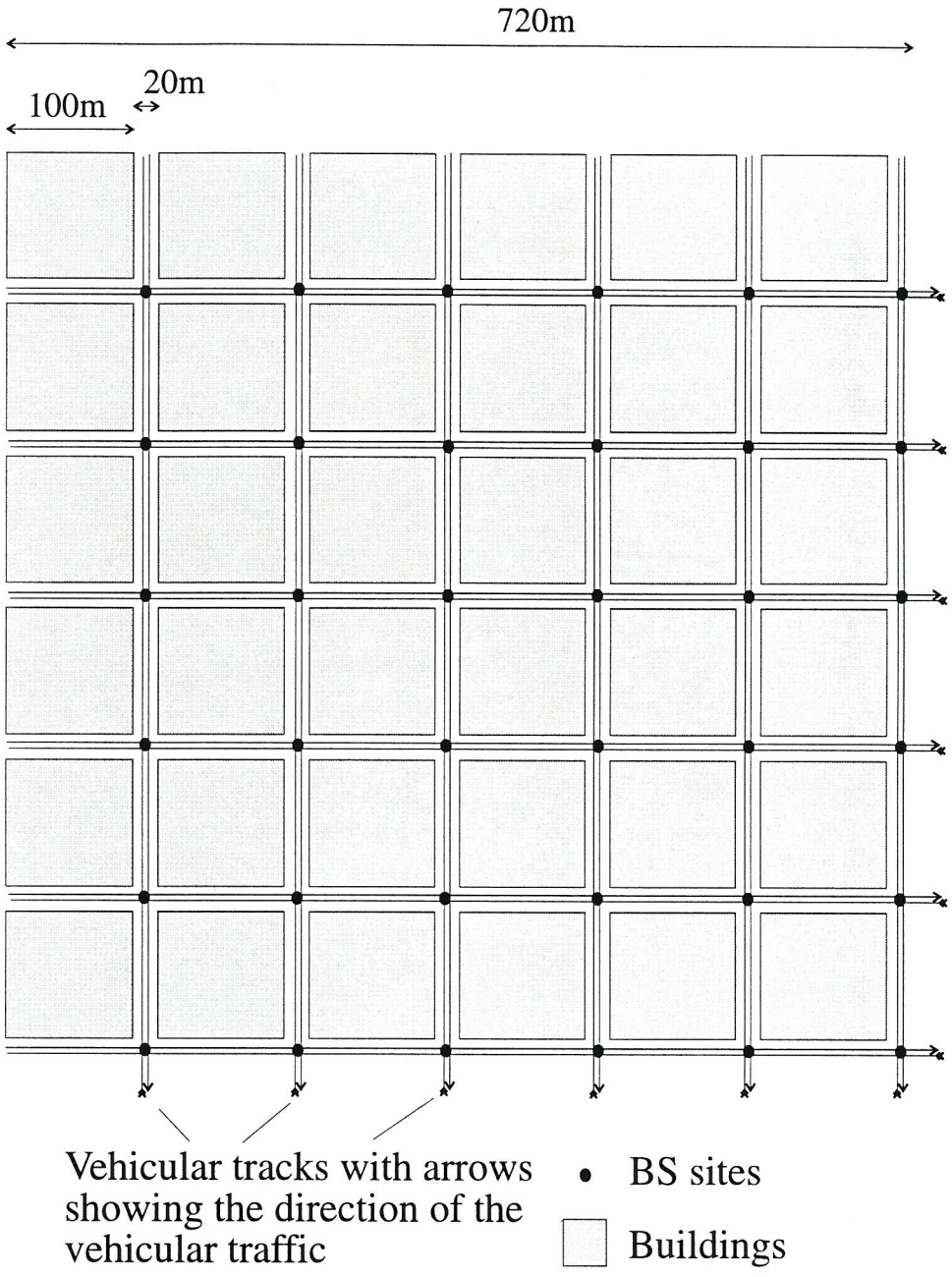

Figure 1.5: Rectilinear Manhattan mode

A dropped call is perceived as more annoying than a new call being blocked. Therefore the HO failure rate must be kept low even at the expense of higher new call blocking probabilities. This brings us to the HO priority schemes. The handover guard channel scheme and the handover queueing scheme have been studied for macrocellular systems [7, 12, 13, 14, 8, 15]. We will study the effectiveness of these two schemes in the first part of Chapter 2 when they are applied to our street microcellular scenario. In particular, their performances for high HO rates are studied, as this thesis is only concerned with MSs that are mounted on vehicles.

Multiple access (MA) is the method that divides the radio bandwidth into radio channels [16, 17, 18, 19, 20, 21]. Time division MA (TDMA) allows users to transmit data in periodic bursts using the entire bandwidth assigned to a radio carrier. Frequency division MA (FDMA) scheme allows radio channels to transmit all the time but only in an assigned frequency sub-band. Radio channels in code division MA (CDMA) have access to all frequencies and all time. Each channel is given a pseudo-random (PN) code sequence that is used to spread the source data to occupy the whole allocated frequency band. The receiver separates the channels on a code basis. In this thesis we are mainly concerned with the assignment of radio channels, and therefore the underlying MA scheme is not important. However, for completeness, we assume our system to be a TDMA system with multiple carriers, like GSM.

We recall that radio channels must be reused in order to achieve higher capacities. However cochannel interference forbids the same radio channel to be used by two BSs that are less than the minimum reuse distance apart. Some channel assignment scheme must be adopted to control the allocation of radio channels to the BSs. Here we will briefly describe some of the channel assignment schemes in order for readers to understand the rest of the thesis. Readers can pursue the references for more details.

A fixed channel assignment (FCA) scheme partitions radio channels into sets, and assigns a set permanently to each cell. The assignment is pre-planned, taking the cochannel interferences into account, before the installation of the BSs.

In a dynamic channel assignment (DCA) scheme, there is no fixed relationship between cells and channels [22]. A pool of channels is available to all BSs. A DCA scheme has the ability to meet the peak of teletraffic, and generally performs better than the FCA scheme. However some form of channel

re-arrangement algorithm is needed to reduce the average reuse distance.

A hybrid channel assignment scheme divides the channels into two groups; fixed channels and dynamic channels. The fixed channels are assigned to the BSs using a FCA scheme, and have a fixed relationship with their associated BSs. The remaining channels are dynamic channels. They are reserved in a central pool, and available for dynamic assignment in any coverage area as long as they are not simultaneously used closer than a reuse distance. Different ratios of these two types of channels were studied in references [23, 24, 25].

A channel borrowing scheme pre-assigns each BS with a nominal channel set as in a FCA scheme. However, a BS can also access the non-nominal channels when it exhausts all of its nominal channels. A channel is said to be "borrowed" by this BS. A borrowed channel is forbidden to be used by the lending cell and by some of the cochannel cells that are originally given this channel as the nominal channel. This borrowed channel is said to be locked in these cells. There are proposed algorithms that minimise or eliminate locking of a borrowed channel [26, 27, 28, 29, 30, 31].

Channel segregation is a self-learnt distributed assignment scheme [32, 33]. It does not require cell planning and is highly adaptive to the change of propagation conditions. Channel allocation is determined in each BS in a distributed manner, and global information is not required. Each BS captures its own channel using its internal priority function that is updated with the probabilities of success of each channel assignment.

Before channel assignment takes place, a BS must first be selected to serve the mobile. Many research papers assume that the cells have clear borders and can be tessellated over the service area without any cell overlap region; for example, the cell arrangement in Figure 1.1. In these cases the BS selection algorithm is trivial as there is only one BS that covers a given location. In reality radio cells do not have regular shapes nor well defined borders. Consequently adjacent cells must be overlapped in order to provide seamless coverage [34]. A MS near the border of a cell can often receive radio signals from more than one BS due to the overlapped radio coverage between adjacent cells. By adopting a suitable BS selection algorithm, we can exploit the overlapped radio coverage to further enhance the system's teletraffic performance [35, 36, 37, 38, 39, 40, 40]. We will propose our BS selection algorithms in the latter part of Chapter 2.

Mobile operators have to plan their networks carefully before becoming committed to acquiring a BS site [41]. They often use software planning tools in addition to field measurements in order to estimate the radio coverage of a given site. To maximise the returns the operators must estimate the expected teletraffic that will be generated in the area and allocate capacities to the BSs accordingly [42]. The cost of acquiring a BS site is expensive, and the choice of location is often restricted as planning permission is required from the local councils. To realise a microcellular network, a large number of BS sites are required and the bulk of the investment would be spent on the network infrastructure. However the levels of teletraffic generated by the users vary geographically and the teletraffic hot spots change during the course of a day. As the teletraffic demand is difficult to predict, it is difficult to plan a network that would provide the optimal coverage. This motivates us to investigate the adoption of moving BSs (MBSs) - BSs that are mounted on vehicles and move with the road traffic.

In this thesis, both the MSs and the MBSs are mounted on the same type of vehicles. These vehicles travel around the city randomly at constant speed. Traffic jams can be artificially created by reducing the speed of the vehicles in certain areas of the city. Consequently teletraffic hot spots are generated. However, the densities of MBSs in the traffic jam areas are also increased as the MBSs are mounted on vehicles. Our goal is to devise some channel assignment schemes that can be adopted by the MBSs. The normal BSs that have fixed locations are still needed as they have fixed connections to the rest of the network and can act as gateways. We refer to these normal BSs as the fixed BSs (FBSs). The aim is to let the FBSs carry most of the teletraffic while the MBSs accommodate the teletraffic hot spots. We assume the MBSs have some method to download the teletraffic back to the fixed networks (e.g. relay data back to the FBSs using repeaters, use of macrocellular links, etc). We have left this issue for future research.

This section has only discussed aspects of cellular radio that are pertinent to this thesis. However, cellular radio is a vast subject and the reader who wishes to acquire a wide knowledge of the subject is recommended to consult references [1, 43, 4, 44, 45, 46, 47, 48, 49, 50, 51, 52, 53, 54, 55, 56].

1.2 Organisation of Thesis

This thesis is organised into five chapters. Chapter 2 presents a street microcellular network in a rectilinear city. The dimensions of the city and the mobility issues of the vehicles are described. The former part of Chapter 2 is devoted to an investigation of the applications of the two handover priority schemes, namely the handover guard channel scheme and the handover queueing scheme, for a microcellular network. Both mathematical analysis and computer simulation results are given. In the latter part of Chapter 2, we propose two BS selection algorithms, namely the base station load equalisation (BSLE) and the re-arrangement upon blocking (RAUB) algorithms. The results from these algorithms will be compared against the standard directed-retry algorithm.

Chapter 3 begins our investigations into moving BSs (MBSs). We start our study with a simple scenario where the fixed BSs (FBSs) and the MBSs have their own allocated spectrum. The FBSs are allocated radio channels using a fixed channel assignment (FCA) scheme, while each MBS is given an unique channel set. This channel assignment method is not practical as the radio spectrum would be quickly exhausted when the MBSs are introduced. However, this simple channel assignment scheme allows us to study the basics of the MBSs and serves as a stepping stone to Chapter 4 when a more complex scheme is introduced.

In Chapter 4 we propose a dynamic channel assignment (DCA) scheme that allows both the FBSs and the MBSs to share the same radio spectrum. Two network access schemes are studied in this chapter. Finally, our conclusions are drawn and further work suggested in Chapter 5.

Chapter 2

Teletraffic Study of Urban Cellular Network

The equivalent of a hexagonal cellular structure for microcells is the rectilinear city grid shown in Figure 1.5. The roads of the grid are bordered by square cross-sectional buildings, each of 100m length. The roads are 20m wide, and have four lanes supporting two-way traffic. The BS transceivers are placed at the middle of each road intersection. They are mounted at lamp-post height, i.e., well below the urban skyline, and therefore the height of the buildings are of no consequence. The radio coverage of each transceiver is confined by the topology of the roads producing microcells in the shape of a cross. Figure 2.1 shows the coverage of five microcells. We purposely place the microcells close together, so that there is an extensive overlapping area to provide seamless radio coverage. The distance from the centre of a cell to its border is L, and the length of the overlapping region is W.

2.1 Street Microcells

While dynamic channel allocation (DCA) techniques are being investigated for third generation mobile systems, all the current cellular systems use fixed channel allocation (FCA) methods. Accordingly we are concerned here with the deployment of base stations (BSs) for systems that use FCA in microcellular environments.

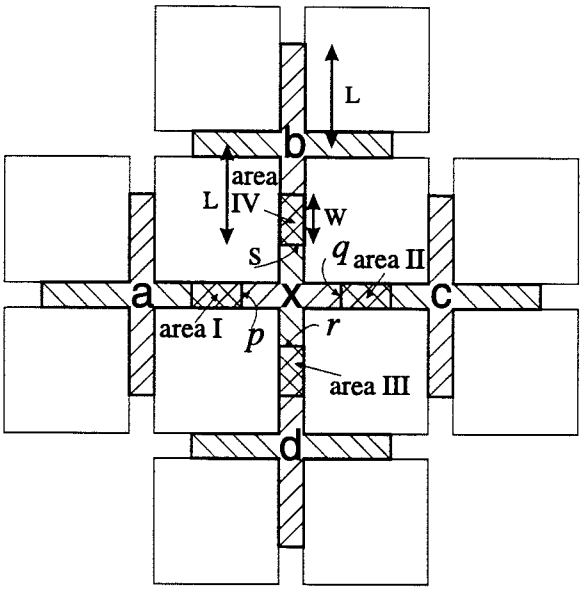

Figure 2.1: Radio coverage of five neighbouring microcells

We assume that each BS is assigned an equal number of channels, and the reuse distances of these channels are sufficient large that the respective cochannel interference is acceptable. As in GSM, time-division multiple access (TDMA) with frequency-division duplex (FDD) is employed. In this microcellular scenario, the radio link between the serving BS and the servicing MS is in line-of-sight (LOS). Thus the transceivers are able to accommodate multipath fading as the radio links are designed for larger cells where the excess delays are much greater. Path loss is the only form of signal deterioration in our model, with both up-links and down-links having the same path loss, which is position dependent. In our scenario, a MS is allowed to establish a connection when it is within the cell area, and no connection when it is outside the cell area.

To avoid edge effects, we allow the city to wrap around from the East-most edge to West-most edge, and from South-most to North-most edges. For example, if a user reaches the East-most edge of the city, he will re-enter the city from the West-most edge. The same argument applies for the radio coverage. Therefore the number of MSs residing in the simulated city remains constant.

We only consider vehicular mounted mobile stations (MSs). In our simula-

Speed (miles per hour)	Stopping distance (meters)
20	12
30	23
40	36
50	53
60	73
70	96

Table 2.1: Shortest stopping distances for various travelling speeds

tions for this dense urban area, each vehicle travels at a constant speed of 6 m/s (13.4 miles/hr). When the vehicle reaches the junction, it has a probability of 0.8 to continue travelling straight, and a probability of 0.1 of either turning left or right. Each MS serves one user. Each idle user is arranged to generate a new call according to a Poisson distribution, with mean rate λ_{nu}. The call duration is negative exponentially distributed, with mean $1/\mu_c$. We fix the mean idling time, $1/\lambda_{nu}$, to be 20 minutes and the mean call duration, $1/\mu_c$, to be 2 minutes. Thus the offered traffic per user is 0.1 Erlangs. Once a call commences a specific call duration is assigned to a mobile. Failure to achieve this call duration is logged as a dropped call. Alternatively, when a MS makes a call attempt and there are no available channels the call is said to be blocked. The user arrival rate and departure rate are the same for all simulation runs. We vary the offered traffic by altering the number of users present in the city. The positions from where the mobiles make new calls are randomly chosen within the city area. We only consider traffic initiated by MSs and destined for the PSTN/ISDN network. Mobile-to-mobile and PSTN/ISDN network-to-mobile traffic is not considered.

Given the dimensions of a vehicle, length of the road and the separation between vehicles, we can calculate the maximum number of MSs that the city can accommodate. Table 2.1 gives the stopping distances for different travelling speeds [57]. A natural cubic spline is used to interpolate these data points [58, 59]. The stopping distance is found to be 4.9 meter when the vehicle is travelling at 6 m/s. Vehicles in the simulation are 4.1 meter long and 1.7 meter wide. Therefore when they are travelling at 6 m/s, the effective distance between the centres of consecutive vehicles is 9 meters. Figure 2.2 shows a segment of the 20 meters wide road having two lanes in each direction.

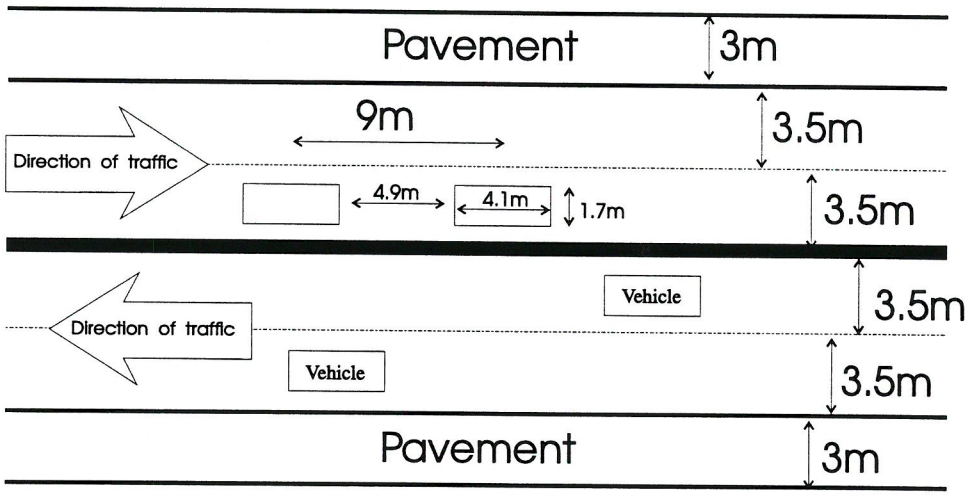

Figure 2.2: A segment of the road

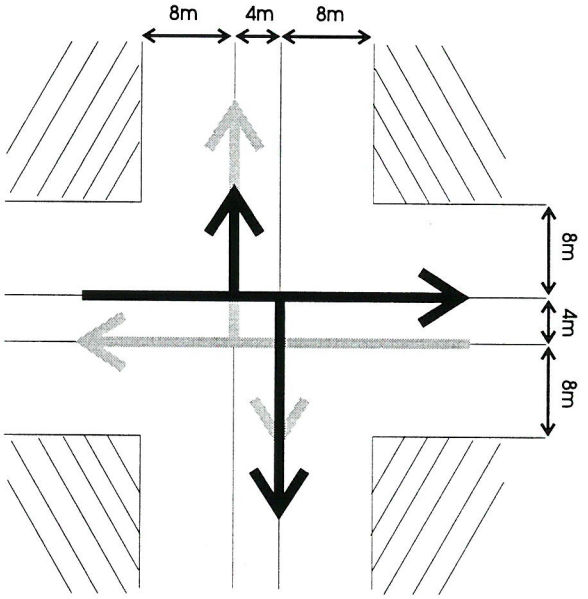

Figure 2.3: Directions of the flow of vehicular traffic (black arrows for traffic that approaches the junction from the left, grey arrows for traffic approaches from the right)

For the convenience of programming, the two lanes per direction are mapped onto a single line. Figure 2.3 shows the possible routes when a vehicle reaches a road junction. Each road is 720 meters long and consists of four lanes. There are six horizontal and six vertical roads running in the city. Thus the total length of the roads is 34560 meters. As the effective distance between consecutive vehicles is 9 meters, the city can maximally contain 3840 vehicles. This limits the highest offered traffic that can be generated in the city.

In order to reduce the computational cost, the simulation program only keeps track of the positions of the active MSs, i.e., calls in progress. When a MS becomes active, it will appear in the city at a randomly assigned coordinate. The simulation model will update the position of this MS during the period of its call. When the MS disconnects from the system, it will be given a new spatial coordinate, next call time and the call duration of its next call. Positions of the inactive MSs are not important to the system, thus the inactive MSs simply "vanish" from the city. The positions of the active MSs are updated every second, which is the smallest unit of time in our simulation program.

Both the analytical and the simulation models will be presented. The simulation program is written in C++ in object-oriented programming style. The program is developed on a UNIX[1] platform with X Window[2] display capability. This allows visual inspection during the development.

2.2 Handover (HO) Priority Schemes

We will examine two handover (HO) priority schemes, namely the HO guard channel scheme [60, 7, 12] and the HO queueing scheme [15, 8]. The former reserves a number of guard channels exclusively for the use of the HO calls. The latter allows the otherwise rejected HO requests to be queued. Both schemes aim to reduce the forced termination probability by giving some form of priority to the HO calls over the new calls. Both schemes have been studied by other researchers in macrocellular networks. Our aim here is to compare their performances when they are applied to an urban microcellular scenario.

[1]UNIX is a trademark of the Open Software Foundation

[2]The X Window System is a trademark of The Massachusetts Institute of Technology

2.2.1 Handover Guard Channel Scheme

The concept of guard channels is to reserve a number of channels, N_h, exclusively for the use of handover (HO) calls. Consequently a BS cannot serve a new call when it has no more than N_h number of channels free. In our scenario each cell consists of two areas; they are the non-overlapping area where the radio coverage is provided solely by one BS, and the overlapping area where the radio coverage is provided by two BSs. In the overlapping area, a MS can be served by either one of the two BSs. In this case the method of directed-retry [61] is employed to set up a new call. This means that a new call always makes its first request to the nearest BS. However, if this BS does not have any vacant channel to serve the call, the other BS will be asked to oblige. A new call generated in the overlapping area will be blocked if both BSs do not have a vacant channel.

An analytical model of our scheme will be presented, and the results compared with those extracted from a computer simulation model.

The following assumptions are made in our analysis.

1. The teletraffic load is evenly distributed in space, and therefore evenly distributed over each microcell coverage area.

2. The number of users is finite as users are confined to the coverage area of a microcell. Therefore the finite quasi-random traffic model is used.

3. The call duration has a negative exponential distribution with mean $T_c = 1/\mu_c$.

4. The residing time of a MS in a microcell has a negative exponential distribution.

5. The channel holding time of all calls handled by the BS has a negative exponential distribution.

6. No fading effects are considered.

7. Each cell has a clearly defined border. Perfect signal reception is assumed within the confined cell area, and no signal reception outside the cell area.

8. When a MS is served by a BS, it is assumed that the BS continues to provide service to that MS until it leaves the coverage area.

9. A subset of channels, N_h, of the total N channels at a BS is reserved exclusively for handovers.

10. A new call originating in a non-overlapping area will be carried by the BS for that area, provided the BS has more than N_h channels free. Otherwise, it is blocked. In contrast, a HO call will only be forced to terminate if the BS has no free channel.

11. A new call originating in overlapping area will first request a connection with the BS that provides the stronger signal. If this BS has N_h or less channels available, the other BS will be asked for assistance. The call is blocked if the second BS also has less than or equal to N_h available channels. Note that handovers only take place when users cross the serving cell's border. Thus HO requests are always made in the non-overlapping area of a cell.

Let the number of users in the coverage area of a microcell be M_u, and M be the total number of users in the city. The ratio of the cell area to the city area is ϵ. Thus

$$M_u = M \ \epsilon \ . \tag{2.1}$$

The carried traffic per microcell is A_c, and the portion of it that is generated by users residing in the overlapping region of the cell is A_{cn}. As every user occupies one channel, A_c also represents the average number of active users connected to a microcell. Similarly, A_{cn} represents the average number of active users who reside in the overlapping region of the cell.

We define ζ to be,

$$\zeta \triangleq \frac{\text{non-overlapping area}}{\text{ovelapping area}} \ . \tag{2.2}$$

On average, traffic originating in an overlapping area is evenly shared between the two BSs. Therefore the total number of active users residing in

an overlapping area, regardless of their serving BS, is $2A_{cn}$. In addition, the number of active users residing inside the cell area, regardless of the BSs they are connected to, is $A_c + A_{cn}$.

Hence,

$$\begin{aligned} \frac{2A_{cn}}{A_c + A_{cn}} &= \frac{\text{size of microcell's overlapped area}}{\text{size of a microcell}} \\ &= \frac{1}{1+\zeta} \\ A_{cn} &= \frac{A_c}{1+2\zeta} \,. \end{aligned} \tag{2.3}$$

Each idle user generates new calls at a rate of λ_{nu}, and the average new call arrival rate at a microcell is λ_n. The average new call arrival rates for the non-overlapping and the overlapping regions are λ_a and λ_b, respectively, viz:

$$\begin{aligned} \lambda_a &= (M_u - A_c - A_{cn}) \frac{\zeta}{1+\zeta} \lambda_{nu} \\ &= \left(M_u - \left(1 + \frac{1}{1+2\zeta} \right) A_c \right) \frac{\zeta}{1+\zeta} \lambda_{nu} \end{aligned} \tag{2.4}$$

and,

$$\lambda_b = \left(M_u - \left(1 + \frac{1}{1+2\zeta} \right) A_c \right) \frac{1}{1+\zeta} (1 + P_{B0}) \frac{\lambda_{nu}}{2} \tag{2.5}$$

where P_{B0} is the probability that a BS is unable to service a new call. In the non-overlapping area, P_{B0} is equal to the new call blocking probability. P_{B0} is called the *call congestion probability* of a BS. It is the probability that a new call arrives at a BS when the BS is in one of its congestion states[3]. It is

[3]The state space of a BS is defined by its number of occupied channels. Thus states $N - N_h + 1$, $N - N_h + 2$, ..., N are said to be congestion states. A new call will not be admitted if the BS is in one of these states.

different from the *time congestion probability*, which is the probability that the cell is in its congestion states at any given time.

The total average new call arrival rate per cell, λ_n, is:

$$\lambda_n = \lambda_a + \lambda_b \ . \tag{2.6}$$

We now need to calculate the probability that a given call needs a HO. For new calls originating in the non-overlapping area, the average distance travelled before reaching one of the cell's borders is L. If users are travelling at a speed of v m/s, the average leaving rate, μ_a, is

$$\mu_a = \frac{v}{L} \ . \tag{2.7}$$

From Figure 2.1, we can see that there are four overlapping areas per cell. They are labelled as area I, II, III and IV for cell X. Let's look at area I. Calls originating in this area can either travel to the left or right. T_{br} is the average time between when the call is made and when the MS reaches the right hand side border of the cell. Correspondingly, T_{bl} is the average time a user takes to travel to the left hand side border. These times may be expressed as:

$$T_{br} = \frac{4L - W}{2v} \tag{2.8}$$

and

$$T_{bl} = \frac{W}{2v} \tag{2.9}$$

The same argument applies to areas II, III and IV. Assuming half of the users travel to the left, and half travel to the right, the new call leaving rate in the overlapping area, μ_b, is

$$\mu_b = \frac{2}{T_{br} + T_{bl}} \ . \tag{2.10}$$

Handovers can only take place at borders p, q, r and s shown in Figure 2.1. Therefore the rate of HO calls, μ_h, is

$$\mu_h = \frac{v}{2L - W} \ . \tag{2.11}$$

The corresponding average residing times for new calls originating in non-overlapping areas, new calls originating in overlapping areas and HO calls are T_a, T_b and T_h respectively, having values,

$$T_a = \frac{1}{\mu_a} \ , \tag{2.12}$$

$$T_b = \frac{1}{\mu_b} \tag{2.13}$$

and

$$T_h = \frac{1}{\mu_h} \ . \tag{2.14}$$

A channel is released from a user when the call is completed or when the user leaves the serving cell. Thus, the channel holding time is the shorter time between the residing time and the call duration. The average channel holding time for new calls originating in non-overlapping areas, new calls originating in overlapping areas and HO calls are T_{Ha}, T_{Hb} and T_{Hh} respectively, given by

$$T_{Ha} = \frac{1}{\mu_a + \mu_c} \ , \tag{2.15}$$

$$T_{Hb} = \frac{1}{\mu_b + \mu_c} \tag{2.16}$$

and

$$T_{Hh} = \frac{1}{\mu_h + \mu_c} \ . \tag{2.17}$$

The probability, P_h, that a HO call needs another handover is

$$P_h = \frac{\mu_h}{\mu_h + \mu_c} \ . \tag{2.18}$$

The probabilities that a handover is needed for a new call that originated in the non-overlapping and overlapping areas are P_{ia} and P_{ib} respectively, viz:-

$$P_{ia} = \frac{\mu_a}{\mu_a + \mu_c} \tag{2.19}$$

and

$$P_{ib} = \frac{\mu_b}{\mu_b + \mu_c} \tag{2.20}$$

The HO rate, λ_h, is

$$\begin{aligned} \lambda_h &= \lambda_a(1 - P_{B0})\ P_{ia} + \lambda_b(1 - P_{B0})\ P_{ib} + \\ &\quad \lambda_h(1 - P_{fh})\ P_h \\ \lambda_h &= \frac{(\lambda_a\ P_{ia} + \lambda_b\ P_{ib})(1 - P_{B0})}{1 - P_h\ (1 - P_{fh})} \ , \end{aligned} \tag{2.21}$$

where P_{fh} is the probability that a HO attempt fails.

We have now derived the equations for each of the three types of arrival rates, namely, λ_a, λ_b and λ_h. We have also derived their corresponding channel holding times, T_{Ha}, T_{Hb} and T_{Hh}.

To calculate the overall average channel holding time, T_{ch}, we need to weight the different channel holding times with their respective rate of arrivals. We define α_a, α_b and α_h as follows,

$$\alpha_a = \frac{\lambda_a(1 - P_{B0})}{(\lambda_a + \lambda_b)(1 - P_{B0}) + \lambda_h(1 - P_{fh})} \tag{2.22}$$

$$\alpha_b = \frac{\lambda_b(1 - P_{B0})}{(\lambda_a + \lambda_b)(1 - P_{B0}) + \lambda_h(1 - P_{fh})} \tag{2.23}$$

$$\alpha_h = \frac{\lambda_h(1 - P_{fh})}{(\lambda_a + \lambda_b)(1 - P_{B0}) + \lambda_h(1 - P_{fh})} \tag{2.24}$$

then,

$$T_{ch} = \alpha_a \, T_{Ha} + \alpha_b \, T_{Hb} + \alpha_h \, T_{Hh} \tag{2.25}$$

The probabilities P_{B0} and P_{fh} can be determined in the usual way for birth-death processes [62, 63].

Each microcell partially overlaps with its four neighbouring cells. A five dimensional state space is needed to describe one microcell. We approximate the problem to a one dimensional state space by assuming the adjacent cells are in their statistical average states at all time. The one dimensional Markov chain is shown in Figure 2.4. Each circle in the diagram represents a state. The upper arrows represent the upward transition probabilities, and the lower arrows represent the downward transition probabilities.

Equation 2.4 and 2.5 represent the average new call arrival rates, λ_a and λ_b, for non-overlapping areas and overlapping areas, respectively. By replacing A_c with j in these equations, we obtain the instantaneous new call arrival rates, λ_{aj} and λ_{bj}, for a BS in state j for the non-overlapping and the overlapping areas, respectively as,

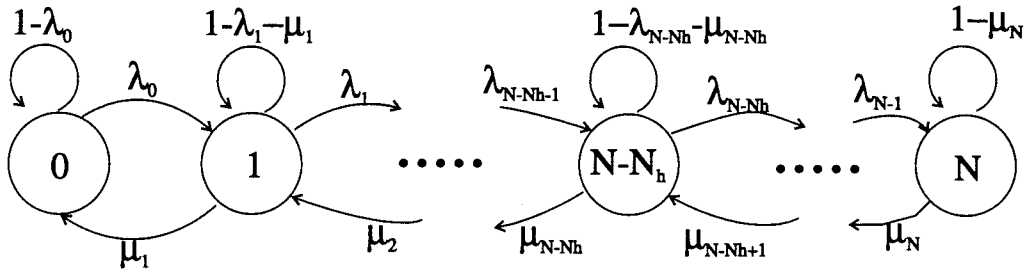

Figure 2.4: Markov chain of a birth-death process

$$\lambda_{aj} = \left(M_u - \left(1 + \frac{1}{1+2\zeta} \right) \; j \right) \; \frac{\zeta}{1+\zeta} \; \lambda_{nu} \tag{2.26}$$

and,

$$\lambda_{bj} = \left(M_u - \left(1 + \frac{1}{1+2\zeta} \right) \; j \right) \; \frac{1}{1+\zeta} \; (1 + P_{B0}) \; \frac{\lambda_{nu}}{2} \; . \tag{2.27}$$

The upward transition probability, λ_j, is:

$$\begin{array}{ll} \lambda_j = \lambda_{aj} + \lambda_{bj} + \lambda_h & \text{for } 0 \leq j \leq N - N_h - 1 \\ \lambda_j = \lambda_h & \text{for } N - N_h \leq j \leq N - 1 \; . \end{array}$$

The downward transition probability, μ_j, is:

$$\mu_j = j \; \mu \qquad \text{for} 1 \leq j \leq N$$

where

$$\mu = \frac{1}{T_{ch}} \; .$$

At equilibrium,

$$P_j \; \lambda_j = P_{j+1} \; \mu_{j+1}$$

where P_j is the probability of being in state j

$$
\begin{aligned}
P_0 &= P_0 \\
P_1 &= \frac{\lambda_0}{\mu_1} P_0 \\
P_2 &= \frac{\lambda_0}{\mu_1} \frac{\lambda_1}{\mu_2} P_0 \\
&\vdots \\
P_j &= \frac{\lambda_0 \ \lambda_1 \ \lambda_2 \ \ldots \ \lambda_{j-1}}{\mu_1 \ \mu_2 \ \mu_3 \ \ldots \ \mu_j} P_0 \ .
\end{aligned}
$$

Using the normalisation condition

$$\sum_{j=0}^{N} P_j = 1$$

$$
\begin{aligned}
\frac{1}{P_0} &= 1 + \frac{\lambda_0}{\mu_1} + \frac{\lambda_0}{\mu_1} \frac{\lambda_1}{\mu_2} + \ldots + \frac{\lambda_0 \lambda_1 \lambda_2 \ldots \lambda_{N-1}}{\mu_1 \mu_2 \mu_3 \ldots \mu_N} \\
P_0 &= \frac{1}{1 + \sum_{i=1}^{i=N} \left(\prod_{j=0}^{j=i-1} \frac{\lambda_j}{\mu_{j+1}} \right)} \ . \qquad (2.28)
\end{aligned}
$$

The carried traffic, A_c, is the expected value of the system's state, j,

$$A_c = \sum_{j=0}^{N} (j \ P_j) \ . \qquad (2.29)$$

The call congestion probability, P_{B0}, which also represents the new call blocking probability in the non-overlapping area is,

$$P_{B0} = \frac{\text{no. of new calls arrive when } N_h \text{ or less channels are free}}{\text{total no. of new call arrivals}}$$

$$= \frac{\sum_{j=N-N_h}^{N} (\lambda_{aj} + \lambda_{bj})\ P_j}{\sum_{j=0}^{N} (\lambda_{aj} + \lambda_{bj})\ P_j}$$

Substituting λ_{aj} and λ_{bj} from Equations 2.26 and 2.27 into P_{B0} yields

$$P_{B0} = \frac{\sum_{j=N-N_h}^{N} \left(M_u - \left(1 + \frac{1}{1+2\zeta}\right)\ j\right)\ P_j}{\sum_{j=0}^{N} \left(M_u - \left(1 + \frac{1}{1+2\zeta}\right)\ j\right)\ P_j}$$

$$= \frac{\sum_{j=N-N_h}^{N} \left(M_u - \left(1 + \frac{1}{1+2\zeta}\right)\ j\right)\ P_j}{M_u \sum_{j=0}^{N} P_j - \left(1 + \frac{1}{1+2\zeta}\right) \sum_{j=0}^{N} j P_j}$$

and on rearranging,

$$P_{B0} = \frac{\sum_{j=N-N_h}^{N} \left(M_u - \left(1 + \frac{1}{1+2\zeta}\right)\ j\right)\ P_j}{M_u - \left(1 + \frac{1}{1+2\zeta}\right)\ A_c} \ . \tag{2.30}$$

The probability that a new call originating in overlapping area is blocked, P_{B1}, is

$$P_{B1} = P_{B0} \cdot P_{B0} \ .$$

The probability that a given HO will be forced to terminate, P_{fh}, is

$$P_{fh} = \frac{\text{no. of HO calls arriving when all N channels are busy}}{\text{total no. of HO call arrivals}}$$

$$= \frac{\lambda_h\ P_N}{\sum_{j=0}^{N} (\lambda_h\ P_j)}$$

that is,

$$P_{fh} = P_N \ . \tag{2.31}$$

The forced termination probability is

$$P_F = \frac{\text{no. of force terminated calls}}{\text{no. of successful carried calls}}$$

and it can be expressed in terms of HO rate, new call arrival rates in the overlapping and the non-overlapping area, and their corresponding probabilities of success, which gives,

$$P_F = \frac{P_{fh}\lambda_h}{(\lambda_a + \lambda_b)(1 - P_{B0})} \tag{2.32}$$

To calculate the average new call blocking probability, we define σ as the ratio of the total area of all non-overlapping regions in the city to the total area of all overlapping regions in the city. Note that σ is not the same as ζ, because our microcells are not tessellated over the city, but partially overlapped.

Figure 2.5 shows five microcells. The dotted squares can be tiled over the city area. The borders of the squares lie at the mid-points of the overlapped regions of the respective cells. Let y be the area of the non-overlapping region of a cell and x be the area of the overlapping region of a cell, then

$$\zeta = \frac{y}{x} \ .$$

Within the dotted square, the area of the overlapping region is $x/2$. Therefore,

$$\sigma = \frac{y}{x/2}$$

and

$$\sigma = 2\zeta \ . \tag{2.33}$$

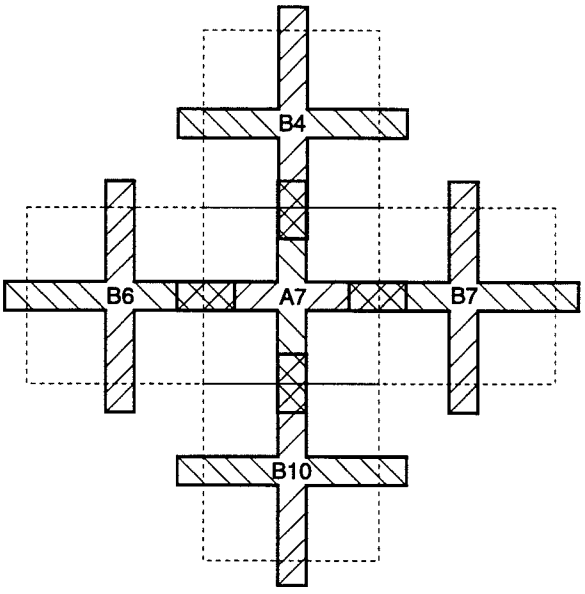

Figure 2.5: A diagram showing five microcells

Thus, the average new call blocking probability, P_{Bav}, is

$$P_{Bav} = P_{B0}\ \frac{\sigma}{1+\sigma} + P_{B1}\ \frac{1}{1+\sigma}$$

and

$$P_{Bav} = \frac{P_{B0}\ \sigma + P_{B1}}{1+\sigma}\ . \tag{2.34}$$

We chose the length of the microcell, L, and the length of the overlapping area, W, to be 80 and 40 meters, respectively. The ratio of the non-overlapping area to the overlapping area, ζ, is 1. The ratio of the cell area to the city area, ϵ, is 1/27. The new call arrival rate per user, λ_{nu}, is set to be 1/1200 $\sec^{-1}$, and the mean call duration, $1/\mu_c$, is 120 sec. Thus the offer traffic per user is 0.1 Erlangs.

To simulate the urban traffic condition, we set the vehicular speed to be 6 m/s. The average new call blocking probabilities, P_{Bav}, and the forced termination probabilities, P_F, for systems having 8, 16 and 24 channels per

BS are shown in Figure 2.6, 2.7 and 2.8, respectively. Both the new call blocking probabilities and the forced termination probabilities were reduced when the number of channels per BS was increased from 8 to 16 and 24. As the blocking probabilities decrease the simulation program needs to be run for a longer time in order to record the same number of block calls. For this reason we were only able to simulate the system that operates with eight channels per BS. Theoretical results, however, were given for all three systems (8, 16 and 24 channels per BS).

Theoretical results were plotted as lines in Figure 2.6 to 2.8, while the simulation results were drawn as markers (Figure 2.6 only). Figure 2.6 shows that the simulation results agree closely with the theory. The differences in the two models' results are partly contributed by the time-driven nature of the simulation program that rounds all event occurrences to the nearest second.

The number of HO guard channels was varied in order to study the trade-off between the new call blocking probabilities and the forced termination probabilities. By increasing the number of guard channels, the new call blocking probabilities are significantly increased while the forced termination probabilities are only marginally decreased. It is therefore evident that the concept of HO guard channels is inefficient when applied to scenarios where HO activities are high.

However, in reference [60] it was shown that in a macrocellular system where HO activities are low, a HO guard channel scheme can significantly reduce the forced termination probabilities with only a marginal increase in the new call blocking probabilities. To simulate low level of HO activities, we reduced the MS speed from 6 m/s to 1 m/s. Figure 2.9, 2.10 and 2.11 show the new call blocking probabilities and forced termination probabilities for systems having 8, 16 and 24 channels, respectively, when the MS speed is reduced to 1 m/s. Again the simulation program was only used to evaluate the eight channels per BS system, while theoretical results were given for all three systems. In comparison with Figures 2.6 to 2.8, Figures 2.9 to 2.11 show that when the MS speed is reduced from 6 m/s to 1 m/s, the increase in P_{Bav} is smaller, while the decrease in P_F is greater.

In order to study the performance of the HO guard channel scheme versus the level of HO activities, we fixed the total number of channels to be eight, and initially there were no HO guard channels. We calculated the number of MSs required to produce a new call blocking probability of 2% for this

system configuration. With the same number of MSs present in the city we calculated the forced termination probability. Then we increased the number of HO guard channels to one and re-calculated the corresponding new call blocking probability and forced termination probability for the same number of MSs in the city. The percentages of increase in P_{Bav} and the percentages of decrease in P_F for different MS speed are shown in Figure 2.12. It can be seen that the percentage of increase in P_{Bav} increases exponentially with the MS speed and the percentage of decrease in P_F decreases exponentially with the MS speed. With this system configuration, the increase in P_{Bav} is always greater than the decrease in P_F. (Notice that by definition the percentage of decrease is always less than 100% although the percentage of increase can be greater than 100%).

We repeated this analysis with $N = 16$. The results are shown in Figure 2.13. This time the percentage of increase in P_{Bav} is less than the percentage of decrease in P_F when the MS speed was less than 0.1 m/s. Thus we conclude that a system will benefit from the HO guard channel scheme if each BS in the system is given a large number of channels and the HO rate is low. Consequently, although the HO guard channel scheme can benefit a macrocellular system, it is not suitable for a microcellular system.

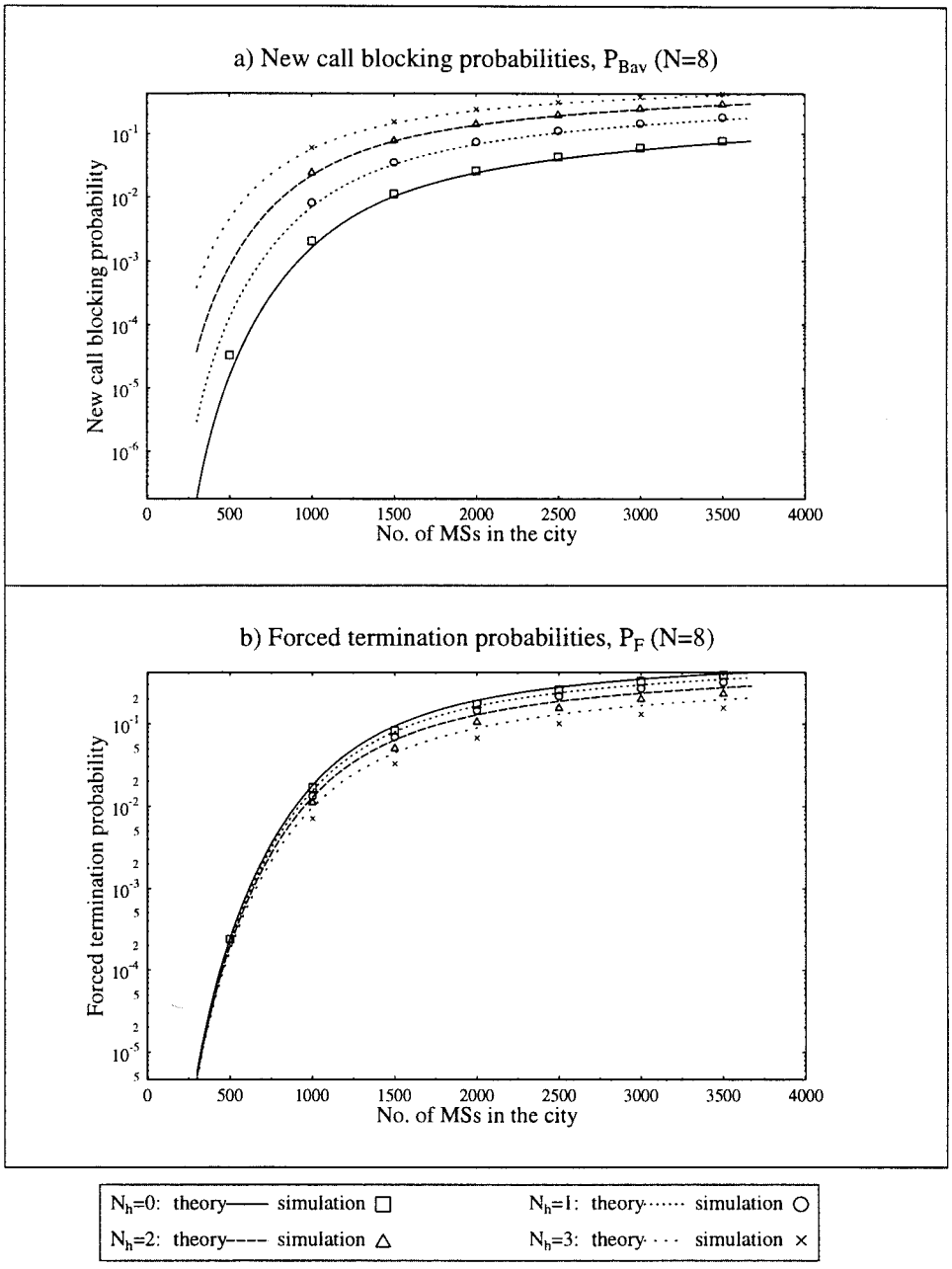

Figure 2.6: a) New call blocking probabilities b) Forced termination probabilities for 8-channels BS and the MS speed is 6 m/s.

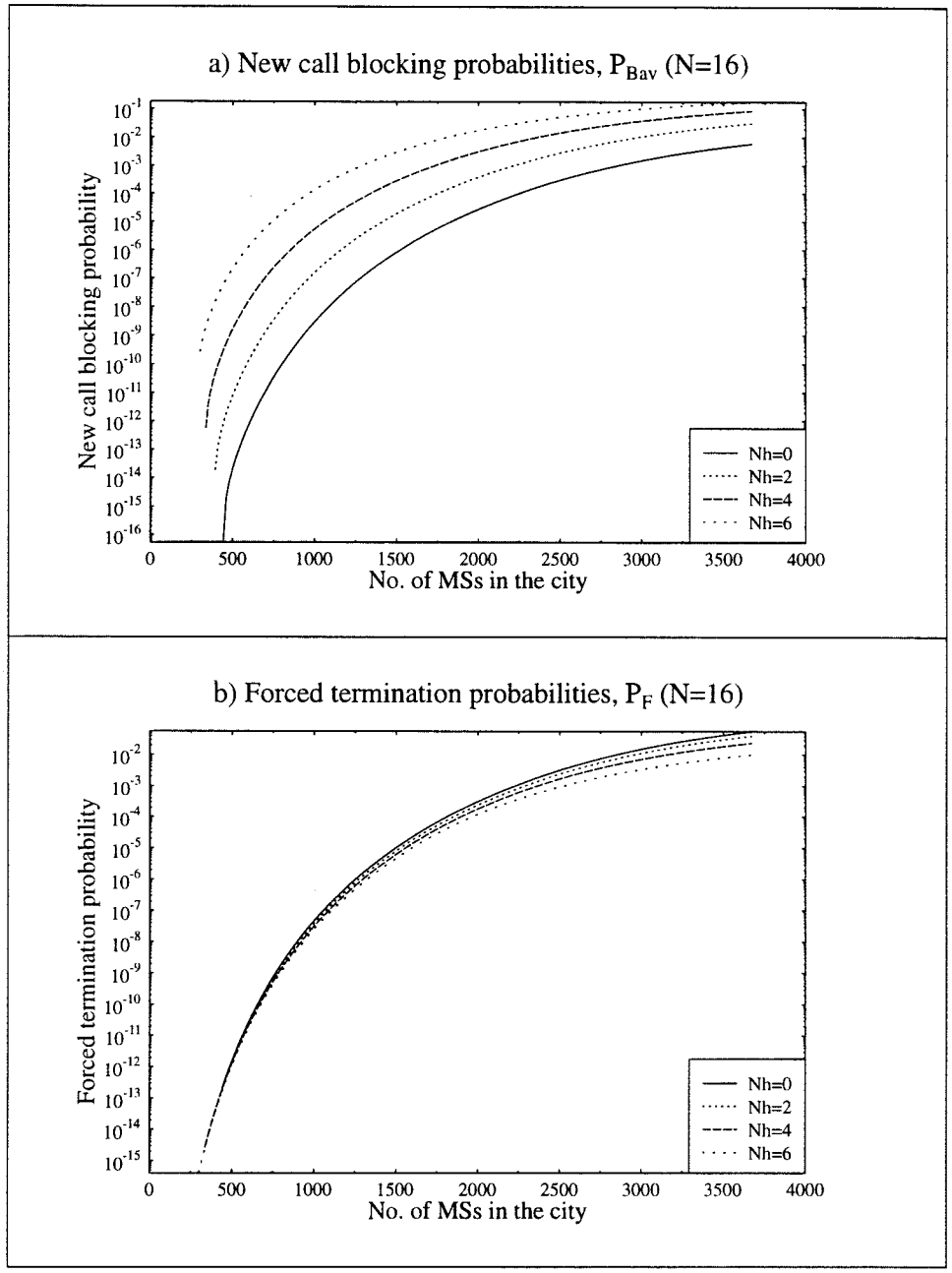

Figure 2.7: a) New call blocking probabilities b) Forced termination probabilities for 16-channels BS and the MS speed is 6 m/s.

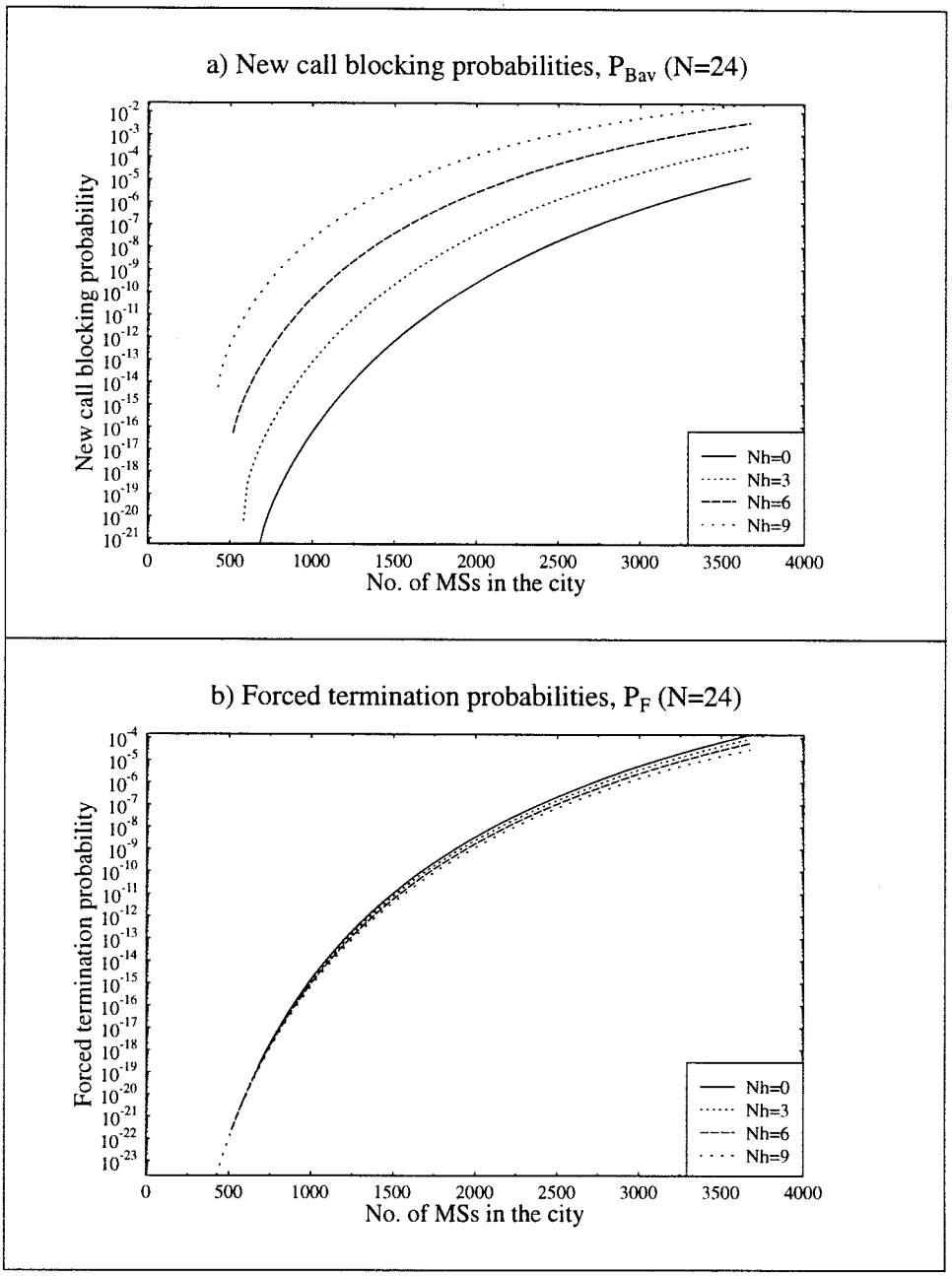

Figure 2.8: a) New call blocking probabilities b) Forced termination probabilities for 24-channels BS and the MS speed is 6 m/s.

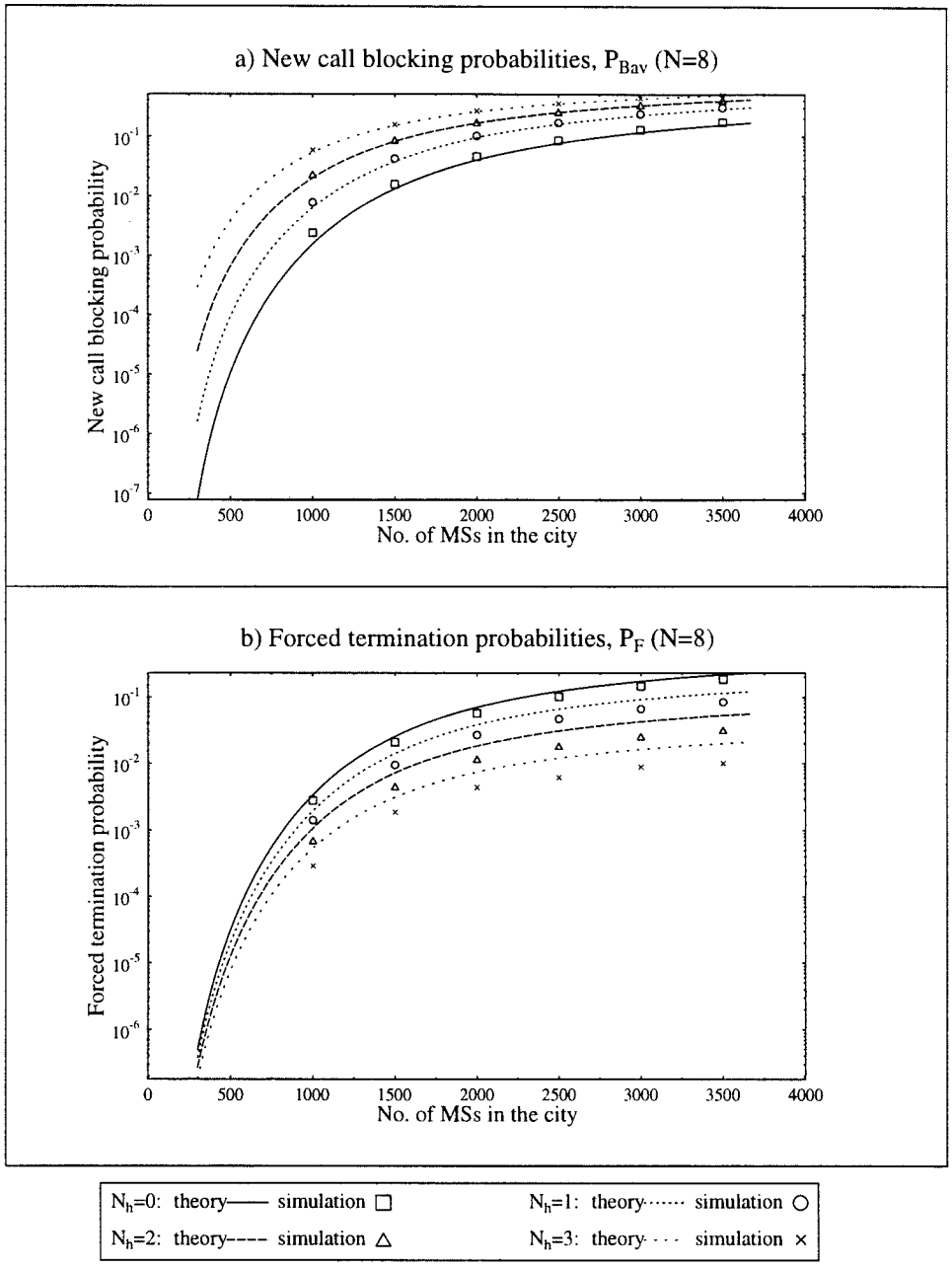

Figure 2.9: a) New call blocking probabilities b) Forced termination probabilities for 8-channels BS and the MS speed is 1 m/s.

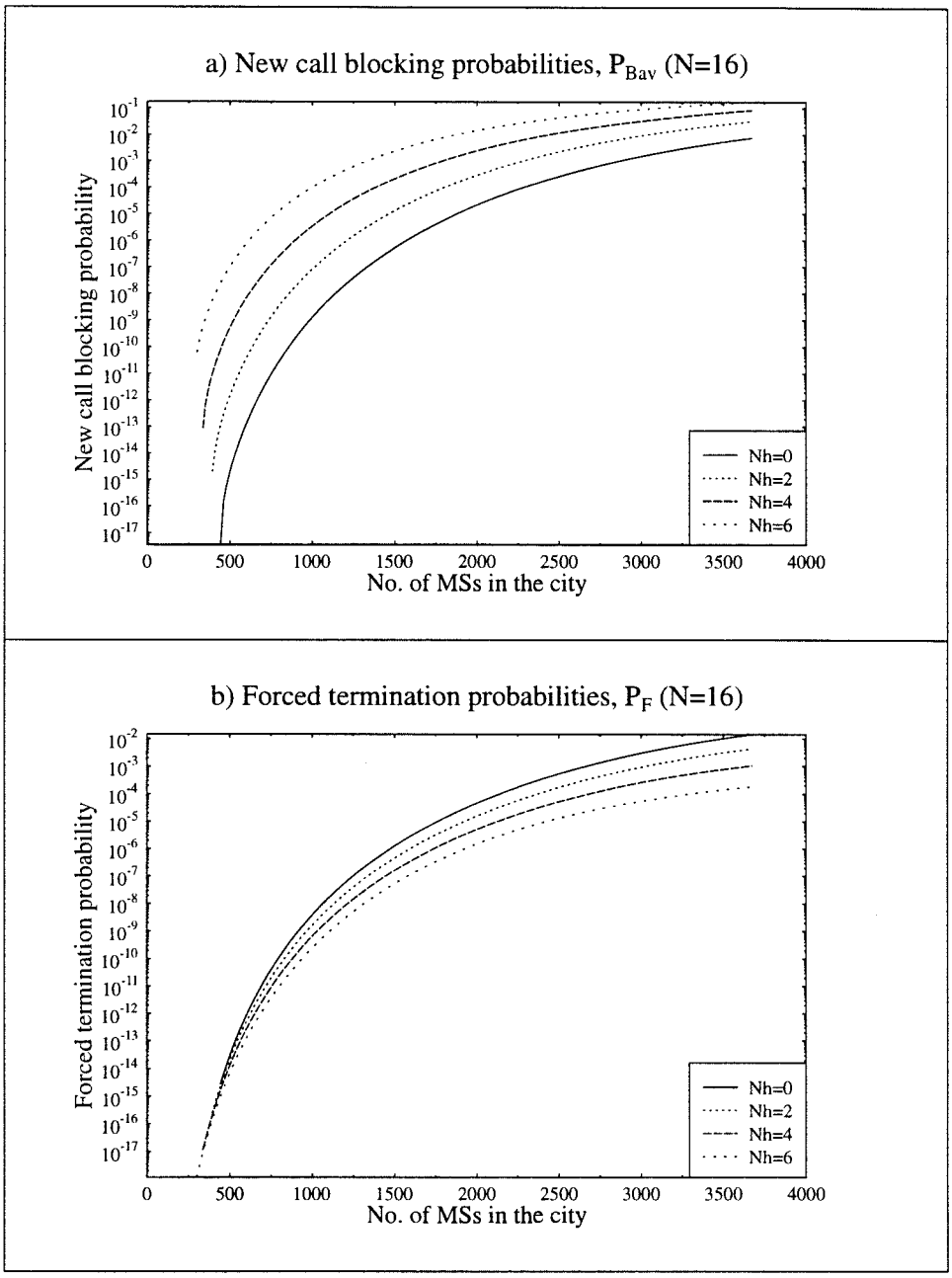

Figure 2.10: a) New call blocking probabilities b) Forced termination probabilities for 16-channels BS and the MS speed is 1 m/s.

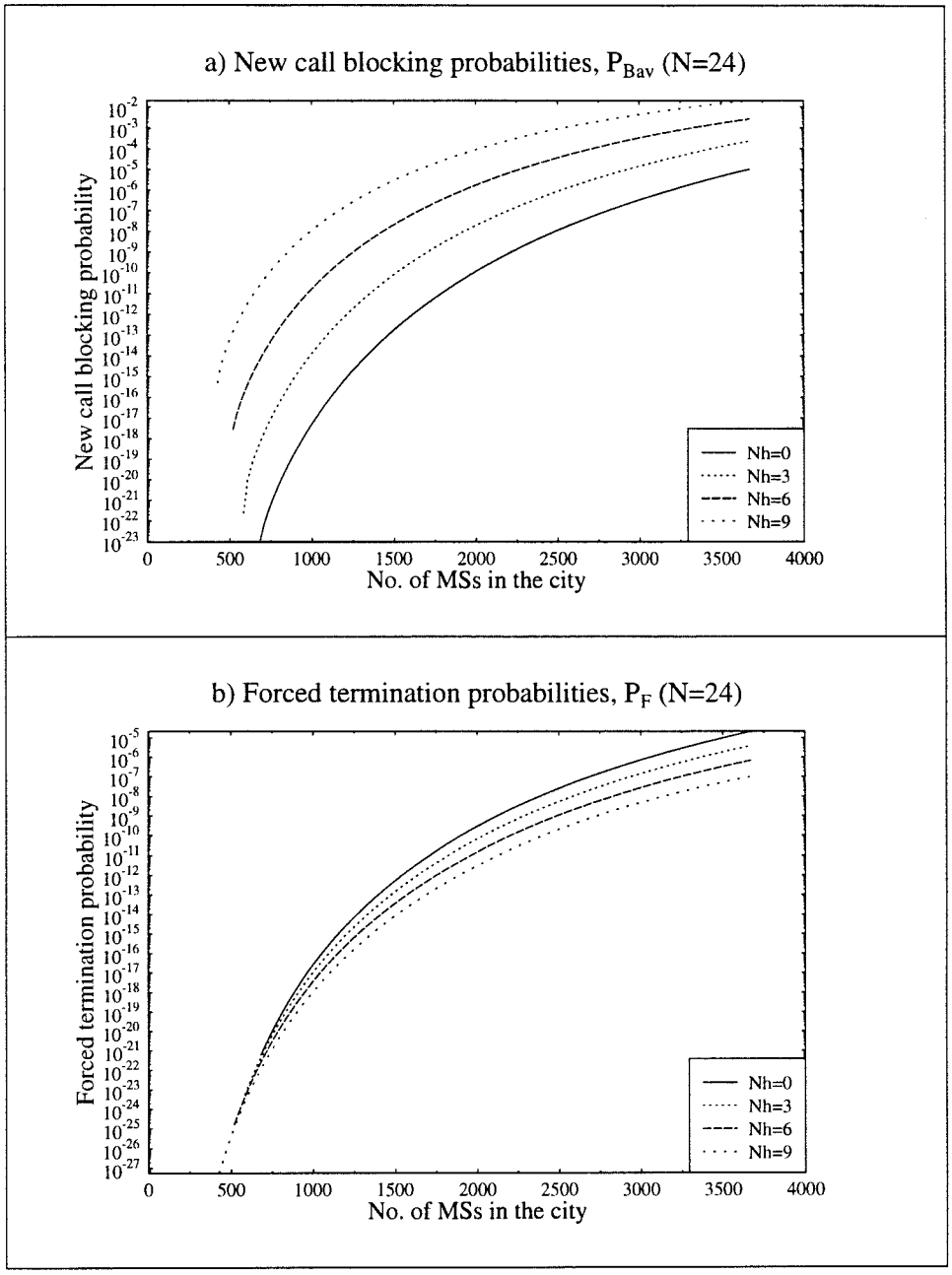

Figure 2.11: a) New call blocking probabilities b) Forced termination probabilities for 24-channels BS and the MS speed is 1 m/s.

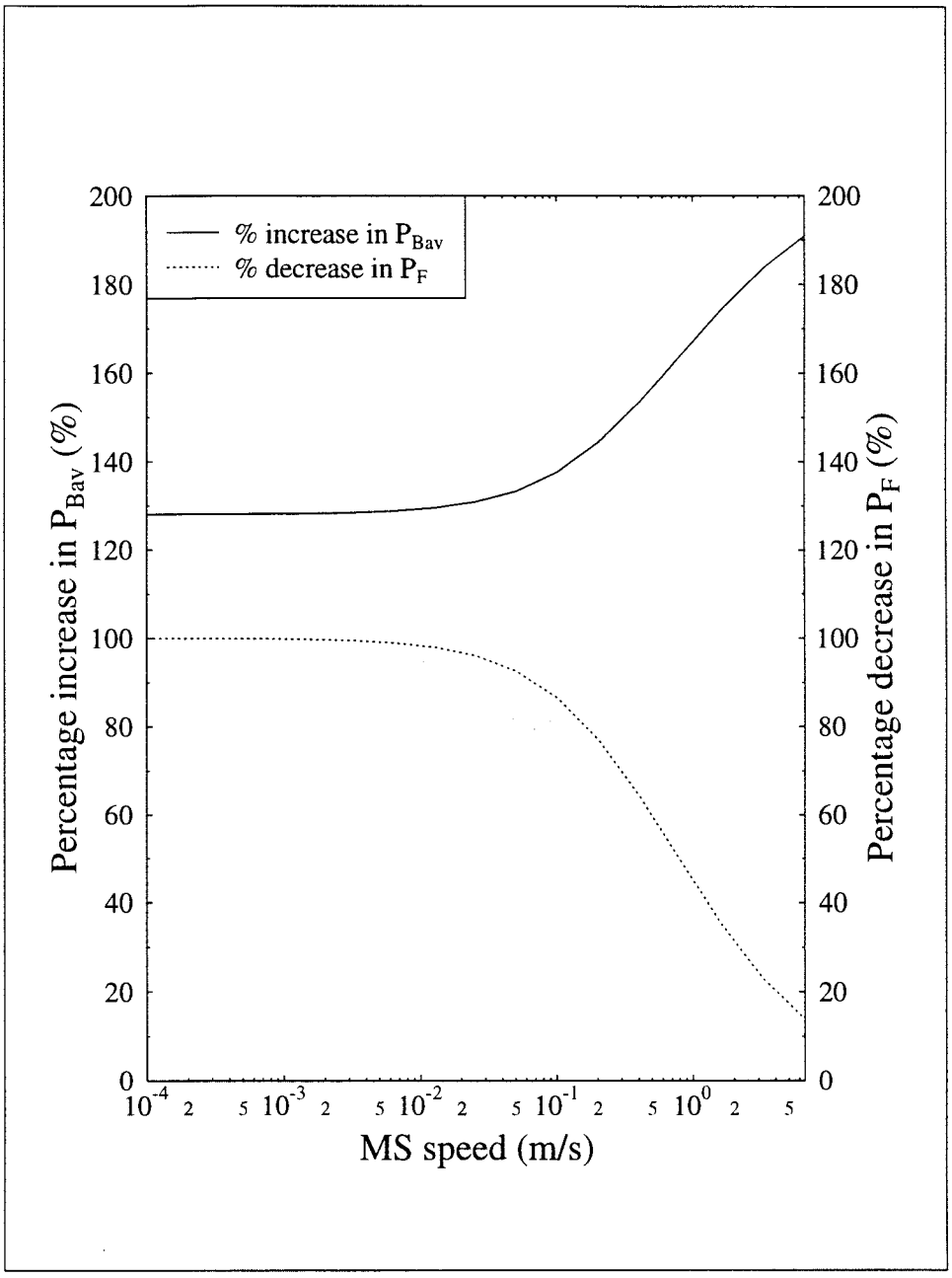

Figure 2.12: The percentage increase in new call blocking probabilities and the percentage decrease in forced termination probabilities versus the MS speed for an 8 channels per BS system.

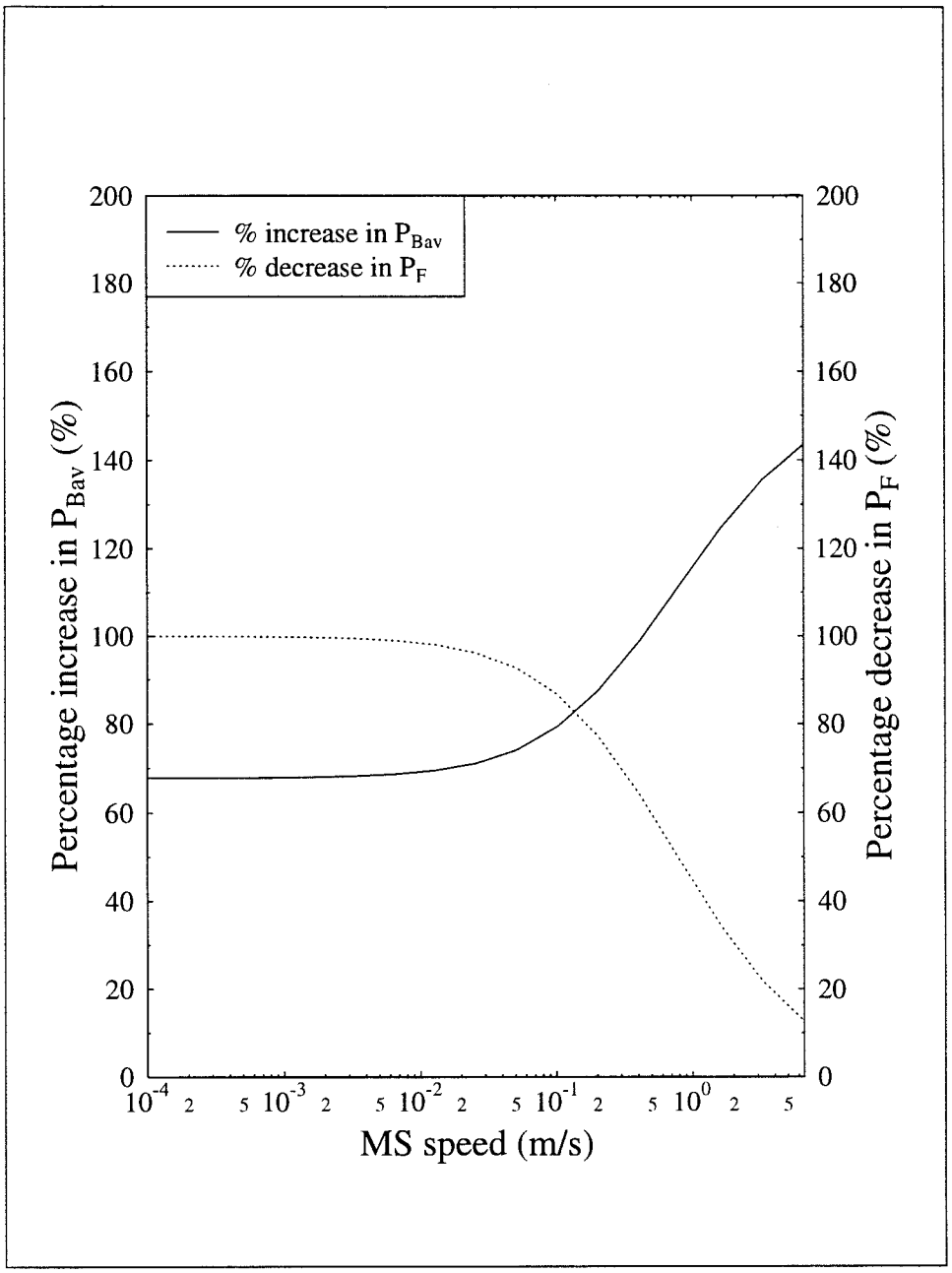

Figure 2.13: The percentage increase in new call blocking probabilities and the percentage decrease in forced termination probabilities versus the MS speed for a 16 channels per BS system.

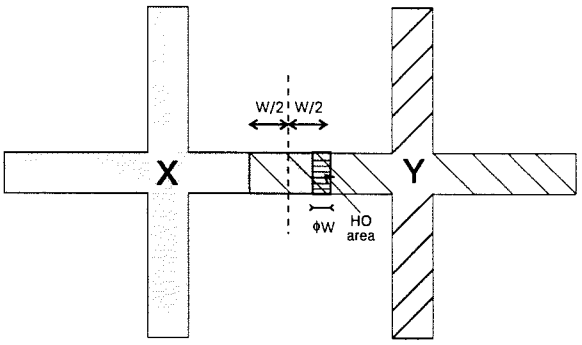

Figure 2.14: Handover area of a cross-shaped microcell.

2.2.2 Handover Queueing Scheme

Queueing of HO calls is another method to give priority to HO calls over new calls. As a MS travels nearer to the border of its current serving BS, it has an increasingly strong received signal strength from the adjacent BS. When the reception from the adjacent BS is better than the current serving BS by some threshold, a HO request is made. In practice, this threshold needs to be carefully determined to avoid repeated HOs between the two BSs. In our idealistic model, where path loss is directly related to distance, we can use distance to define where a HO request should be made. Figure 2.14 shows two adjacent BSs, X and Y. The radio coverage of BS X is shaded in grey. The length of the overlapped area between BS X and BS Y is W.

When the MS is at a distance less than $W/2$ from the border of its current serving cell, the adjacent BS provides a stronger received signal strength for the MS. We define the HO area as the area where the distance between the MS and its serving cell's border is less than ϕW, where ϕ is between 0 to 0.5. When a MS first enters the HO area, a HO request is made to the adjacent BS. If the HO request is not granted, the call is placed in a queue and it remains in communication with its present BS. As soon as the adjacent BS has an available channel, the first HO call in the queue will be served. The queue operates on a first-come-first-served basis. A queued HO call would be forced to terminate when it moves out of its current BS's coverage.

For new calls generated in the overlapped area, the request is made to the strongest BS first and then to the second BS if the request was not granted by the first BS. In the latter case, where the MS is connected to the weaker

BS, if the MS resides in the HO area of the weaker BS, a HO request is made immediately to the stronger BS and would be placed in that BS's queue. If the MS travels towards its server (the weaker BS) and eventually leaves the HO area, the previously placed HO request will be cancelled. On the other hand, if the MS travels away from the server and leaves the cell without having successfully handed over to the adjacent BS, the call is dropped.

The HO queueing scheme was simulated and the results obtained from the computer model. Figure 2.15 shows the new call blocking probabilities and the forced termination probabilities for a system that has eight channels per BS and the MSs travel at 6 m/s. The size of the HO area is varied by changing ϕ from 0.2 to 0.4. As ϕ is increased, the HO calls can stay in the queue for longer periods thus improving their chances of successful HOs. The decreases in the forced termination probabilities are shown in Figure 2.15b. Consequently the amount of carried traffic due to the HO calls is increased. However this causes an increase in the new call blocking probabilities, as depicted in Figure 2.15a, in order to balance the overall carried traffic. For this configuration, the relative increases in the new call blocking probabilities are of the same order as the relative decreases in the forced termination probabilities.

We repeated the same simulation but with the MS mobility reduced to 1 m/s. The results are shown in Figure 2.16. The decreases in the forced termination probabilities in this figure are more than those shown in Figure 2.15. In addition, the increases in the new call blocking probabilities are reduced to an insignificant amount. This is because, as the MS speed is reduced, the time a HO call can spend in the queue is increased, and as a result, the forced termination probability is reduced. The increased carried HO traffic would cause an increase in the new call blocking probability in order to balance the overall carried traffic. However in this case the reduced MS speed also lowers the HO rate, thus the overall increases in HO carried traffic is small.

Similar to the HO guard channel scheme, this HO queueing scheme operates more efficiently when the HO activities are low.

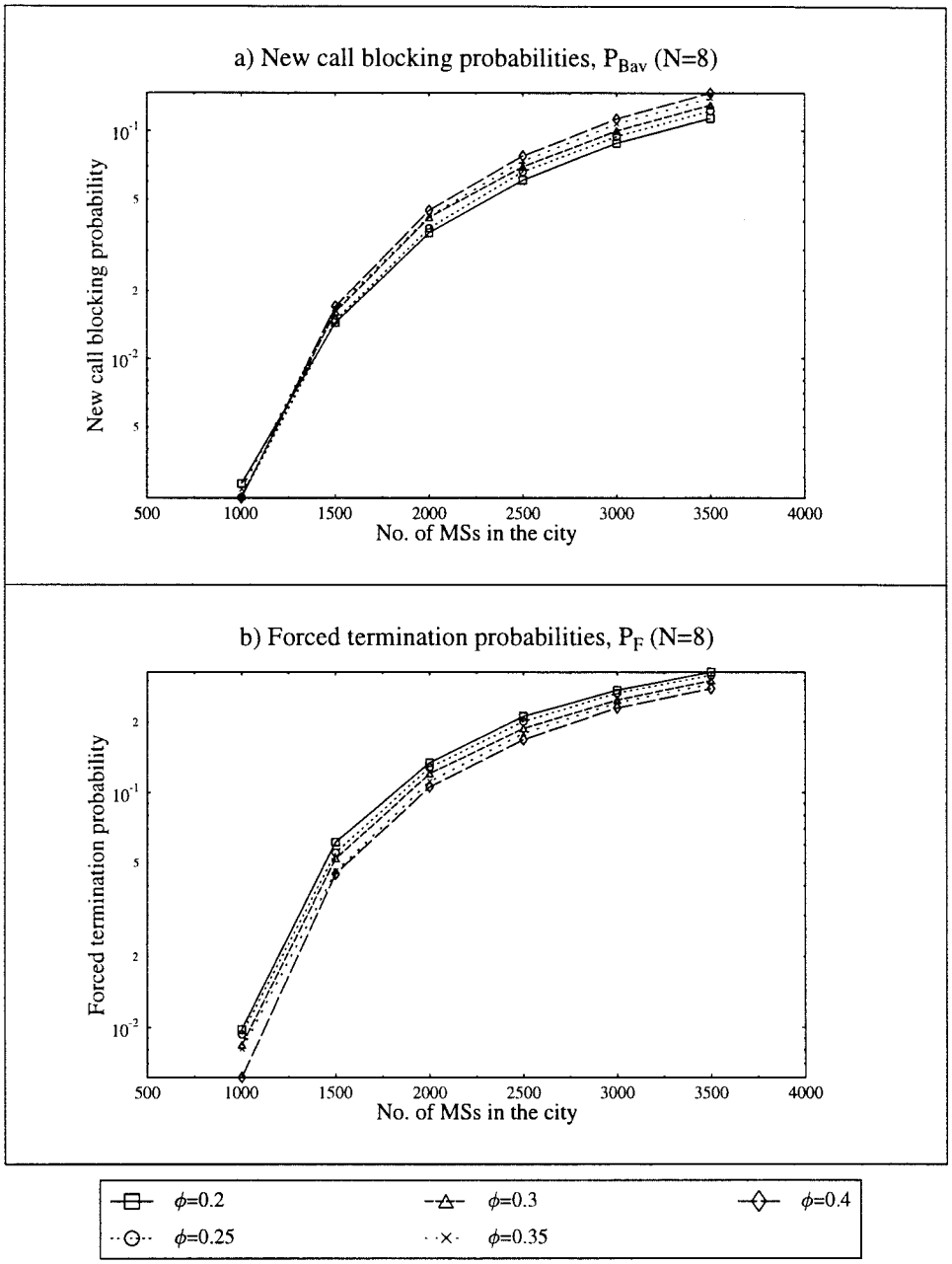

Figure 2.15: a) New call blocking probabilities and b) forced termination probabilities for HO queueing scheme, with MS mobility of 6 m/s and 8 channels per BS.

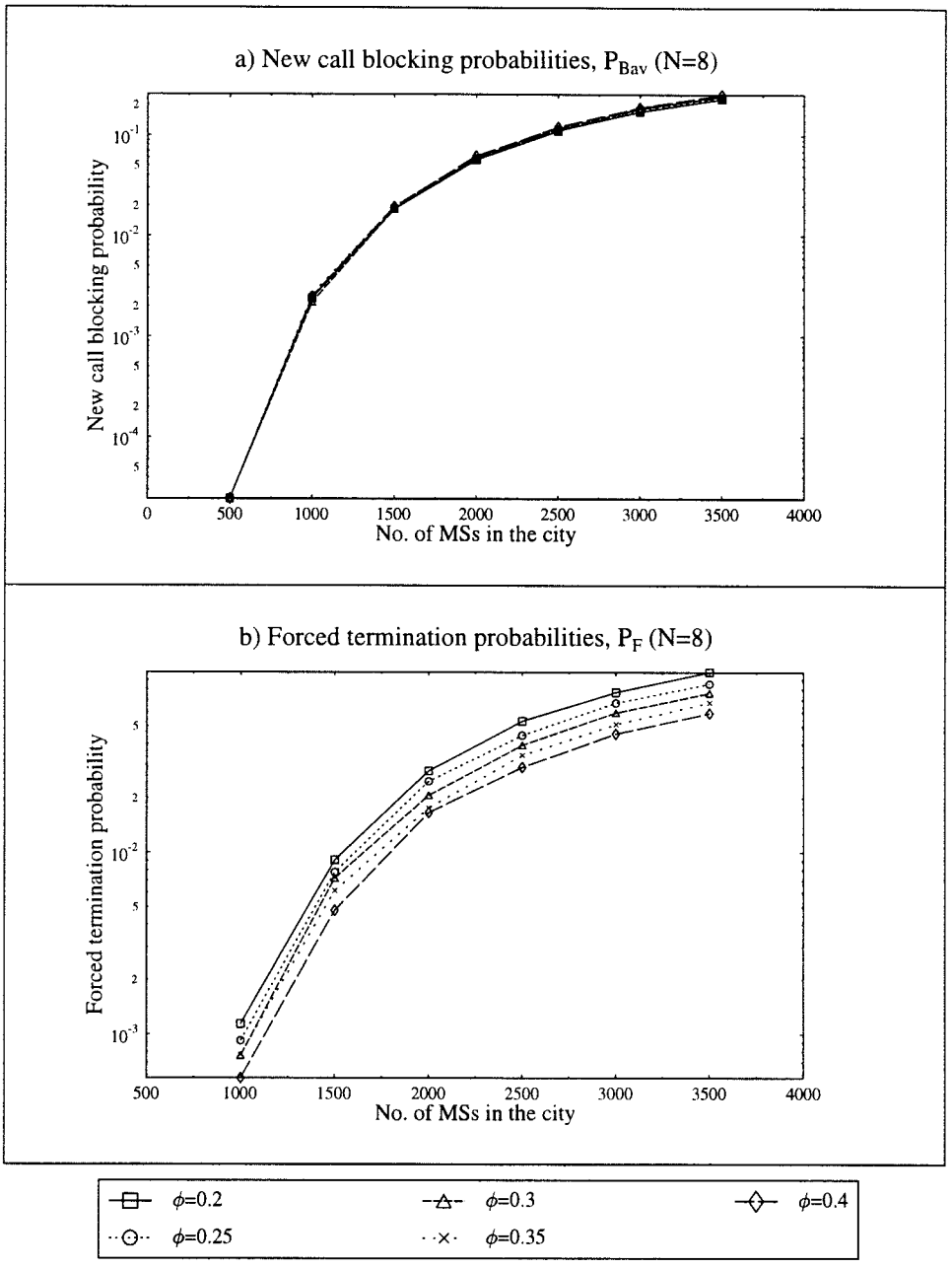

Figure 2.16: a) New call blocking probabilities and b) forced termination probabilities for HO queueing scheme, with MS mobility of 1 m/s and 8 channels per BS.

2.2.3 Conclusions

We have shown that both the HO guard channel and the HO queueing schemes operate more efficiently when the HO activities are low. For comparison, the results from the two schemes are plotted on the same graph shown in Figure 2.17 and 2.18 for the MS speed of 6 m/s and 1 m/s respectively. The results shown are for a system that has eight channels per BS. The solid lines shown in the Figures represent the HO guard channel scheme with N_h = 0, 1, 2 and 3. The dotted lines represent the HO queueing scheme with ϕ = 0.2, 0.25, 0.3, 0.35 and 0.4. For the ranges of ϕ simulated, the forced termination probabilities of the HO queueing scheme are close to those obtained from the HO guard channel scheme with N_h between 1 and 2. However, the corresponding new call blocking probabilities are significantly higher in the HO guard channel scheme. Consequently the HO queueing scheme offers a better trade-off between the new call blocking probability and the forced termination probability than the HO guard channel scheme does. However, the value of ϕ is restricted and not easily controlled in practice. In addition the reduction of the forced termination probability offered by the HO queueing scheme is small. The HO guard channel scheme, on the other hand, offers a large reduction in the forced termination probability, although accompanied by a large increase in the new call blocking probability. Also, in practice, the HO guard channel scheme is easier to implement than the HO queueing scheme.

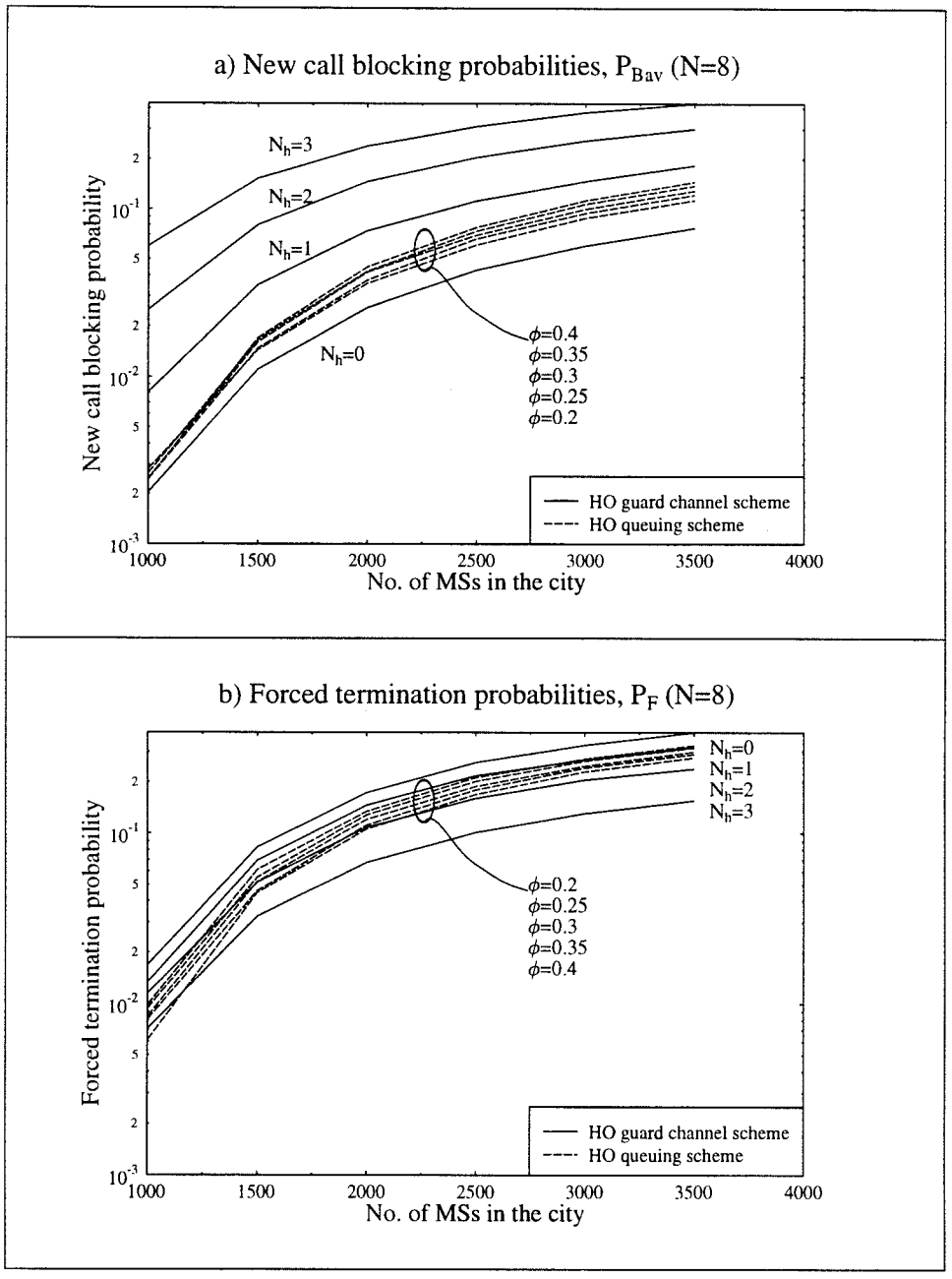

Figure 2.17: a) New call blocking probabilities and b) forced termination probabilities for the HO guard channel scheme and the HO queueing scheme, with MS mobility of 6 m/s and 8 channels per BS.

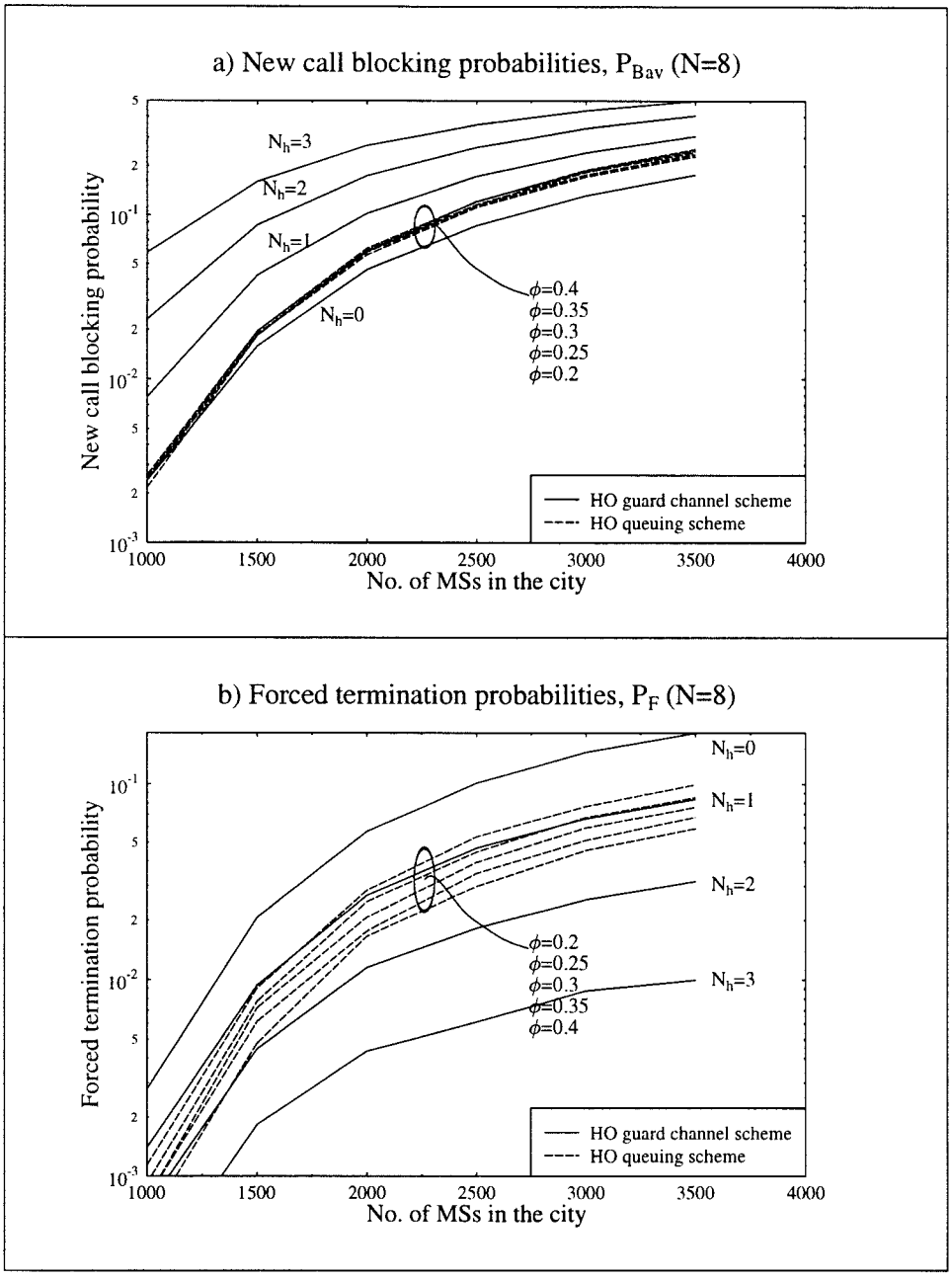

Figure 2.18: a) New call blocking probabilities and b) forced termination probabilities for the HO guard channel scheme and the HO queueing scheme, with MS mobility of 1 m/s and 8 channels per BS.

2.3 Base Station Selection Algorithms

In an overlapping area, where a mobile can receive sufficient signal power from more than one BS, the choice of BS used to communicate with the mobile affects the teletraffic performance of the system. We will study three BS selection algorithms. The first one is known as the directed retry [61, 35], and the other two we name as the Base Station Load Equalisation (BSLE) and Rearrangement Upon Blocking (RAUB) [40]. The BSLE system regularly checks the number of available channels of all BSs in the vicinity of the mobile, and informs the mobile to change its BS when another BS has more capacity. The RAUB system, on the other hand, only rearranges the BS and mobile connections when another call would otherwise be lost.

We use the same city layout as before, that is, a rectilinear city with six by six building blocks and BSs placed at the centres of the road intersections. The HO guard channel scheme is employed to improve the forced termination probability. Each BS has eight channels and the number of guard channels, N_h, is one. The mobiles are travelling at a fixed speed of 6 m/s.

2.3.1 Directed Retry

Directed retry recognises the blocking of a call, and searches for alternative BSs to handle the call. The performance of the directed retry scheme is used as the benchmark for our other two algorithms. Users residing in the overlapping areas benefit from the retry algorithm. However, the retry facility does not enhance service to users residing in non-overlapping areas. We now describe the new call set-up and call maintenance procedures used in the retry process.

New Call Set-up procedure Each MS monitors all known broadcast control channels (BCCH), and measures their respective signal strengths. BSs that can provide acceptable signal strength to the MS are eligible for connection. A call request is made to the BS that provides the strongest signal. If this BS is able to serve the call a connection is made. Otherwise, the MS will make a second request to the next strongest BS, and so on. If none of the covering BSs can serve this MS, the call is blocked.

Call Maintenance procedure A MS continues at regular intervals, here every second, to measure all known BCCH signal strengths. It reports the measurements to the network via the serving BS. When a MS exits from its serving cell, a HO procedure is initiated. We refer to this type of HO as level-1 HO. The network selects the new BS using the same criteria as in the set-up procedure. If the handover is successful, the MS will re-synthesis to the newly assigned radio channel. If the HO request fails, the call is forced to terminate and is recorded as a dropped call.

2.3.2 Base Station Load Equalisation (BSLE)

The BSLE [64] scheme requires the system load, i.e., the number of channels occupied, in all covering BSs to be known for call set-up and maintenance procedures. New calls that are generated in the overlapping areas are made to the BS with the most available channels. Channel re-assignment is allowed if the current serving BS is no longer the least loaded. As a consequence, we introduce an extra level of handovers, which we call level-2 HOs. Level-1 HO takes place when a MS reaches the border of its serving cell. A new BS must be available to serve this roaming MS, otherwise the call is dropped. Level-2 HO, on the other hand, will never result in a dropped call as it is basically a reassignment of available channels. This algorithm minimises the instantaneous variation in the loading of the BSs, thereby minimising the number of occurrences of intermittent teletraffic hot spots.

New Call Set-up procedure Each MS measures all known BCCH signal strengths and reports its measurements to the network. The network then makes the decision on which BS will be used based on the respective BS loadings. The BS with the least loading is assigned to serve this MS. If the loadings are the same, then the one with the strongest received signal level will serve this MS. This procedure minimises the interference level.

Call Maintenance procedure A MS continues to report to the network, every second, the identities of the covering BSs and their respective received signal strengths. The network then decides which is the 'best BS' to serve this MS based on the reports available at this instant. The BS selection is made on the same basis as used in the set-up procedure described above.

If the MS resides in an overlapping region it will be instructed to switch to another BS that has more capacity.

2.3.3 Re-Arrangement upon Blocking (RAUB)

The BS selection procedure in the RAUB scheme is also based on the BS loadings. Unlike BSLE, however, it does not attempt to equalise the BS loadings. It invokes level-2 HO to re-arrange channels only when failure to do so would result in a new call being blocked, or that a call in progress would be dropped. In addition to the new call set-up and call maintenance procedure, the RAUB scheme has an *assistance* procedure. This procedure is responsible for invoking a level-2 HO, and it is initiated by the network. RAUB invokes a smaller number of HOs (level-1 and level-2) than BSLE, thereby decreasing the amount of control traffic required.

New Call Set-up procedure This is the same as in the BSLE scheme, except that when all covering BSs have no available channels, the call is not necessary blocked. In this case, an *assistance* procedure is invoked. This procedure attempts to make a level-2 HO for an existing MS served by the BS, so that a connection can be cleared from the current saturated BS allowing the new mobile to be accommodated. If this fails, the new call is blocked.

Call Maintenance procedure In contrast to the BSLE scheme, a MS keeps the same channel while within the serving BS's coverage area. When the MS leaves its serving cell's coverage area, it initiates a level-1 HO. The selection method for the new BS to continue the call is the same as for RAUB's new call set-up method. The network will invoke the *assistance* procedure if none of the BSs can serve this roaming MS. If the *assistance* procedure fails to free an existing connection, the call will be dropped.

Assistance procedure Suppose a MS resides in the non-overlapping area of BS X, and BS a, b, c and d are the four neighbouring BSs as shown in Figure 2.19. If this MS requires a connection to BS X and BS X currently does not have any vacant channels, the network must then invoke the assistance procedure in order to free up a channel from BS X. The first task is to identify

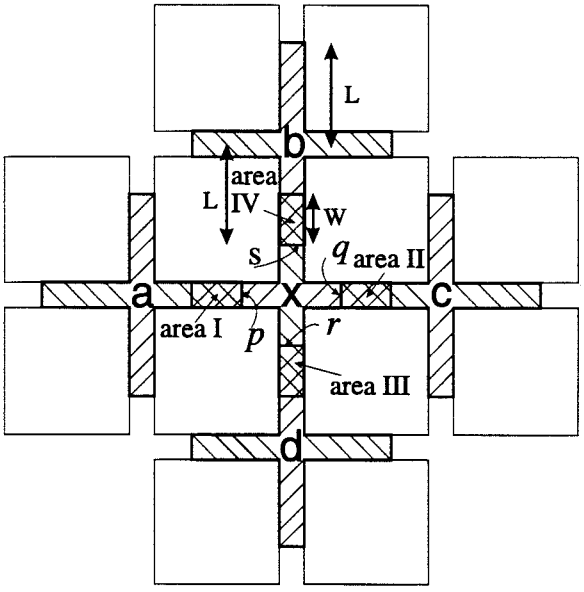

Figure 2.19: Radio coverage of five neighbouring microcells

the neighbouring BSs. BS X will then be instructed to examine each of its connected MSs. These MSs will report back to BS X if they are in any of the overlapping areas. If more than one MS resides in the overlapping areas, the MS that can communicate to the BS that has the least loading will be chosen for level-2 HO. If there are more than one MS that meets this requirement, then we choose the MS whose channel holding time with BS X is the longest. After invoking level-2 HO, BS X can then use the just vacated channel to serve the otherwise blocked MS. The assistance procedure fails if none of the MSs that are currently connected to BS X reside in the overlapping areas, or all neighbouring BSs are fully loaded.

If the requesting MS resides in the overlapping area between BS X and Y, then BS a, b, c, d, e and f are the six neighbouring BSs as shown in Figure 2.20. The assistance procedure in this case is more complex but the principle remains the same. Both BS X and BS Y will examine their connected MSs' availability for level-2 HO. If level-2 HO can be made to BSs a or b or f, then BS X can use the just vacated channel to serve the requesting MS. Similarly, if a level-2 HO can be made to BSs c or d or e, BS Y can serve the requesting MS.

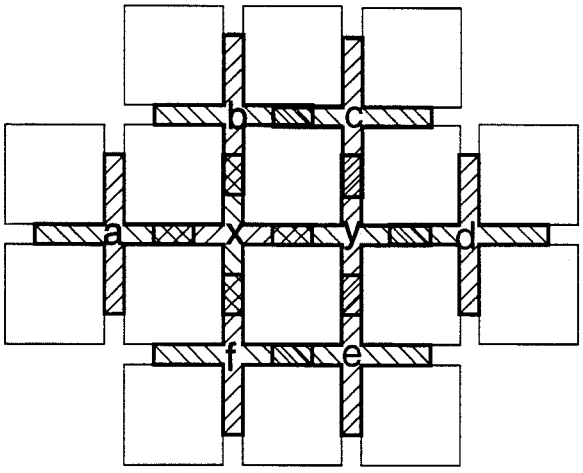

Figure 2.20: The six neighbouring microcells around cell x any y

2.3.4 Results

The performances of the three algorithms were evaluated using computer simulation. Figure 2.21 shows the average number of level-1 plus level-2 HOs a successfully connected user will experience for different levels of channel utilization. The channel utilization, ρ, is the proportion of time a channel is being used, and it can be expressed as,

$$\rho = \frac{A_c}{N}, \tag{2.35}$$

where A_c is the carried traffic of the BS whose total number of channels is N.

The MSs in the BSLE system experienced the highest number of HOs per call, while the MSs in the RAUB system experienced nearly the same number of HOs as the MSs in the directed retry system did. The number of HOs experienced by a successfully connected MS decreased for all three systems when the channel utilization level was increased. This was because there were more calls in progress that were dropped as the system reached saturation.

Figure 2.22 shows the HO failure probability. Note that the HO failure probability differs from the forced termination probability. The former is the probability that a HO call will fail, and the latter is the probability that a

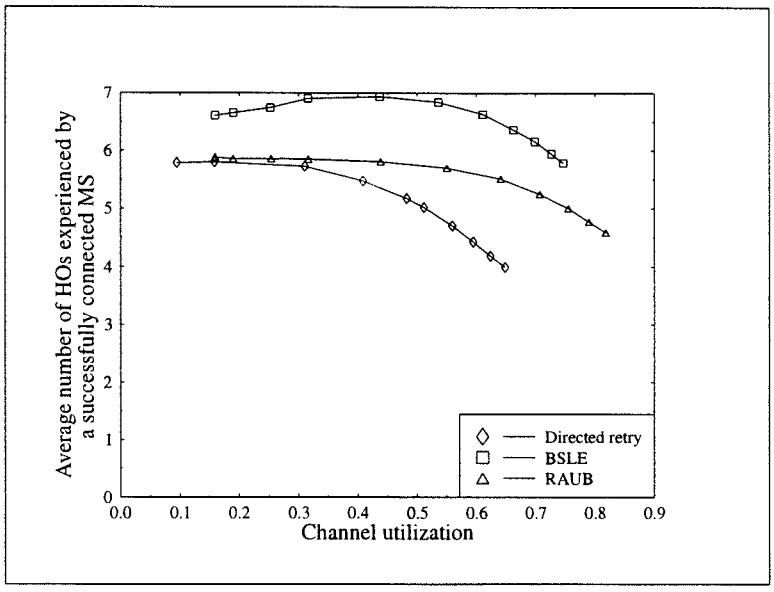

Figure 2.21: Average number of level-1 plus level-2 HOs a successfully connected user experiences

successfully connected call will be forced to terminate. The RAUB system gave the best results, followed by the BSLE system.

Figure 2.23 shows the average new call blocking probabilities for all three systems. Figure 2.24 displays the corresponding forced termination probabilities. For a new call blocking rate of 2%, the directed retry system, the BSLE system and the RAUB system were operated at channel utilization levels of 0.38, 0.5 and 0.64, respectively. Using the directed retry system as the benchmark, the BSLE system and the RAUB system improved the channel utilization by 32% and 68%, respectively. For the same level of channel utilization of 0.38, the forced termination probabilities for the directed retry system, the BSLE system and the RAUB system were 4.5%, 0.45% and 0.3%, respectively.

2.3.5 Conclusions

Both the BSLE and the RAUB systems gave better new call blocking probabilities and forced termination probabilities than the directed retry system.

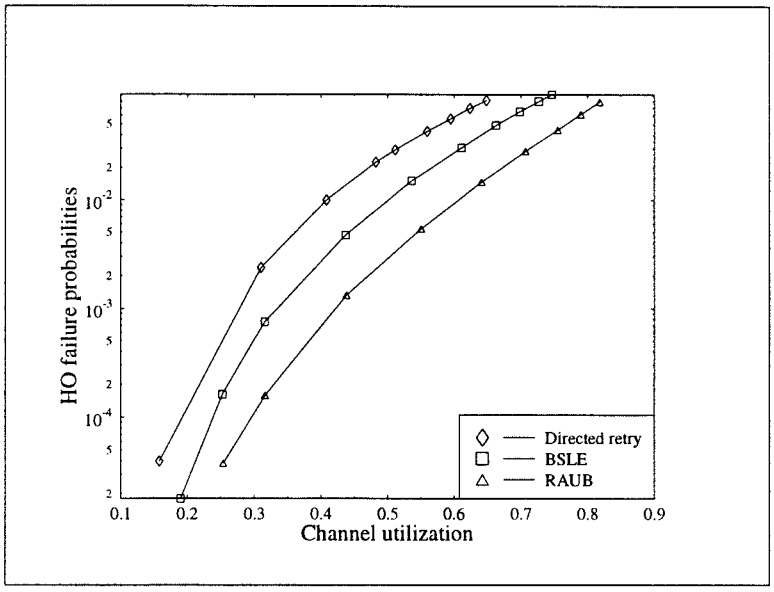

Figure 2.22: Probability that a handover call fails

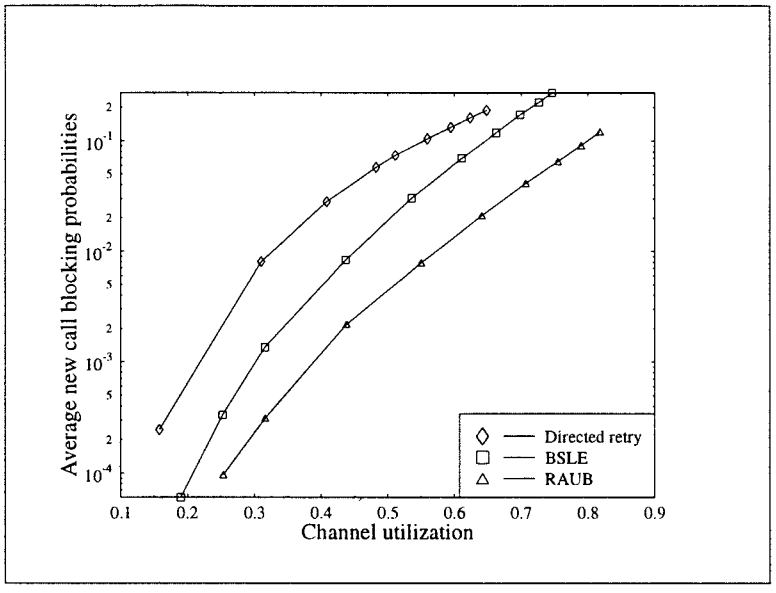

Figure 2.23: Average new call blocking probabilities at different levels of channel utilization

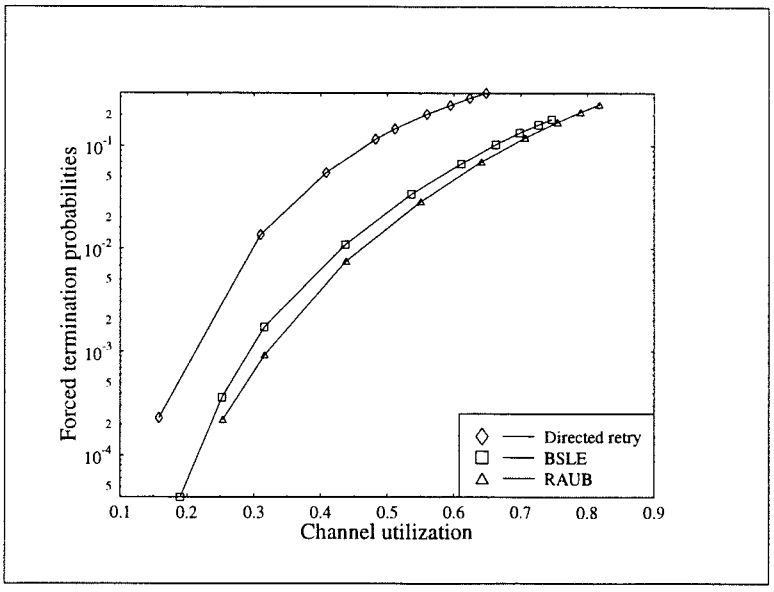

Figure 2.24: Forced termination probabilities of a successfully connected call

The BSLE system achieved better blocking rates at the expense of increased HO traffic. Impressively, the RAUB system gave the best blocking rates over the other two systems without introducing any more HO traffic.

Chapter 3

Moving Base Stations (MBSs) with Fixed Channel Assignment (FCA) Scheme

The task of pre-designing a network of BSs is referred to as cell tailoring. In rural areas, the density of BS sites is low. These BSs transmit with high power in order to provide large radio coverage areas, known as macrocells. Smaller cells can be employed in areas where user demand is expected to be high. For example, microcells can be employed in urban outdoor areas while picocells provide indoor communications. There is a trade-off between spectral efficiency and the cost of installing extra BS sites. In previous chapters, we have studied the performance of street microcells where the teletraffic demand was assumed to be uniform throughout the city. However, in practice teletraffic demand varies in both space and time. One approach to accommodate a variable traffic density is to employ microcellular clusters with overlaying macrocellular clusters [7, 65]. The majority of the teletraffic will be carried by the microcells, but excess teletraffic generated by the microcells will be carried by the macrocells.

Our approach here is to allow BSs to have mobility to move into areas where extra capacity is needed. We call them moving base stations (MBSs). Fixed base stations (FBSs) that have permanent fixed sites are still needed to provide the basic service. MBSs are mounted on vehicles, such as buses and taxis. Assuming teletraffic demand is related to vehicular traffic density, the

MBSs will often be found in or near teletraffic hot spots. A power control scheme is employed to reduce cochannel interference. Effectively, the cell tailoring procedure is done dynamically in real time.

A method to download the data from the MBSs back to the fixed network is necessary. One approach is to use another radio link to carry the data from the MBSs back to the fixed network via some collection points. The collection points, or nodes, can be the FBSs, an overlaying macrocell, or a set of repeaters using high frequency line-of-sight links. The objective of our work is to study the benefits of employing MBSs. In doing so, we hope our findings will encourage further research and development to bring about the realisation of our MBS system.

One may argue that if the MBSs need radio links to network nodes to download the data, then why not let the MSs access these nodes directly. First of all, MBSs can afford to be bulky as they are installed on vehicles. In addition car batteries are readily available to the MBSs for high power transmissions that are required if the network nodes are macrocellular BSs located at far distances. Handheld MSs have neither of these features. While the MSs use omni-antenna, the MBSs could use phase array with steerable beams. If the MBSs are mounted on buses, the additional height would also mean less shadow fading.

In previous chapters we adopted a simple model where we assumed perfect signal reception inside the cell area and no signal reception outside the cell's borders. However when the BSs have mobility, the distance between two interfering BSs can no longer be pre-determined. Thus a pathloss model must be incorporated into the program in order to calculate the received signal strength and the cochannel interference in real time. In the next section, we will describe the pathloss model we adopt. In section 3.2, we will describe the features of our simulation program for the MBS system. In the final section of this chapter we will present a simple system where the spectrum is allocated separately to the FBSs and the MBSs. The spectrum allocated to the FBSs is partitioned into groups (channel sets). Each FBS in the same cluster has a different set of channels. The same spectrum is then reused at other clusters. Each FBS can only use channels from its own group. This method of spectrum allocation is called fixed channel assignment (FCA).

The MBSs have their own spectrum. Each MBS has its own uniquely assigned

group of channels, that are not reused by other BSs in the city. We introduce this hypothetical system solely for the purpose of making some preliminary observations, knowing that this method of spectrum allocation is impractical. As each MBS has its own channel set, its presence does not interfere with other FBSs or MBSs in the vicinity. Thus it allows us to study the teletraffic characteristics of the MBSs, in the absence of cochannel interference. A more sophisticated channel assignment scheme will be studied in chapter 4, where the FBSs and the MBSs share the same spectrum.

3.1 Pathloss Model and System Configuration

3.1.1 Pathloss Model

In a microcellular network, BS antennas are mounted well below the urban skyline. This leads to very different radio propagation characteristics comparing to a conventional macrocellular system that installs BS antennas on high towers. Harley reported his measurements for short distance, low antenna height signal attenuation in reference [66]. His measurements showed that the extrapolation of the formulas used in a macrocellular system for low antenna heights, short distance areas were invalid. His measurements were made with the BS antenna installed at a height of 5 to 20 metres while the MS antenna was fixed at a height of 1.5 metres. The measurements made covered a distance of 1km in a line-of-sight (LOS) path at both 870.15 MHz and 1.8 GHz. Bultitude and Bedal reported their results of wide-band measurements made under similar conditions [67]. Their paper includes cumulative distribution functions for envelop fading, as well as delay spread and frequency correlation statistics. Both Rustako and Erceg used multi-ray models to predict microcellular propagation [68, 69]. Their results were compared with their field measurements. Rustako made his measurements on LOS transmissions for transmitting powers of 1 watt and 20 mW for narrow-band signals at 900 MHz and 11 GHz, respectively. Erceg measured both the LOS and out-of-sight (OOS) signal attenuation when transmitting a direct sequence (DS) spread spectrum signal at 1956 MHz with a chip rate of 24 Mb/s. Berg proposed an empirical path loss model, a slow fading model and a fast fading model in reference [70]. Although his proposed models are simple enough for simulation purposes, they require parameters from field measure-

ments. All of the reported measurements give similar characteristics. The path loss seems to roll-off at a slope of 20 dB/decade for distances close to BS antenna. Then at some breakpoint, the slope increases to 40 dB/decade. For OOS case, there is a sudden drop of 15 to 25 dB when the BS antenna becomes OOS. In addition, the slope increases to 40 to 80 dB/decade. These characteristics are outlined in reference [71].

Due to computational cost, our simulation model assumes that path loss is the only form of signal attenuation. Fast fading due to the multipath effect is assumed to be taken out by the equaliser, forward error correction (FEC), interleaver, ..., etc. Diffraction loss at corners is included. We adopt the pathloss model used by Erceg [69], which was modelled theoretically in reference [72]. It is described below.

For a given BS antenna height, h_b, and MS antenna height, h_m, transmitting a radio wavelength of λ, the breakpoint distance, R_b, can be calculated as follows,

$$R_b = \frac{4h_b h_m}{\lambda} \quad . \tag{3.1}$$

Line-of-sight (LOS) pathloss in dB, PL_{los}, at a distance, r, from the transmitter is

$$\mathrm{PL}_{los}(r) = \begin{cases} L_b + 20\log_{10}\dfrac{r}{R_b} & 1 \le r \le R_b \\ L_b + 40\log_{10}\dfrac{r}{R_b} & r > R_b \end{cases} \quad , \tag{3.2}$$

where $L_b = |20\log_{10}(\lambda^2/8\pi h_b h_m)|$. The PL_{los} for $r < 1$ is undefined.

Out-of-sight (OOS) pathloss in dB, PL_{oos}, at a distance, d_1, from the transmitter to the corner and distance, d_2, from the corner to the receiver is

$$\mathrm{PL}_{oos}(d_1, d_2) = \mathrm{PL}_{los}(d_1) + 20 + 40\log_{10}\left(\frac{d_1 + d_2}{d_1}\right) \quad . \tag{3.3}$$

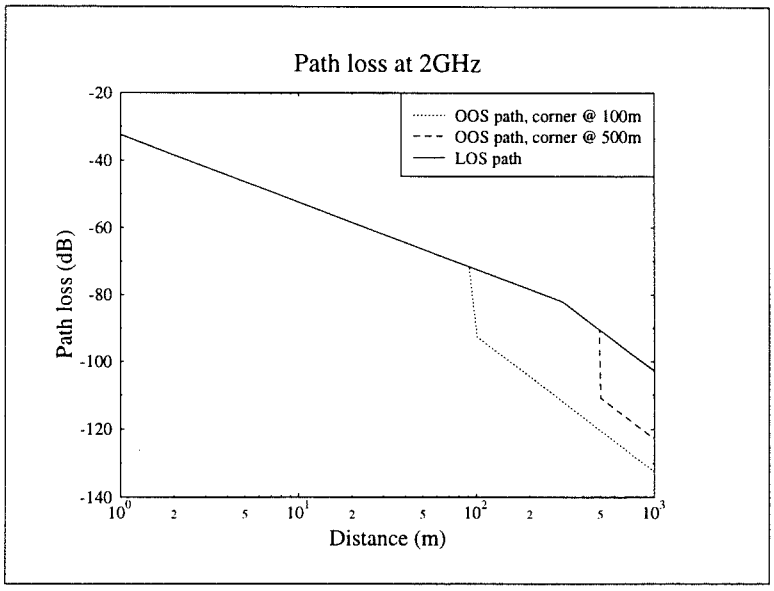

Figure 3.1: Path loss at 2GHz

Employing parameters, h_b=7.6m, h_m=1.5m and transmission frequency of 2 GHz, the breakpoint distance, R_b, is 304 metres and the path loss at one metre distance is 32 dB.

Figure 3.1 shows the path loss in negative values for a transmission frequency of 2 GHz. Three curves are shown in the figure. One of the curves represents the path loss experienced by the receiver when it moves away from the transmitter along a LOS path. The other two curves show the path losses when the receiver turns to travel along a side street located at a distance of 100m and 500m, respectively, from the transmitter, and becomes OOS from the transmitter.

For a given transmitter power T, the received power R can be calculated from,

$$\mathrm{R} = \mathrm{T} - \mathrm{PL} \quad . \tag{3.4}$$

PL is the path loss value calculated from Equation 3.2 for the LOS case, and Equation 3.3 for the OOS case.

3.1.2 City Cell Scenario and System Configuration

The equivalent of a hexagonal cellular structure for microcells is the rectilinear city grid. The roads of the grid are bordered by square cross-sectional buildings, each of 100m length. The roads are 20m wide, and have four lanes supporting two-way traffic. The fixed BS (FBS) transceivers are placed at the middle of each road intersection. They are mounted at lamp-post height, i.e., well below the urban skyline, and therefore the height of the buildings are of no consequence as we assume that there is negligible diffraction over the roof-tops. The radio coverage of each transceiver is confined by the topology of the roads producing microcells in the shape of a cross.

In our simulations, we allow the city to wrap around from the East-most edge to West-most edge, and from South-most to North-most edges in order to avoid edge effects. For example, if a user reaches the East-most edge of the city, he will re-enter the city from the West-most edge. The same argument applies to radio coverage.

As in GSM, time-division multiple access (TDMA) with frequency-division duplex (FDD) is employed. Radio channels are grouped to form channel sets. Control signalling is not simulated. In addition, we only consider traffic initiated by MSs and destined for the PSTN/ISDN network. Mobile-to-mobile and PSTN/ISDN network-to-mobile traffic are not considered.

Fixed channel assignment scheme (FCA) is used for the FBSs. In order to ensure that both the uplink and the downlink signal-to-interference ratios (SIRs) are within the specified system parameter at all times, the worst cases of the two SIRs must be calculated. We shall examine a two-cell cluster and a four-cell cluster configuration. Their corresponding uplink and downlink SIRs for the worst cases will be determined, and the most appropriate configuration will be chosen for our future work.

Notice that each BS is surrounded by four LOS cochannel BSs as we place BSs at the road junctions. Although we allow the city to wrap around in order to avoid edge effects, the size of the simulated city must be large enough to include these four significant cochannel BSs. Therefore the simulated city must be at least six by six building blocks for a two-cell cluster configuration. Similarly a minimal size of 12 by 12 building blocks is needed for a four-cell cluster configuration. The computational cost increases dramatically as the cluster size increases.

The minimum SIR a system can tolerate depends on a number of factors, e.g. the multiple access scheme, the modulation method, ... , etc. As we do not simulate the physical layer of the system, i.e., the underlying modulation scheme, interleaver, channel coding, equalisation, ... , etc, the value for the minimum SIR is chosen arbitrarily. A value that is small enough to permit the smaller cluster size, and yet reasonable in practice is required. The following system parameters are chosen: minimum SIR, $\mathrm{SIR_{min}}$, 10 dB; maximal power available at the transmitter, $\mathrm{Tx_{max}}$, 0 dBm; receiver threshold, $\mathrm{Rx_{min}}$, -70 dBm.

Figure 3.2 shows a two-cell cluster configuration. Due to the 20 dB power drop round the corner, we assume the interference contributed by OOS FBSs is negligible. Figure 3.3 shows the FBS, FBS_X, and its four closest LOS cochannel neighbouring FBSs, FBS_O, FBS_P, FBS_Q, and FBS_R. These cochannel FBSs are 240 m apart. Interferences caused by other cochannel FBSs are assumed to be negligible. Substituting receiver threshold, $\mathrm{Rx_{min}}$, for R and maximum transmission power, $\mathrm{Tx_{max}}$, for T into Equation 3.4, yields a distance of 75.5 metres, that is the length of each arm of the cross-shaped microcells, L.

In Figure 3.3, the mobile, MS_X, is connected to the FBS, FBS_X. The worst interference on the uplink channel of MS_X happens when the same channel is used by the four LOS neighbouring FBSs, FBS_O, FBS_P, FBS_Q and FBS_R, to serve the mobiles, MS_O, MS_P, MS_Q and MS_R respectively. The most severe interference is caused when these four interfering mobiles are at the borders of their cells that are nearest to FBS_X. The wanted uplink signal from MS_X is weakest when MS_X is at one of the borders of FBS_X. Figure 3.3 shows the positions of the mobiles that give the worst uplink SIR. Interferences from other mobiles residing in other cells are assumed negligible.

Using Equations 3.2 and 3.4, the wanted received uplink/downlink signal strength can be calculated as

$$\begin{aligned} \mathrm{Tx}_{max} - \mathrm{PL}_{los}(r = L) &= -70 \text{ dBm} \\ &= 10^{-7}\mathrm{mW} \quad . \end{aligned}$$

The total uplink interference from the four interfering mobiles is

$$4 \times 10^{(\mathrm{Tx}_{max} - \mathrm{PL}_{los}(r=240-L))/10} = 8.4 \times 10^{-8}\mathrm{mW} \quad ,$$

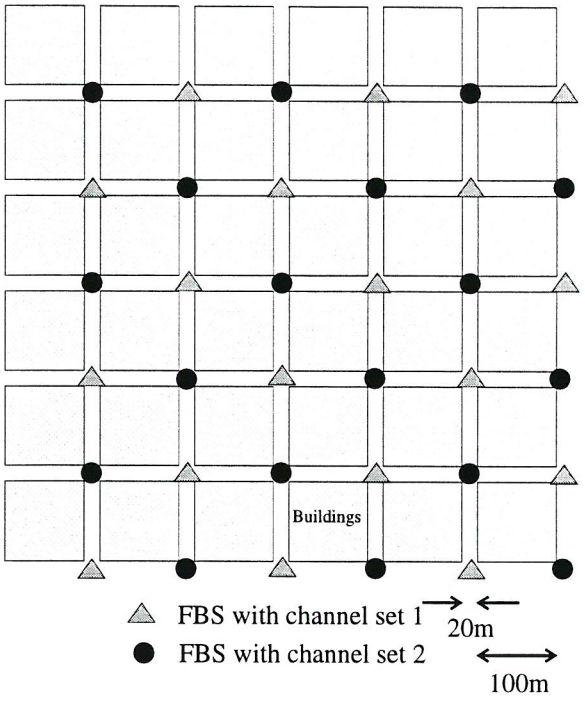

Figure 3.2: Two-cell cluster configuration

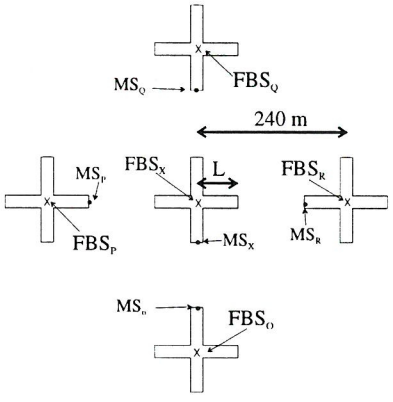

Figure 3.3: Worst uplink/downlink SIR scenario in a two-cell cluster configuration

yielding a worst uplink SIR of 0.76 dB.

The worst downlink SIR occurs when the wanted mobile is at the border of its serving cell as shown in Figure 3.3. Using Equations 3.2, 3.3 and 3.4, the total downlink interference from the four interfering FBSs can be calculated as

$$\begin{aligned} & 10^{(\mathrm{Tx}_{max}-\mathrm{PL}_{los}(r=240-L))/10} \\ & \quad + 10^{(\mathrm{Tx}_{max}-\mathrm{PL}_{los}(r=240+L))/10} \\ & \quad + 2 \times 10^{(\mathrm{Tx}_{max}-\mathrm{PL}_{oos}(d1=240,d2=L))/10} \\ & \qquad\qquad = 2.6 \times 10^{-8}\mathrm{mW} \quad . \end{aligned}$$

This gives a worst downlink SIR of 5.8 dB. Both the uplink and the downlink SIRs are lower than, 10 dB, the value we specify for the simulated system. Thus the two-cell cluster configuration is inadequate in our street microcell scenario. We will now repeat this procedure for a four-cell cluster configuration as shown in Figure 3.4.

Figure 3.5 shows three tiles of mutually interfering cells. The middle cell, coloured black, is the one being measured. All of the surrounding cells shown in Figure 3.5 are interfering ones, but only those six shaded cells contribute significant interference.

The worst uplink/downlink SIR occurs when the wanted mobile is farthest from its cell and the interfering mobiles are closest to the interfered FBS (see Figure 3.3). The received power level of the wanted signal is 1×10^{-7} mW. The total uplink interference from the six interfering mobiles, one from each shaded cells shown in Figure 3.5, is

$$\begin{aligned} & 4 \times 10^{(\mathrm{Tx}_{max}-\mathrm{PL}_{los}(r=480-L))/10} \\ & \quad + 2 \times 10^{(\mathrm{Tx}_{max}-\mathrm{PL}_{oos}(d1=120-L,d2=120))/10} \\ & \qquad\qquad = 7.9 \times 10^{-9}\mathrm{mW} \quad . \end{aligned}$$

The total downlink interference from the interfering FBSs of the shaded cells shown in Figure 3.5 is

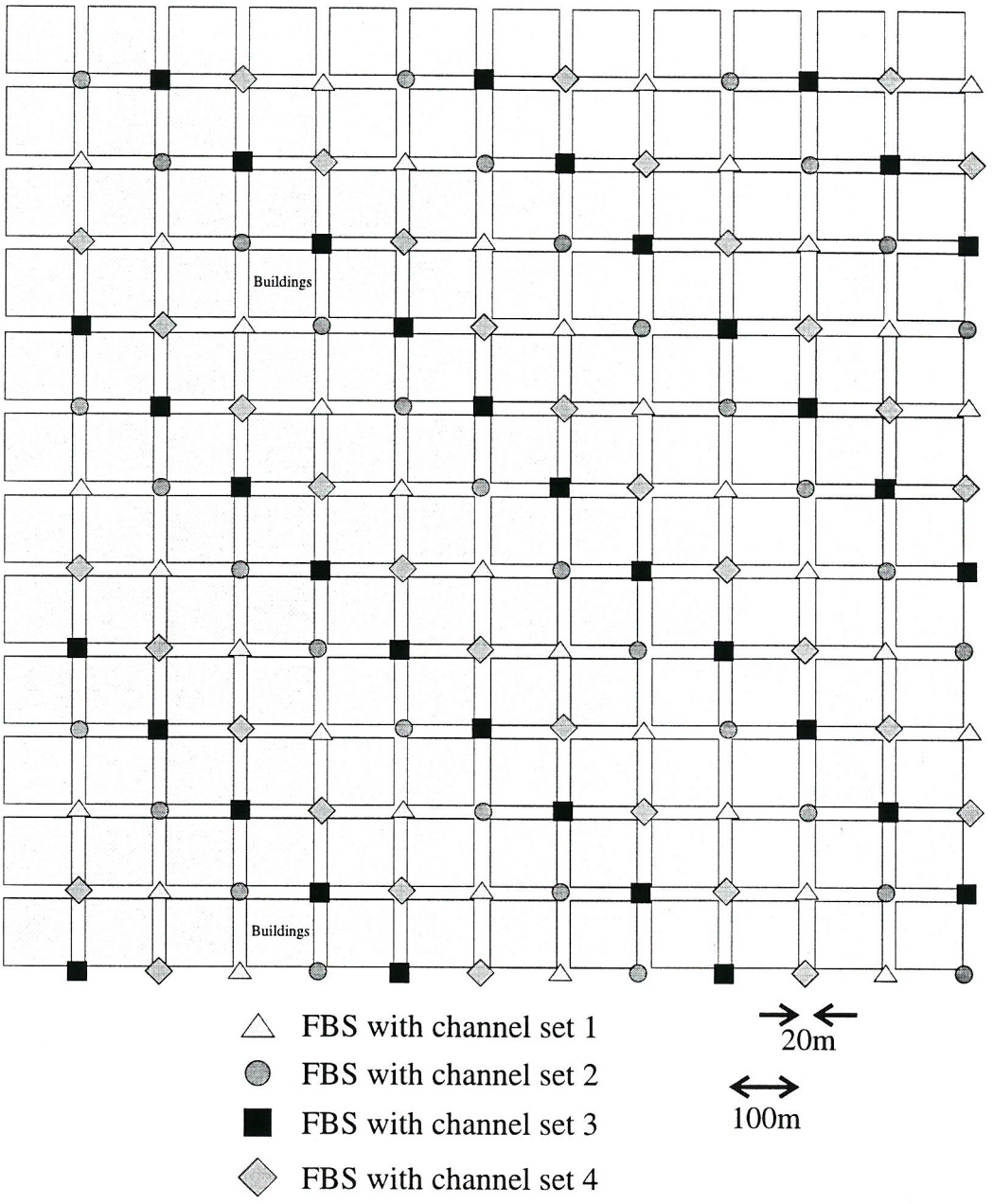

Figure 3.4: Four-cell cluster configuration

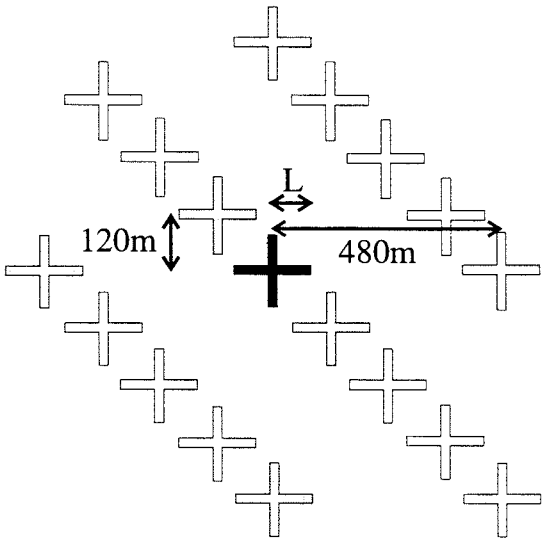

Figure 3.5: The six significant interfering cells in the four-cell cluster configuration

$$
\begin{aligned}
&10^{(\mathrm{Tx}_{max}-\mathrm{PL}_{los}(r=480-L))/10} \\
&\quad + 10^{(\mathrm{Tx}_{max}-\mathrm{PL}_{los}(r=480+L))/10} \\
&\quad + 2\times 10^{(\mathrm{Tx}_{max}-\mathrm{PL}_{oos}(d1=480,d2=L))/10} \\
&\quad + 10^{(\mathrm{Tx}_{max}-\mathrm{PL}_{oos}(d1=120,d2=120+L))/10} \\
&\quad + 10^{(\mathrm{Tx}_{max}-\mathrm{PL}_{oos}(d1=120,d2=120-L))/10} \\
&\qquad\qquad = 2.6\times 10^{-9}\mathrm{mW} \quad .
\end{aligned}
$$

This gives an uplink SIR of 11 dB and a downlink SIR of 15.8 dB. Both of them meet the minimum SIR requirement of our simulated system. Consequently, this four-cell cluster configuration is adopted.

We only consider mobile stations (MSs) housed in vehicles. Each vehicle travels at a constant speed of 6 m/s. When it reaches the junction, we arrange for it to have a probability of 0.8 to continue travelling straight, and a probability of 0.1 of either turning left or right. Each idle user is arranged to generate teletraffic according to a Poisson distribution, with mean rate, λ_{nu}. Call duration is negative exponentially distributed with mean, $1/\mu_c$. Once a call commences a specific call duration is assigned to the mobile. Failure to

Simulated city size	12 × 12 building blocks
FBS cluster configuration	Four-cell cluster
FBS antenna height, h_b	7.6 m
MS antenna height, h_m	1.5 m
Transmission frequency	2 GHz
Maximum transmission power, Tx_{max}	0 dBm
Minimum receiver threshold, Rx_{min}	-70 dBm
Minimum acceptable SIR, SIR_{min}	10 dB
Cell length, L (max. LOS distance for Tx_{max} = 0 dBm and Rx_{min} = -70 dBm)	75.5 m
Vehicular speed	6 m/s
Mean idle time per user, $1/\lambda_{nu}$	20 min
Mean call duration, $1/\mu_c$	2 min

Table 3.1: System parameters

achieve this call duration is logged as a dropped call. Alternatively, when a MS makes a call attempt and there are no available channels the call is said to be blocked. User arrival rates and departure rates are the same for all simulation runs. We vary the offered traffic by altering the number of users present in the city. Table 3.1 summarises our system's parameters.

3.2 Time-driven Simulation Program

A simulation program is written to model a city that consists of 12 by 12 building blocks. Fixed base stations (FBSs) are located at each road intersections. These 144 FBSs are divided diagonally across the city into four groups. Each FBS of the same group is assigned with the same channel set. The simulator uses different colours to distinguish the four channel sets when it displays the radio coverage (path loss less than 70 dB) on the screen. Figure 3.6 shows a snapshot of the simulator's display [1], that shows the radio coverage of those FBSs that are assigned with the purple and the red channel sets, and Figure 3.7 shows those assigned with the blue and the yellow

[1]The display window of the simulator has a dark background and bright foreground. To avoid excessive use of inks during printing, all pictures shown in this thesis are negative images to those captured from the screen of the simulator.

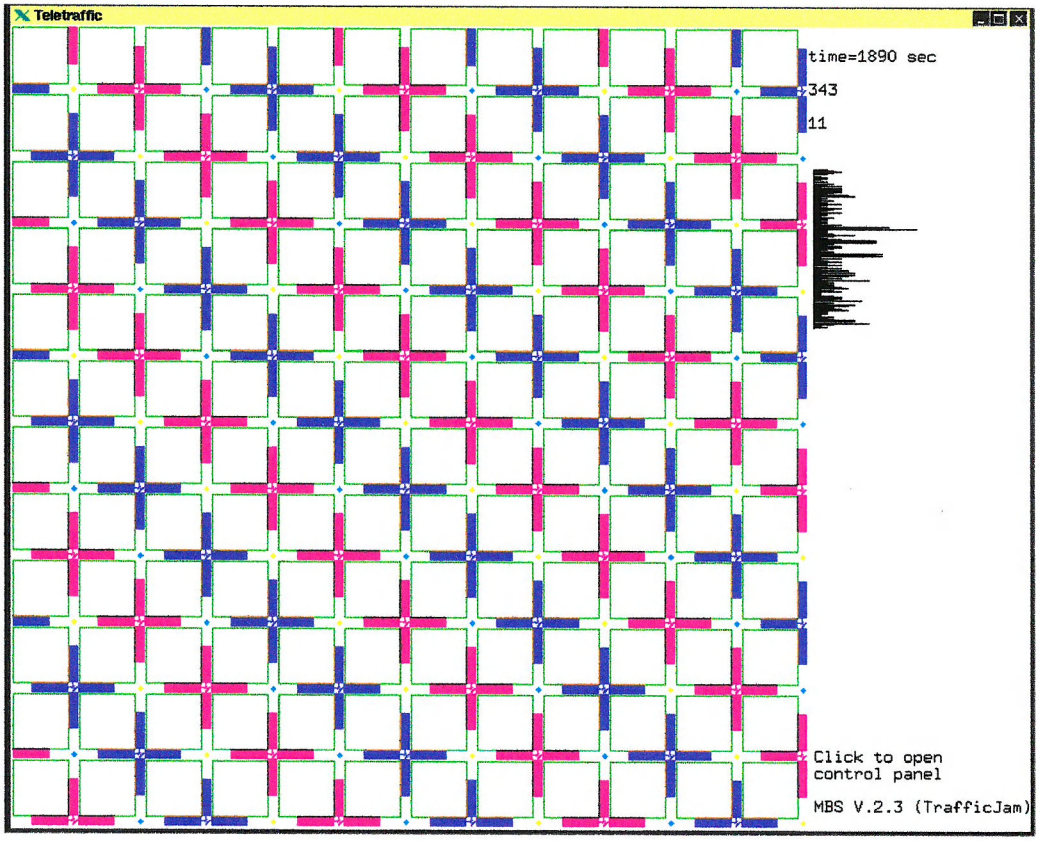

Figure 3.6: Radio coverage of the purple and the red channel sets produced by the FBSs.

channel sets. The locations of the FBSs are marked by dots, and they have the same colour as their assigned channel sets.

In addition to the FBSs, moving base stations (MBSs) are also employed. The MBSs are shown as dots, the same as the FBSs, while the mobile stations (MSs) are represented by tiny pixels. Figure 3.8 shows a snapshot of the simulator's screen, that displays the instantaneous locations of the MBSs and the MSs. Note that the visuals for the FBSs were turned off in that picture.

The simulator is written in C++ with an object-oriented programming style. It is designed to run on the UNIX[2] platform and display on the X Window

[2]UNIX is a trademark of the Open Software Foundation

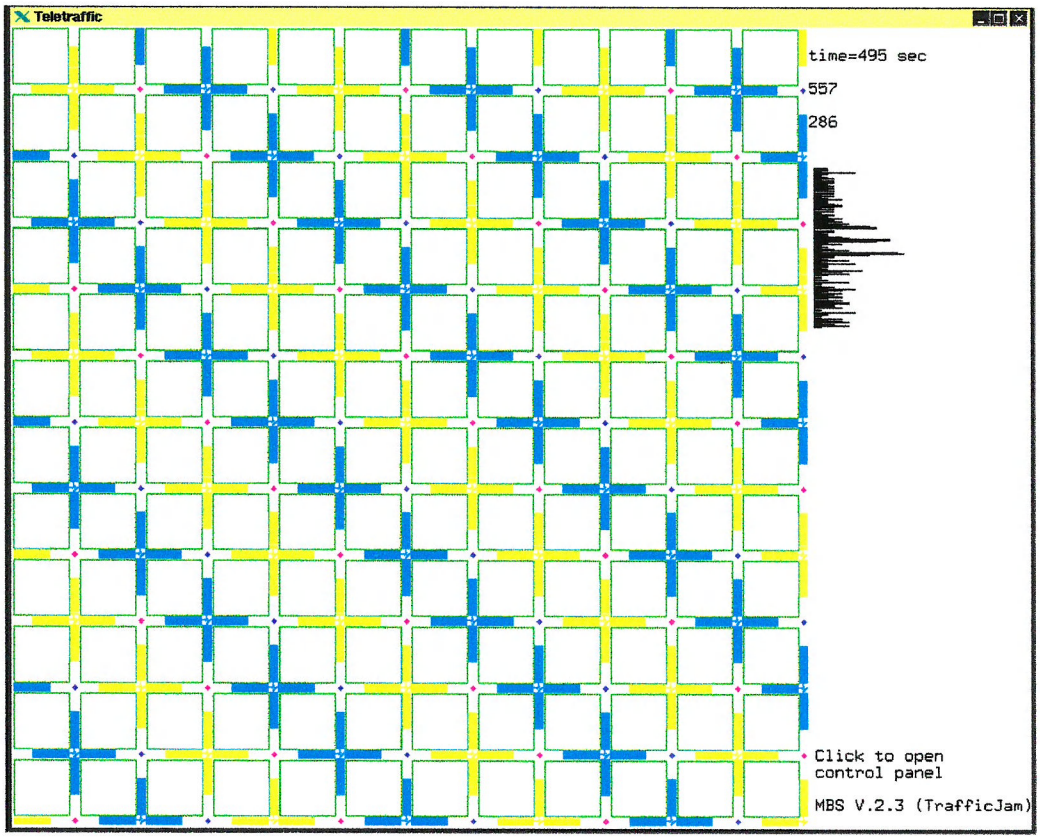

Figure 3.7: Radio coverage of the blue and the yellow channel sets produced by the FBSs.

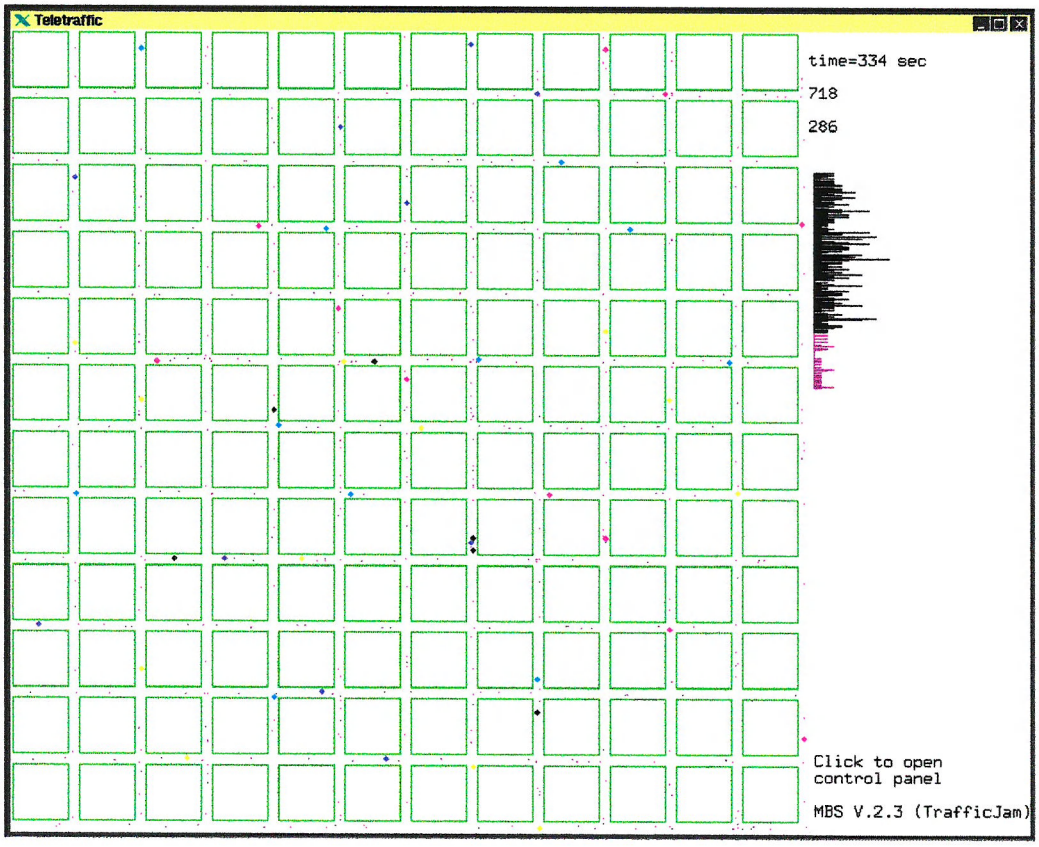

Figure 3.8: An instant of the simulator's display showing the locations of the MBSs and the MSs.

System[3]. The smallest unit of time used in the simulator is one second, and the smallest unit of distance is one metre. The program can run in three different modes; display-mode, transient-mode and steady state-mode.

In display-mode, the state of the simulated system is displayed on the screen in real time. Various display functions are controlled by the two control panels shown in Figure 3.9, namely the main control panel and the radio coverage control panel. The graphical user interface (GUI) is designed using the XForms toolkit[4].

Radio links are displayed in the form of straight lines between the FBS and its MSs as shown in Figure 3.10. The brightness levels of the lines indicate their respective levels of SIR. The radio links between the MBS and its MSs are displayed in a similar way, except for those where both the MBS and the MS are travelling on the same lane. In that case, the radio link is displayed by a zigzag line to give a clearer picture.

Circles of varying sizes are used to represent the teletraffic loadings on all the FBSs as shown in Figure 3.11. The larger the circle the higher the number of users connected to that FBS. This allows us to monitor the spatial distribution of the teletraffic levels across the city. The teletraffic loadings on all the FBSs are also monitored by the histogram on the right hand side of the main window. The locations of the blocked calls and dropped calls are monitored by the simulator and marked by the crosses on the monitor screen as shown in Figure 3.12.

In the transient-mode, the instantaneous traffic carried by the system is recorded for each simulated second. The result can be displayed in a graph with carried traffic versus time. Initially the system starts with zero carried traffic. After a period of time the system settles down. This settling time is a required input parameter when the simulation program runs in steady state-mode. All steady state statistics are recorded after the settling time period. The settling time needs to be measured whenever the system parameters differ (e.g. the MS density, number of MBSs employed, number of radio channels available to the system, ...etc).

The performance of our proposed system is judged by its steady state response. In steady state-mode, relevant statistics for the MBSs and the FBSs

[3]The X Window System is a trademark of The Massachusetts Institute of Technology
[4]Forms Library is Copyright © by T. C. Zhao and Mark Overmars

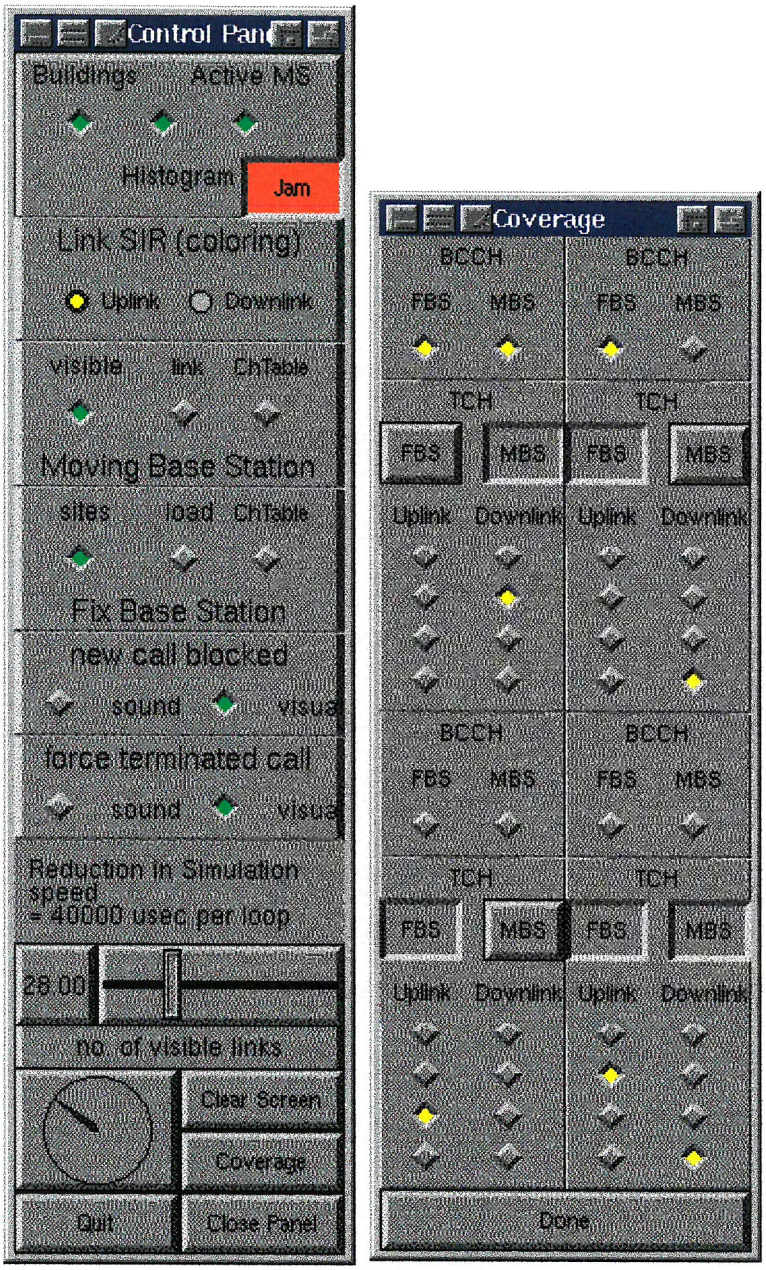

(a) Main control panel **(b) Radio coverage control panel**

Figure 3.9: GUI: The two control panels

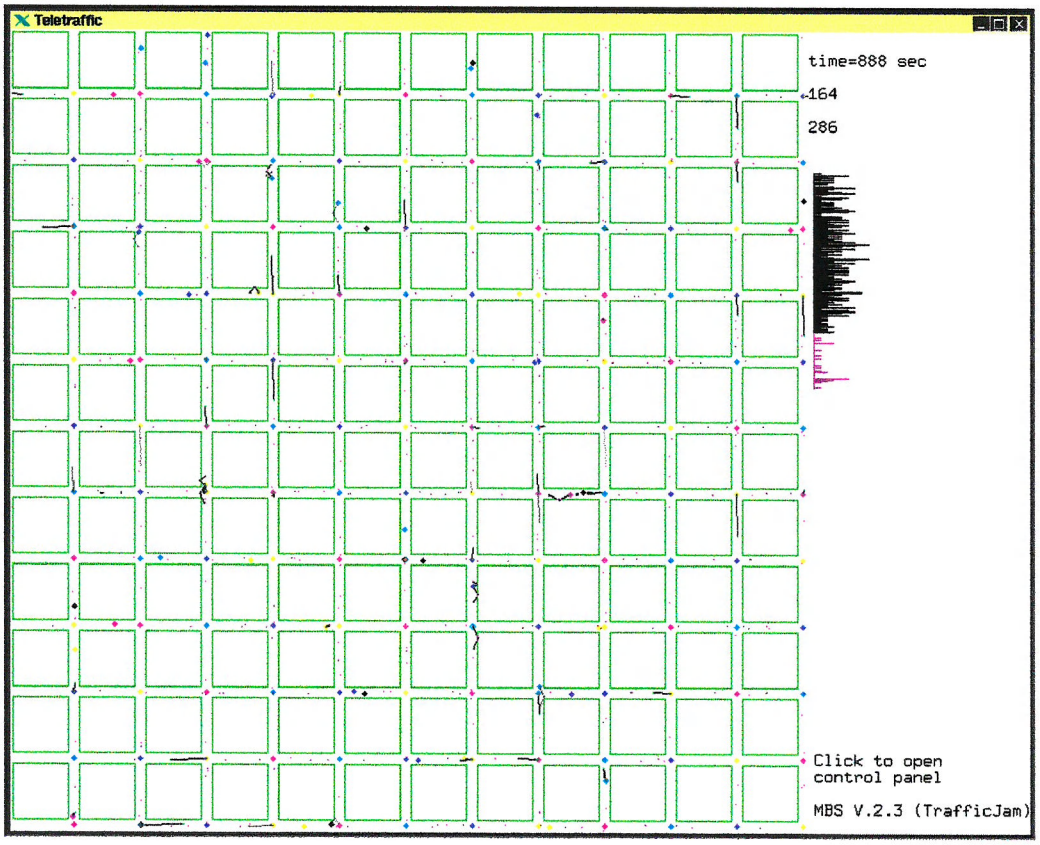

Figure 3.10: Radio links shown by the simulator's display

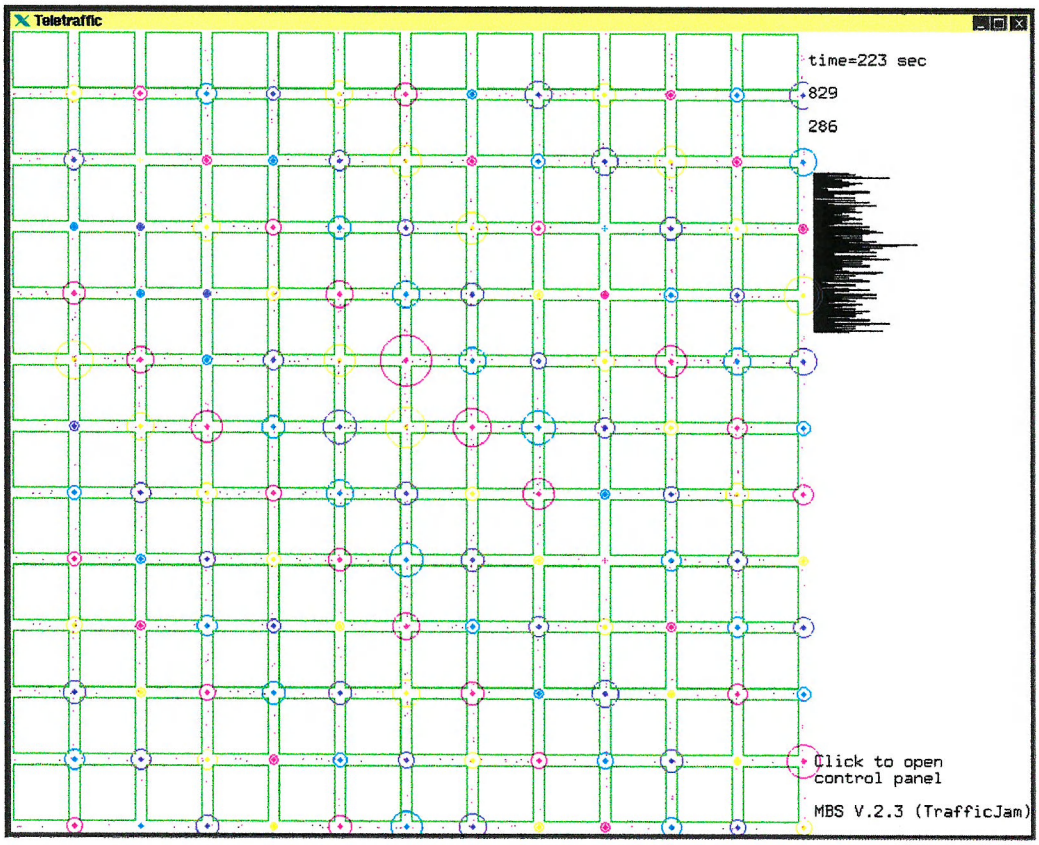

Figure 3.11: The level of teletraffic load on the FBS is shown by the size of its circle

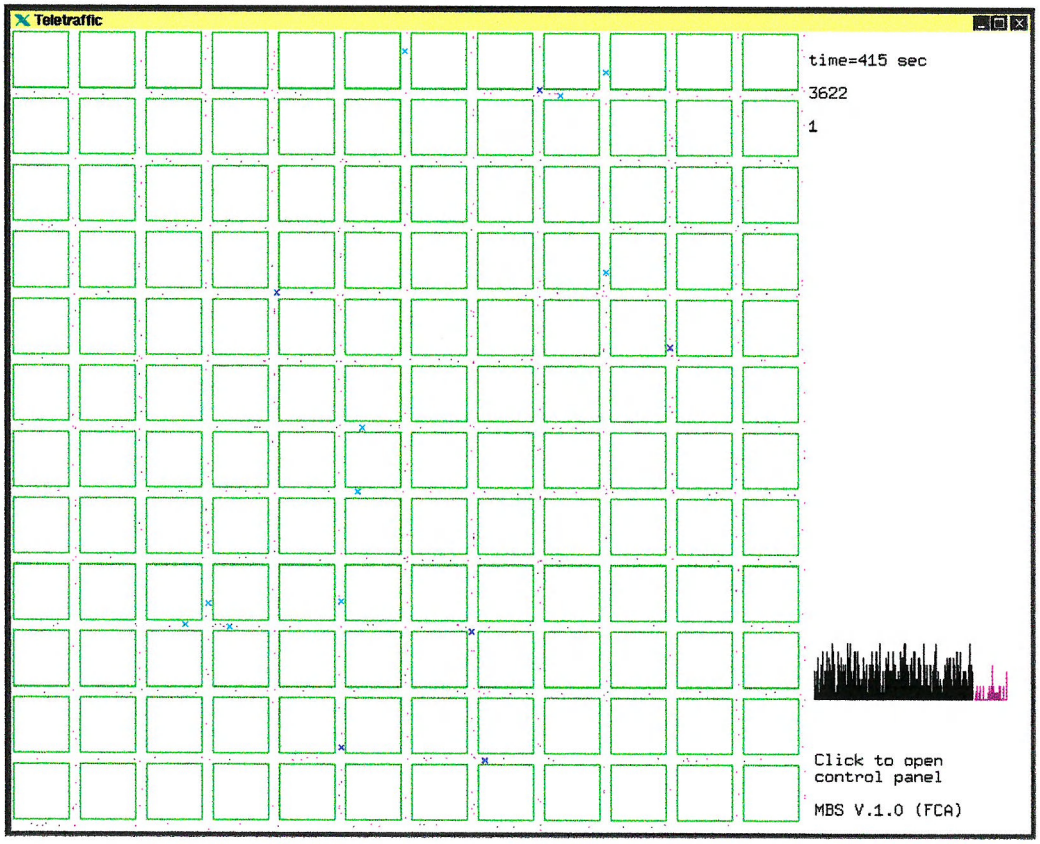

Figure 3.12: Locations of the block calls and dropped calls are marked by the crosses

are collected (e.g. carried traffic, control overheads in terms of the number of intra-handovers, inter-handovers invoked, ...etc). Statistics related to the service provided to the MSs are also collected (e.g. new call blocking probability, forced termination probability, average transmission power, link qualities in terms of the SIRs, ...etc). The performance of the system is evaluated for different offered traffic level. The offered traffic per MS is kept constant, and the total offered traffic is controlled by varying the density of the MSs.

3.3 Fixed Channel Assignment (FCA) Scheme

MBSs have the same mobility characteristics as the MSs, and travel randomly inside the city at a constant speed of 6 m/s. The FBS sites are located at each road intersection. Fixed channel assignment (FCA) is applied to both the FBSs and the MBSs. While the FBSs have to reuse the four assigned channel sets, each of the MBSs is given a unique channel set that is not reused. Although assignment of a unique channel set per MBS is spectrally inefficient, it allows us to study the amount of traffic carried by these MBSs in the absence of cochannel interference.

In addition to the traffic channels (TCHs) that are used to carry the voice and data traffic, control channels (CCHs) are also required in a real system. This thesis, however, is only concerned with the TCHs and one of the CCHs, namely, the broadcast control channel (BCCH). In GSM, the BCCH is used to broadcast information about the BS, e.g. the mobile network code (MNC), the mobile country code (MCC), the cell identity (CI), the base station identity code (BSIC), ... , etc. The BCCH also acts as a beacon channel as it is always transmitted at constant power. The MSs in the simulator measure the received signal strengths of all BCCHs to determine which BS they can connect to. Consequently, the channel sets in the simulator consist of three types of channels; the BCCH, the uplink TCHs and the downlink TCHs.

The MSs can detect a nearby MBS by scanning the BCCH associated with the MBS. The BCCH is transmitted with maximum power (Tx_{max}=1mW) at all times. The TCHs are also transmitted with maximum power as there is no power control. The communication protocols for the FBS and the MBS are the same. There are no priorities between the FBS and the MBS in setting

up a call. Both the FBS and the MBS are simply referred to as BS in the flow charts shown in Figures 3.13 and 3.14. The mechanism for exchanging the data between the MBSs and the fixed wire-network is not implemented in the simulation model.

The flow chart shown in Figure 3.13 describes the routine that each MS undergoes when it wishes to make a new call, or to maintain an already connected call. This routine is repeatedly executed by all busy MSs every second. If the MS wishes to make a new call, it first scans all known BCCHs and then requests a connection. We call this procedure the seekBS function, and it is described later. If the request is granted, connection will be established and a pair of uplink and downlink TCHs will be assigned. The MS will then transmit its data on its assigned uplink channel at a constant power, Tx_{max}. If the request is rejected, the new call is blocked and lost. For a simulation point of view, the MS will be assigned a new next call time attempt and if successful a new call duration. Both variables are from the negative exponential distribution. The MS will also be given new spatial coordinates that are uniformly distributed over the city area. In order to reduce the computational cost, we only keep track of the positions of the busy MSs. Since the MSs are uniformly distributed in space, we assume that the locations where the MSs make new calls are also uniformly distributed. For every second, an idle MS will check its next call time counter. If it is time to make a new call, it will *re-appear* at its new coordinates.

If the MS is maintaining a call, it first checks whether it is time to terminate the call. If so, it releases the channel and turns off its transmission power. The new next call time, call duration and spatial coordinates are assigned. If the call is not yet finished, the MS needs to measure both the uplink and downlink received power. If they are above the system thresholds, the MS then checks their corresponding SIRs. If all measurements are within the system specifications, the MS continues on the same channel. Otherwise, a new channel is needed in order to continue the call. This is done by first invoking the intra-handover (intra-HO) procedure. If this fails, the inter-HO procedure is invoked. If both procedures fail, the call in progress is dropped. The intra-HO procedure instructs the serving BS to execute the seekCH function and the inter-HO procedure instructs the MS to execute the seekBS function. Both functions are described by the flow charts shown in Figure 3.14.

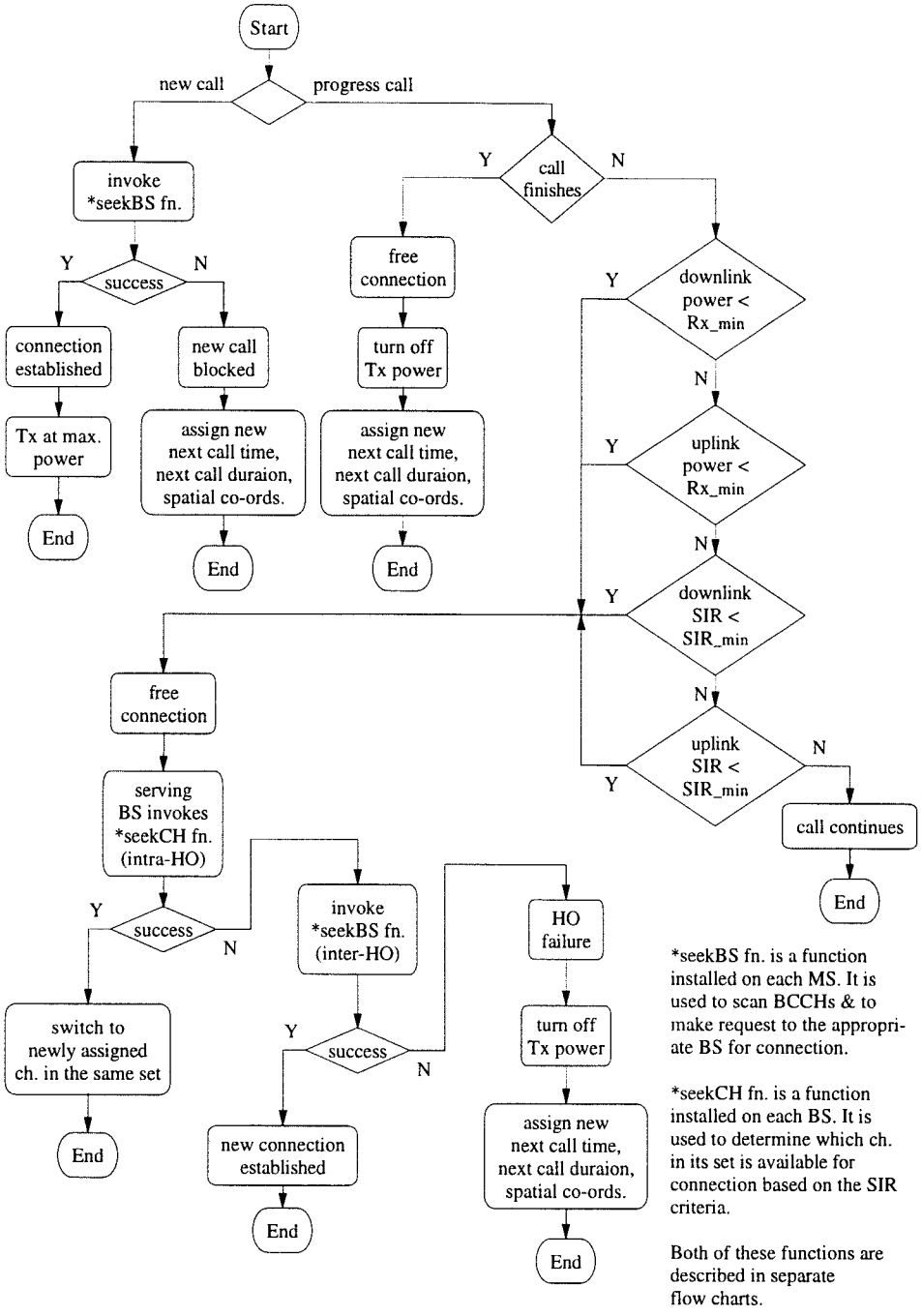

Figure 3.13: A flow chart showing the main communication routine

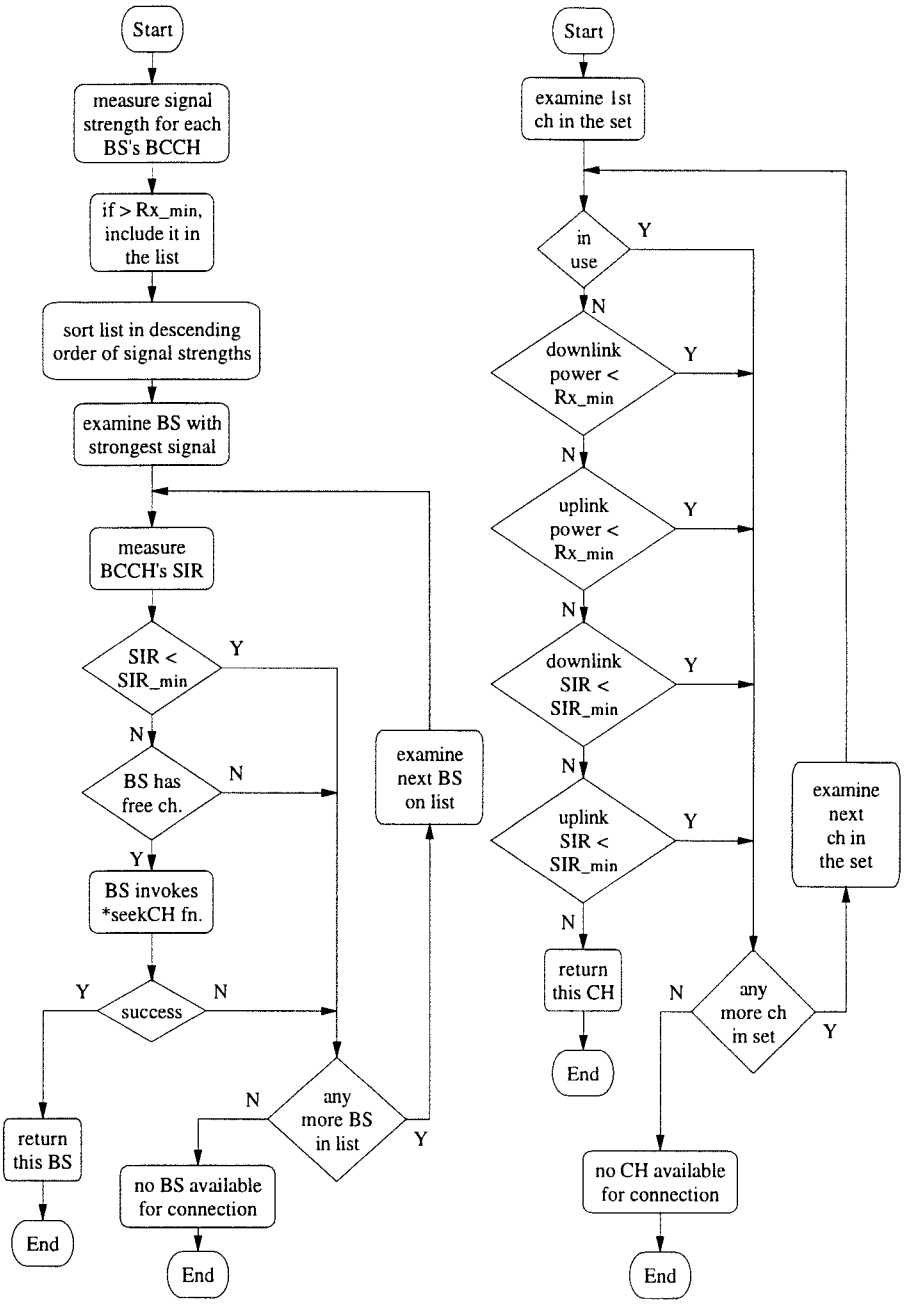

(a) seekBS function

(b) seekCH function

Figure 3.14: Flow charts of the seekBS and the seekCH functions

The seekCH function is executed by a BS. All channels in a given channel set are numbered. The BS examines the lowest numbered channel first. If the examined channel is vacant, the BS measures the signal strength and the SIR of the uplink channel. The MS will then be instructed to report the corresponding downlink signal strength and SIR. If all the acceptance criteria are met, this channel will be used for the connection. Otherwise, the next higher numbered channel will be examined. If none of the channels in the channel set is acceptable, this BS cannot serve this MS.

The seekBS function is executed by a MS. The signal strengths of all BSs' BCCHs are measured. BSs with signal strengths greater than the threshold, Rx_{min}, are included in the list. The list is then sorted in descending order of the BSs' signal strengths. The MS will then examine each of the listed BS in that order. The SIR of the examined BS's BCCH will be measured. If it is above the system threshold, SIR_{min}, the MS will make a request to this BS. This BS will respond by checking whether it has any free channels. If it has, it needs to invoke the seekCH function to check the qualities of these free channels. If it is successful, this BS will serve this MS using the channel returned from the seekCH function. Otherwise, the MS will examine the next BS in the list. If none of the BSs can serve this MS, the call is blocked or dropped.

3.3.1 Cochannel Interferences on FBSs

In this section, we will look at the received signal strengths and the SIRs on the MS-FBS links. Note that with the current scheme there is no cochannel interference on the MBS links. As the mobile moves away from its serving FBS along a LOS path, the received signal power deteriorates exponentially as shown in Figure 3.15.

The level of uplink interference experienced by the FBS is random, because the positions of the cochannel mobiles change. The average value of the uplink interference is recorded when the simulator was run for one hour of simulation time. The maximum level of uplink interference is also recorded. The results are displayed in Figure 3.16 for different mobile populations in the city. As the number of mobiles increases, the average level of uplink interference increases. Notice that, for a given mobile population, the maximum recorded uplink interference is approximately 8 dBm higher than the

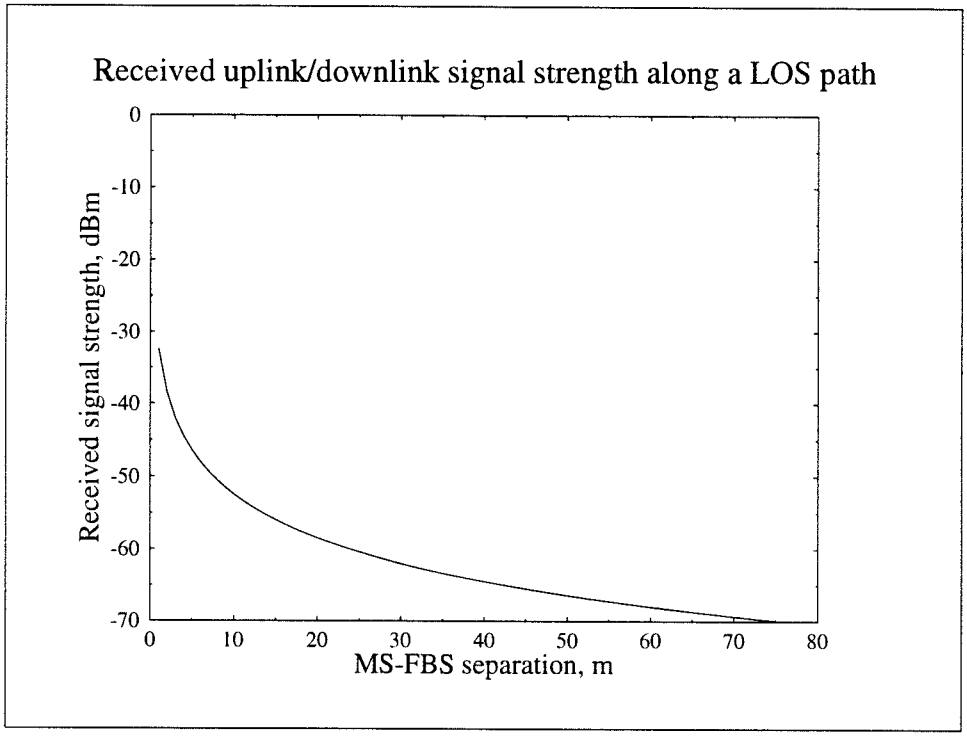

Figure 3.15: Received signal strength Vs FBS-MS separation

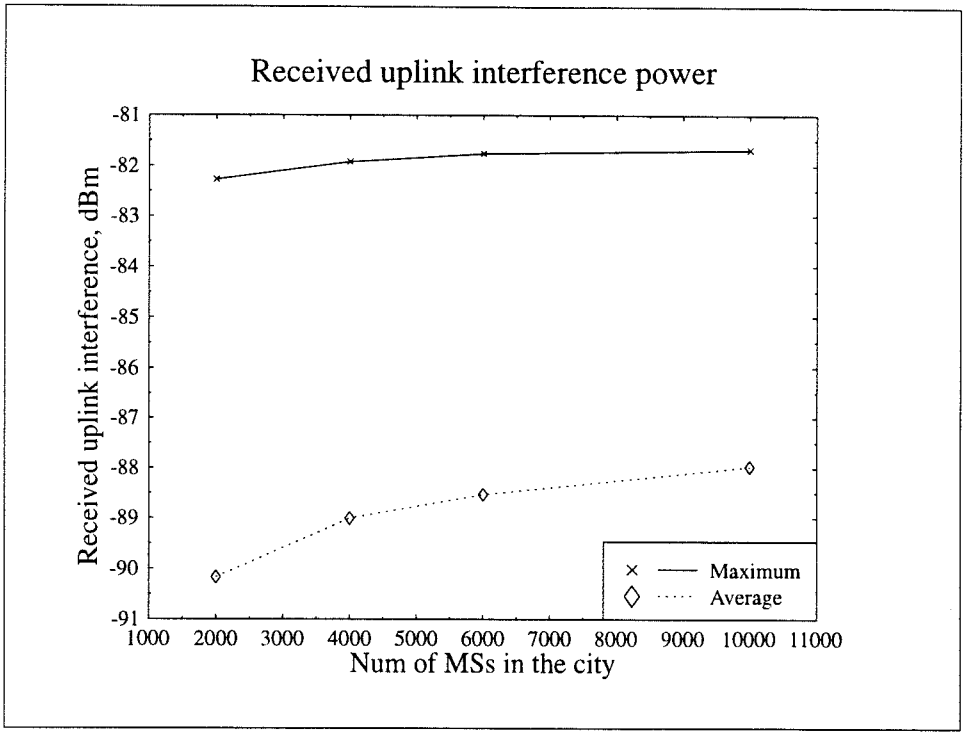

Figure 3.16: The maximum and the average of the received uplink interference power plotted against the number of mobiles present in the city.

average value.

Figure 3.17 shows the uplink SIR recorded by the FBS when the served mobile moves away along a LOS path. Both the average and the maximum uplink SIRs are shown in this figure, for 2000, 4000, 6000 and 10000 mobiles present in the city. The higher the mobile population the lower the uplink SIR.

The level of the downlink interference experienced by the mobile depends on its position. Figure 3.18 shows the level of the downlink interference at the mobile, as it moves away from its serving FBS along a LOS path, for mobile populations of 2000, 4000, 6000 and 10000. The level of interference increases as the population of the mobiles increases.

Referring back to Figure 3.5, we can see that there are four cochannel FBSs in LOS when the mobile is close to its serving FBS. This causes a high level of

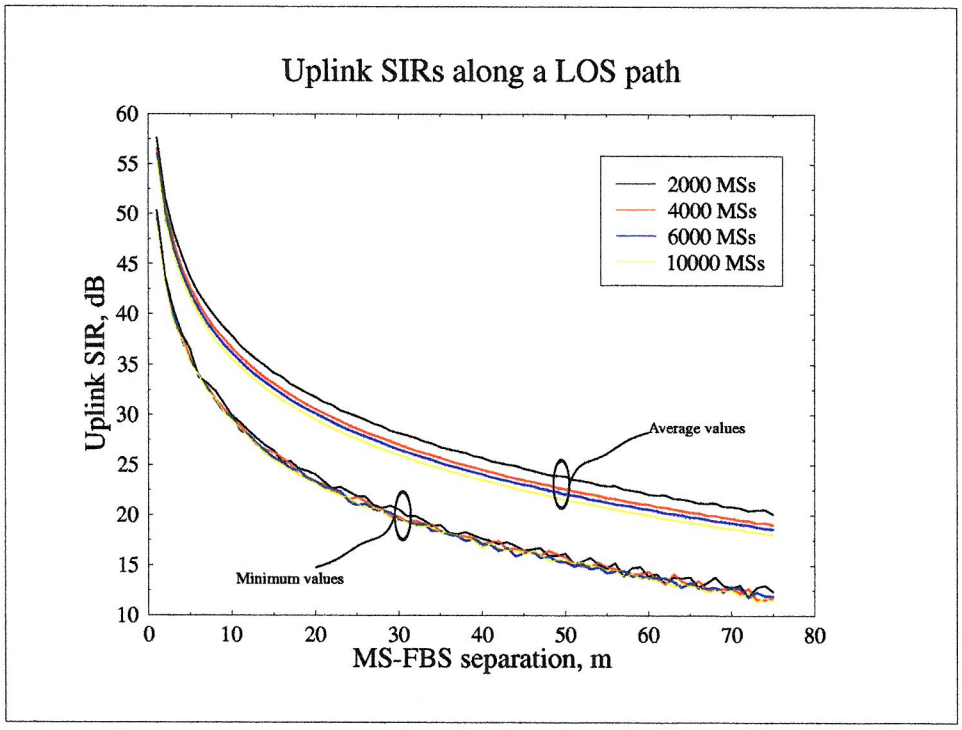

Figure 3.17: Uplink SIR Vs FBS-MS separation distance

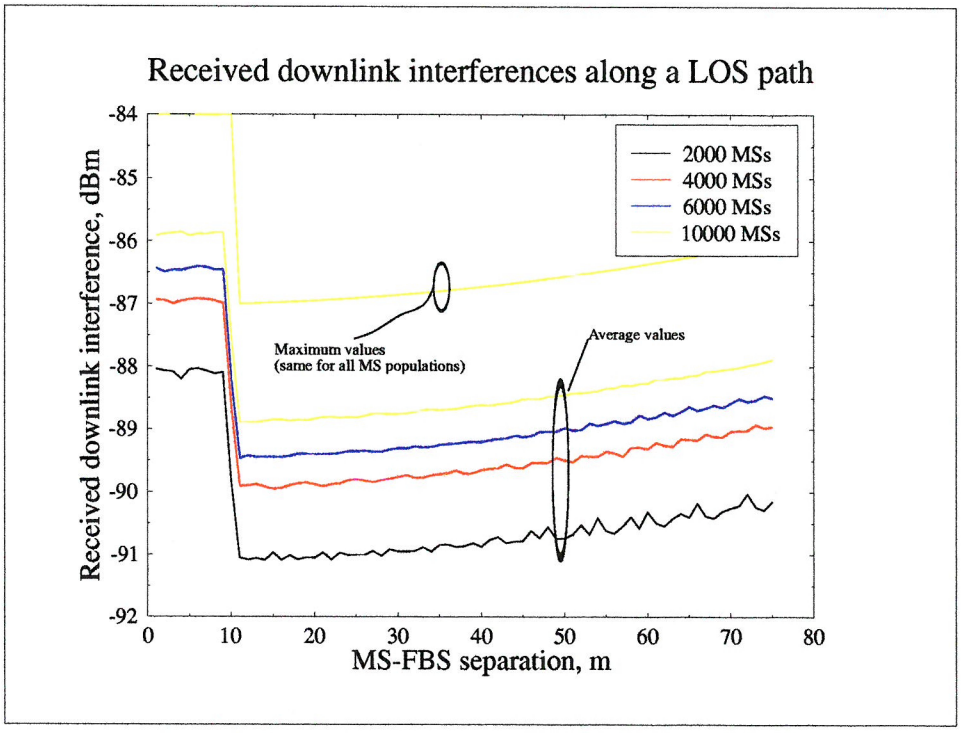

Figure 3.18: The received downlink interference power Vs FBS-MS separation distance

downlink interference. When the mobile moves away from the road junction, there are only two FBSs in LOS. Consequently, the level of interference drops. The two nearest OOS FBSs that are located diagonally to the serving FBS contributes a small amount of interference. As the mobile moves further away from the serving FBS, it moves closer to one of these two OOS FBSs. This is shown by the increasing level of downlink interference after the LOS separation of 10 m in Figure 3.18. The resulting downlink SIR is shown in Figure 3.19.

In order to increase the running time of the simulator, signals that are below two hundredth of Rx_{min} (i.e. 5×10^{-10} mW) are ignored. This increases the speed performance by 30 to 40 percent with insignificant alteration to the result.

The system performance is measured by the new call blocking probability, P_B, and the forced termination probability, P_F. The new call blocking probability

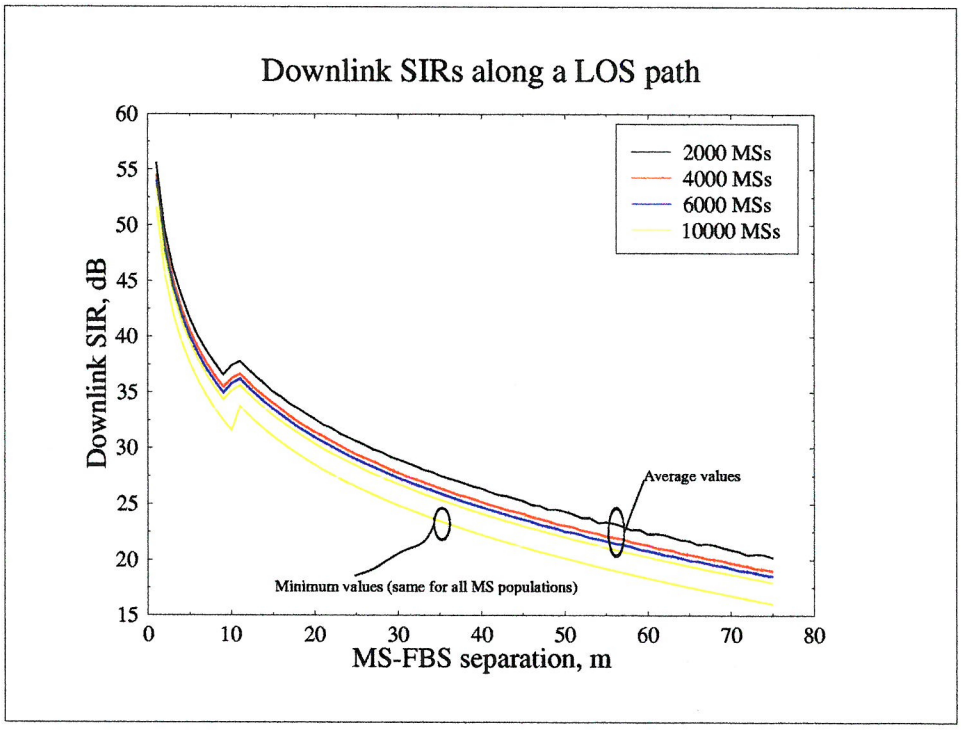

Figure 3.19: Downlink SIR Vs FBS-MS separation distance

is the probability that a newly generated call will be blocked. The forced termination probability is the probability that a call in progress is forced to drop.

Channel utilisation, ρ, is an important system parameter. It represents the fraction of time a channel is being used. From the service provider's point of view, a high channel utilisation means less equipment needs to be deployed. However, a high channel utilisation accompanies a high level of blocking probability, thereby degrading the service provided to the users. Our goal is to develop a system which can lower both P_B and P_F for the same level of channel utilisation.

Figure 3.20 shows the average channel utilisation for the FBS for different mobile populations. As we increase the number of MBS, the channel utilisation for the FBS drops. This is because some of the traffic is now carried by the nearby MBSs. Figure 3.21 shows the average channel utilisation for the MBSs. It is approximately one fourth of that of the FBS. As a MBS moves in the city, the shape of its radio coverage changes. For the majority of the time the MBS is located at the side of the building blocks, producing a rectangular-shaped cell. The size of this rectangular cell is half of the cross-shaped cell produced when the MBS is at a road intersection. The FBSs are permanently located at the centre of the road intersections, thus the average user density per cell area is greater for the FBSs than for the MBSs. In addition, unlike the FBSs, the MBSs are not optimally spaced. Figure 3.22 shows the radio coverage provided by the MBSs.

Figure 3.23 shows the average channel holding time for the FBSs. Users connected to a FBS can be categorised into three types. They can be either a new call user residing within the FBS's coverage area, or a user handed over from the adjacent FBSs, or a user handed over from a nearby MBS. For the first case, the average distance these users travel before reaching the border of the current serving FBS is 75.5m, i.e., the distance from the centre of the cell to its border. As the MSs are travelling at 6m/s, the channel holding time is therefore 12.6 sec.

In the second case, a user who is handed over from an adjacent FBS needs to travel 120m before reaching the current cell's border as shown in Figure 3.24. This gives a channel holding time of 20 sec. For the last case, the average distance a user, who is handed over from a MBS, travels is the same as for a new call user. This is because the borders of a MBS vary as it roams around

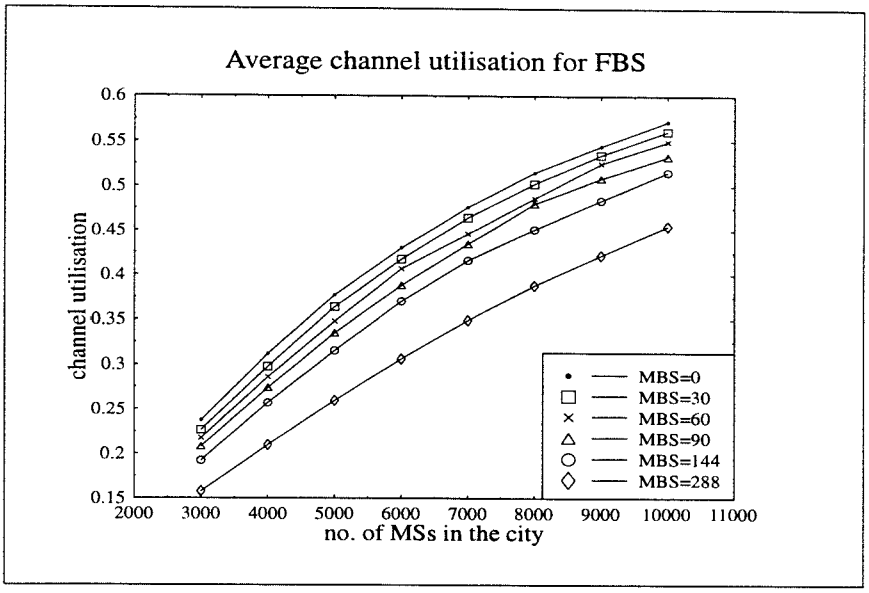

Figure 3.20: Average channel utilisation for FBS

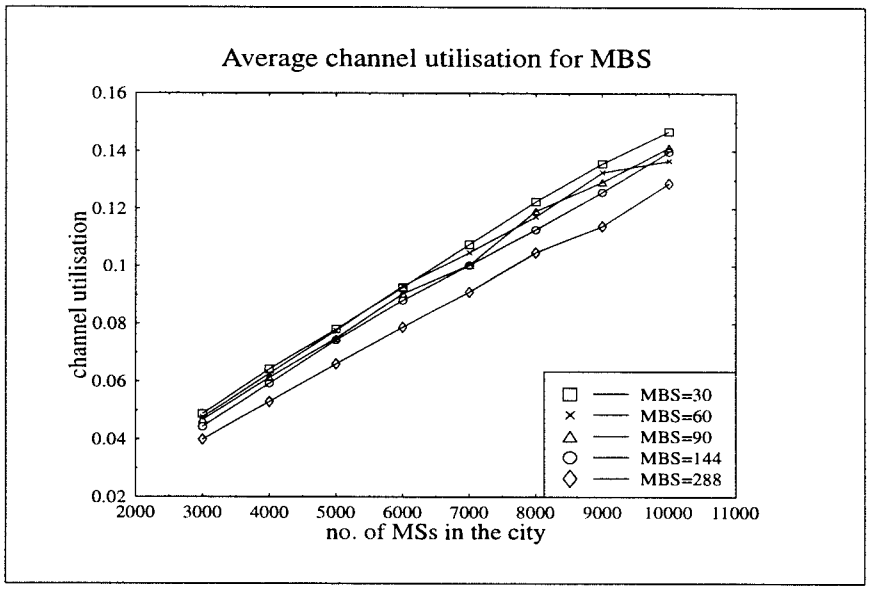

Figure 3.21: Average channel utilisation for MBS

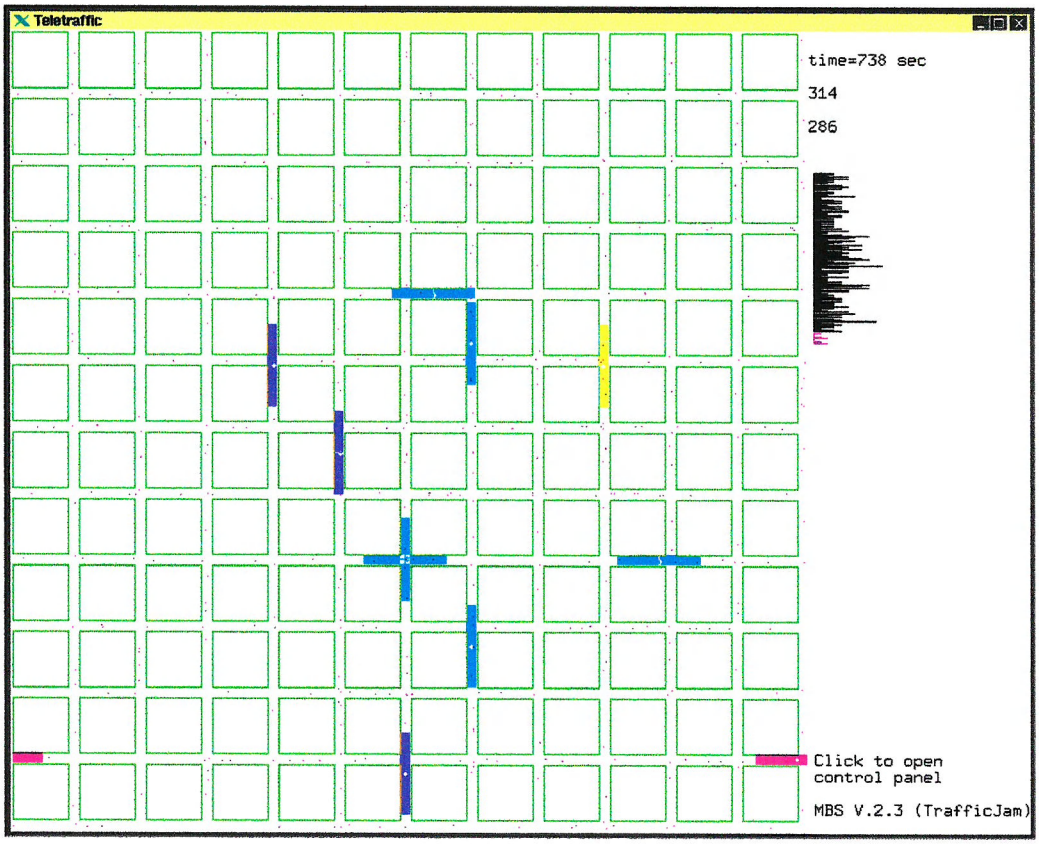

Figure 3.22: Radio coverage provided by the MBSs

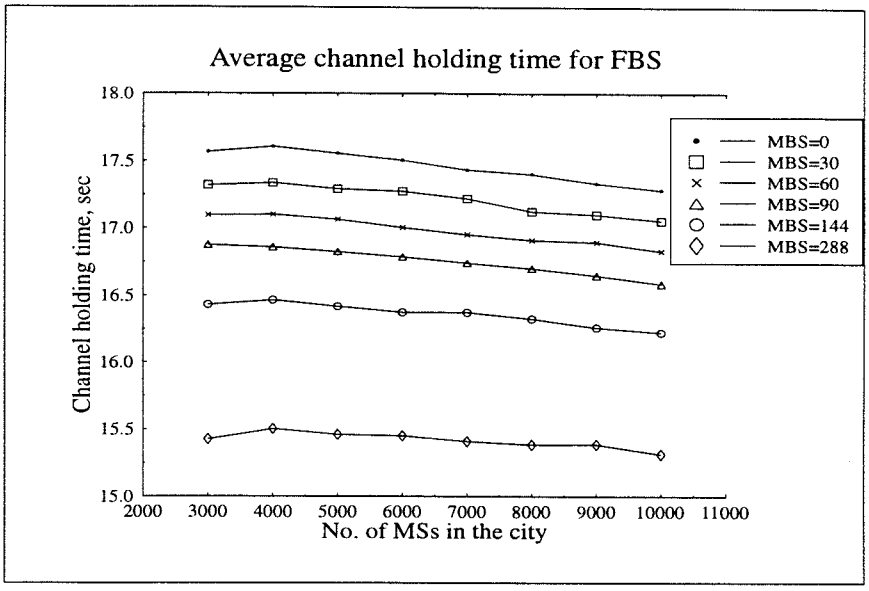

Figure 3.23: Average channel holding time for users connected to a FBS

in the city. Thus the point where the users depart from the connected MBS's coverage can be anywhere relative to the nearby FBS. Table 3.2 to 3.4 give the relevant statistics obtained from simulation.

The average distances shown in Table 3.2 to 3.4 are slightly different than those mentioned in the above paragraph. This is because the simulation program runs in units of a second. As the vehicles are travelling at 6m/s, the point where the handover takes place, for example, can be maximally six metres away from the serving cell's border. The figures in Table 3.2 to 3.4 show that most of the traffic comes from the HO users, only 10-20% is due

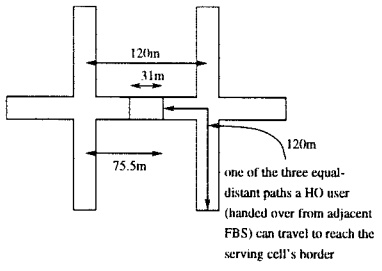

Figure 3.24: Radio coverage of two adjacent FBSs

number of MSs	new users		HO users from FBS	
	%	average distance, m	%	average distance, m
3000	14.8	73.2	85.2	110
6000	15.8	73.3	84.2	110
10000	19.7	73.3	80.3	110

Table 3.2: Statistics of users served by FBS when no MBS is employed

number of MSs	new users		HO user from FBS		HO users from MBS	
	%	average distance, m	%	average distance, m	%	average distance, m
3000	13.1	73.1	65.7	110m	21.2	74.9
6000	13.6	72.9	65	110m	21.4	75.0
10000	15.2	73.1	62.2	111m	22.4	75.0

Table 3.3: Statistics of users served by FBS when 144 MBSs are employed

number of MSs	new users		HO user from FBS		HO users from MBS	
	%	average distance, m	%	average distance, m	%	average distance, m
3000	11.3	72.9	50.1	111	38.5	74.0
6000	11.7	73.7	50.1	110	38.2	74.4
10000	12.7	73.4	48.3	110	39.0	73.8

Table 3.4: Statistics of users served by FBS when 288 MBSs are employed

to new call users. When the number of MBSs is small the majority of the traffic is from the users who were handed over from the neighbouring FBSs, thus the average channel holding time is close to the upper bound of 20 sec. As the number of MBSs is increased, the average channel holding time moves towards the lower bound of 12.6 sec. In addition, as the number of MSs is increased, the average channel holding time decreases. This is because the ratio of traffic generated from new call users to HO users increases. The reason is, as we shall see later, that the HO failure rate deteriorates more severely than the new call blocking rate as the traffic increases.

Figure 3.25 shows the average channel holding times for a MBS. Each data point was collected after one hour of simulation time. This gives a minimum sample size of 2981 (indicated by the program). The sample size increases with increasing number of MSs or increasing number of MBSs. The maximal recorded sample size is 71230. Despite the large sample size (each sample being the holding time of any channel owned by a MBS and held by any MS), the curves in Figure 3.25 oscillate erratically. The channel holding time increases with increasing MS density or increasing MBS density. In all cases, the channel holding times for the MBSs are lower than those for FBSs.

Table 3.5 to 3.7 shows the average distances travelled by each of the three types of users connected to a MBS. As for the FBS, the traffic mainly comes from the HO users. However, when comparing to Table 3.3 and 3.4, the proportion of new call users connected to a MBS is higher than the proportion of new call users connected to a FBS. In addition, the proportion of HO users handed over from a MBS to another MBS is lowered than from a MBS to a FBS. The average distances travelled by each of the three types of users connected to a MBS differs to the corresponding distance when connected to a FBS. For those MSs connected to a MBS and travelling in the same direction as their serving MBS, the connection remains until either the MS or the MBS reaches a junction and decides to turn elsewhere. For those MSs connected to a MBS and travelling in the opposite direction to their serving MBS, the relative speed of these MSs seen from their MBSs is twice their absolute speed, hence the corresponding channel holding times are very brief.

Figures 3.26 and 3.27 show the number of inter-HOs invoked per second for each FBS and for each MBS, respectively. In both cases, the inter-HO rates increase with an increase in the MSs density. Both figures show that the inter-HO rate decreases as the number of MBSs employed increases. This is

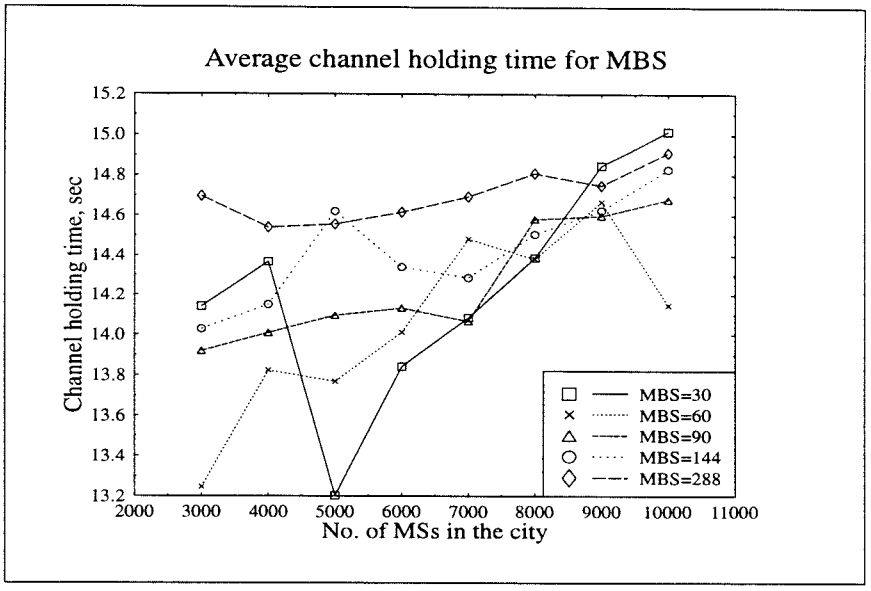

Figure 3.25: Average channel holding time for users connected to a MBS

number of MSs	new users		HO user from FBS		HO users from MBS	
	%	average distance, m	%	average distance, m	%	average distance, m
3000	16.6	115	81.8	76.4	1.6	64.8
6000	17.8	129	80.4	74.4	1.9	85.3
10000	20.5	130	77.5	79.9	2.0	86.8

Table 3.5: Statistics of users served by MBS when 30 MBSs are employed

number of MSs	new users		HO user from FBS		HO users from MBS	
	%	average distance, m	%	average distance, m	%	average distance, m
3000	15.0	126	76.2	77.5	8.8	84.4
6000	15.8	125	75.2	78.3	9.0	83.6
10000	17.9	127	72.3	80.2	9.8	90.0

Table 3.6: Statistics of users served by MBS when 144 MBSs are employed

number of MSs	new users		HO user from FBS		HO users from MBS	
	%	average distance, m	%	average distance, m	%	average distance, m
3000	15.2	128	67.2	79.0	17.6	88.4
6000	15.3	126	67.2	78.7	17.5	83.8
10000	16.4	127	64.7	80.4	18.9	86.0

Table 3.7: Statistics of users served by MBS when 288 MBSs are employed

because there are more BSs to serve, and thus a decrease in carried traffic per BS.

Figures 3.28 and 3.29 show the new call blocking probability and the forced termination probability, respectively, versus the MS density. The introduction of MBSs successfully decreases both the new call blocking probability and the forced termination probability. However, in terms of channel utilisation (which directly relates to spectral efficiency [7, 43]), the performances of the MBSs are poor. In Figures 3.30 and 3.31 the new call blocking probabilities and the forced termination probabilities are plotted against the channel utilisation. For the same level of channel utilisation, both probabilities are highest when the system deploys the most number of MBSs. This is expected as each MBS has an unique channel set which is not re-used. We will study a more effective algorithm in the next chapter when the dynamic channel assignment (DCA) scheme is employed.

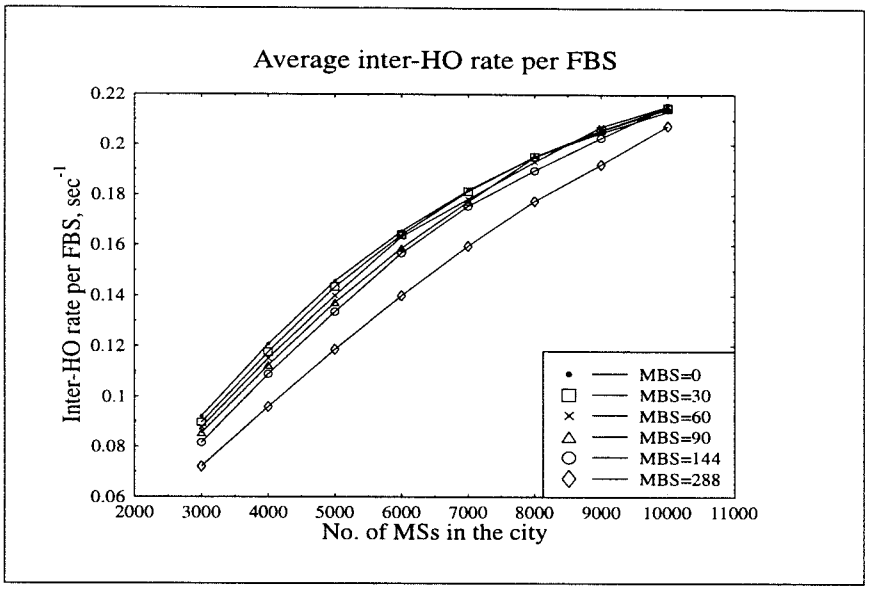

Figure 3.26: Average inter-HO rate invoked per FBS

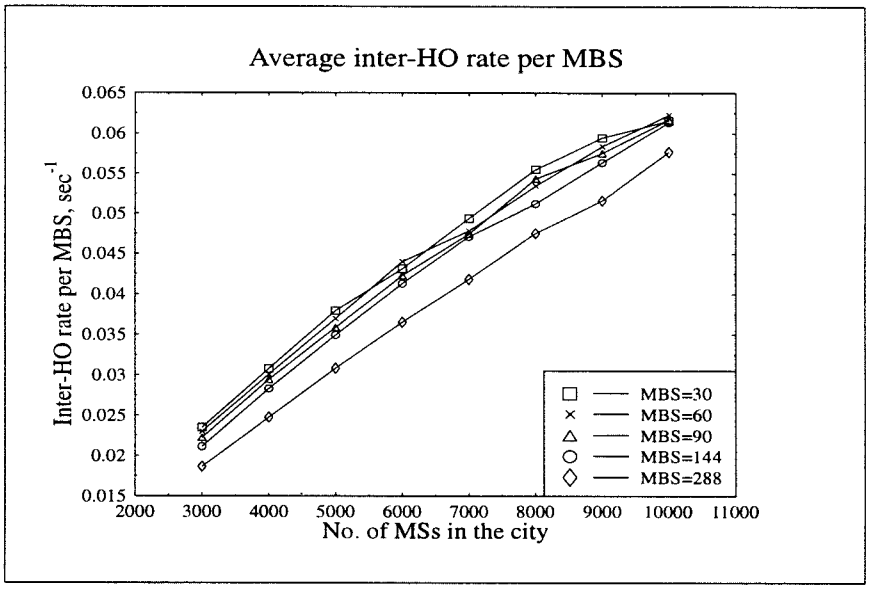

Figure 3.27: Average inter-HO rate invoked per MBS

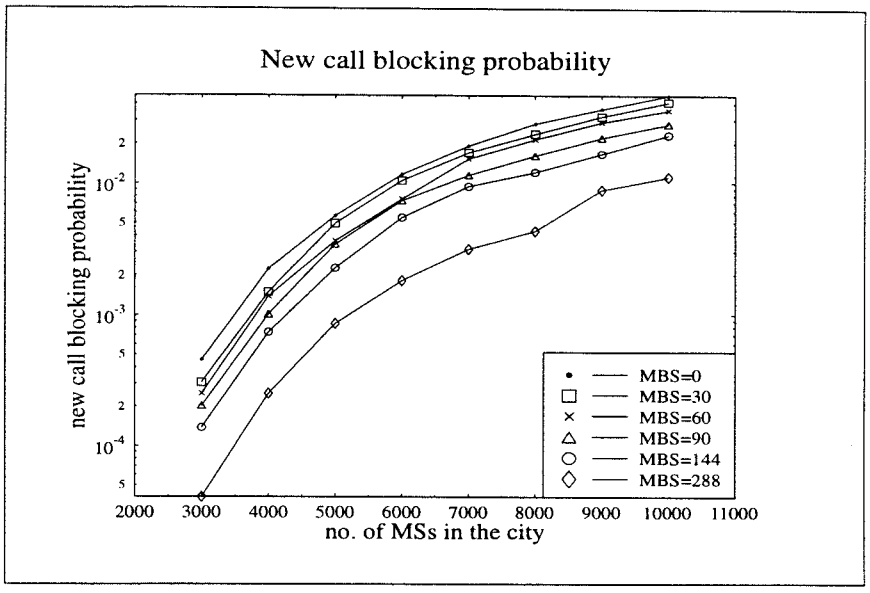

Figure 3.28: New call blocking probability versus MS population when different number of MBSs are employed

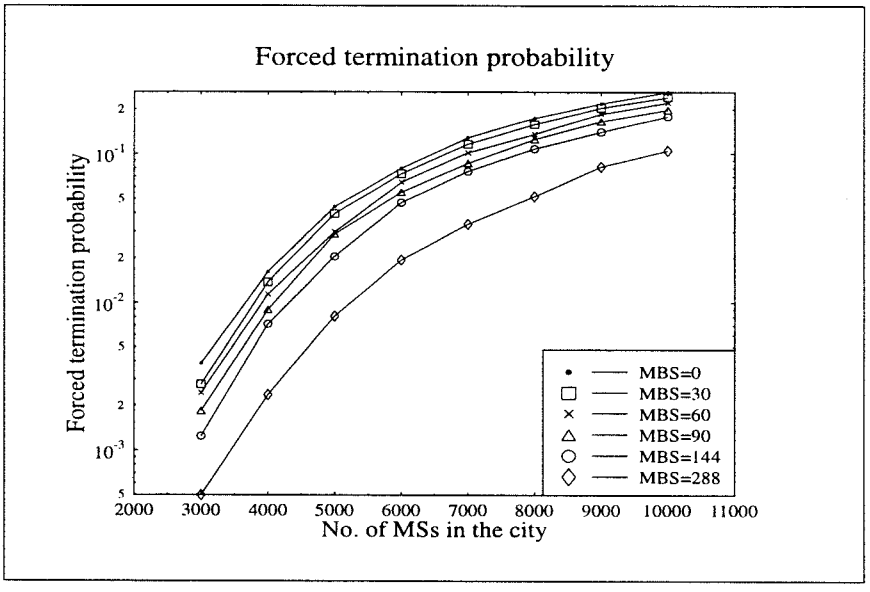

Figure 3.29: Forced termination probability versus MS population when different number of MBSs are employed

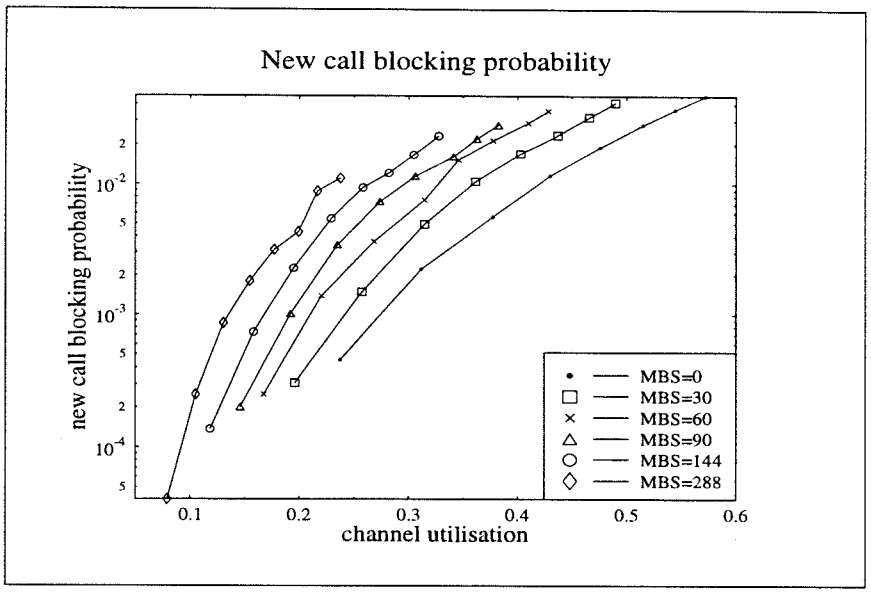

Figure 3.30: New call blocking probability versus channel utilisation when different number of MBSs are employed

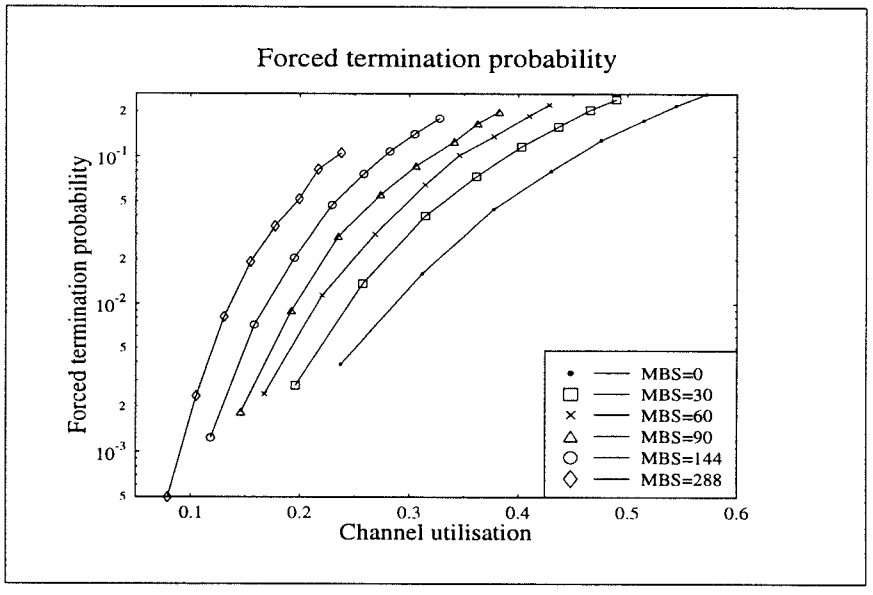

Figure 3.31: Forced termination probability versus channel utilisation when different number of MBSs are employed

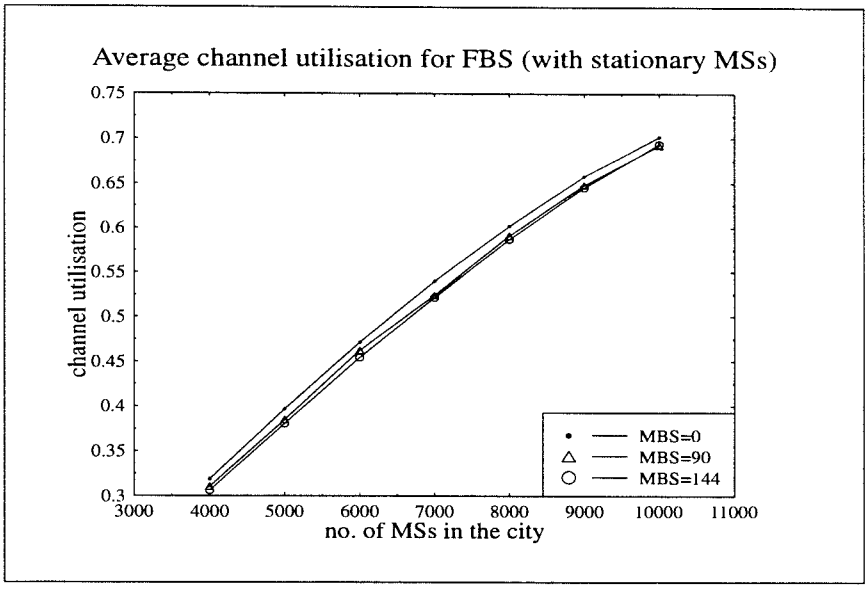

Figure 3.32: Average channel utilisation for FBS (with stationary MSs)

3.3.2 Stationary MSs

So far we have studied the system performance when the MSs are travelling at a constant speed of 6 m/s. At this speed, the level of HO activity is high. In this section, we will reduce the MS speed to zero. The only HO activity taking place is from the MBSs. The results are shown in Figure 3.32 to 3.39 which corresponds to Figure 3.20, 3.21, 3.26 to 3.31 in the last section.

For MSs that are initially connected to FBSs, they will retain the channel for the whole duration of their calls and no handover will ever take place. For MSs that are initially connected to MBSs, the maximum channel holding time with their serving MBSs is 25 sec. This is the time it takes a MBS to travel a full length of its coverage area, i.e., $75.5m \times 2 = 151m$. The mean call duration is 120 sec, and so the MSs are likely to experience handovers. If they are handed over to a FBS, they will remain connected to that FBS for the rest of their call. If they are handed over to a MBS, further handovers may be required. The effect of this is a dramatic increase in channel usage of the FBS, and a dramatic decrease in channel usage of the MBS. This is depicted in Figures 3.32 and 3.33.

Figures 3.34 and 3.35 show the inter-HO rate per FBS and MBS, respec-

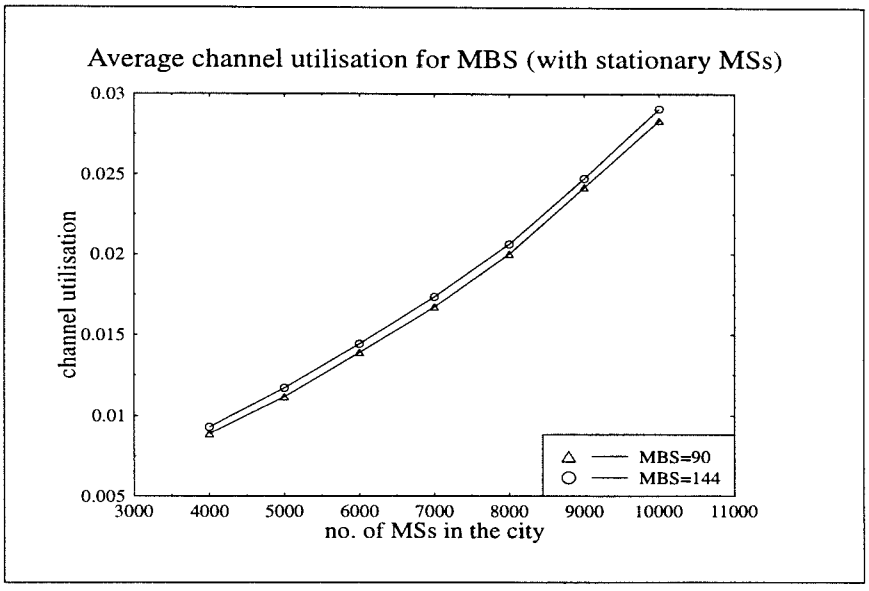

Figure 3.33: Average channel utilisation for MBS (with stationary MSs)

tively. In this case, they represent the handover rate of MBS-to-FBS and the handover rate of MBS-to-MBS, respectively. The curves in these figures are significantly lower than those shown in Figures 3.26 and 3.27 where the majority of handover traffic comes from FBS-to-FBS handovers.

Figure 3.36 shows the new call blocking rate versus the MS density when the MSs are stationary. The curves from Figure 3.28 are also included in this graph to allow comparison. Although it appears that the system has a higher new call blocking rate when the MSs are stationary than when they are moving for the same user density, this does not mean it gives a poorer performance. The actual traffic being carried must also be taken into account. When the MSs are stationary, the probability of premature termination is low. Thus the average channel holding time is longer, giving a higher carried traffic. Therefore when a new call arrives, the probability of finding an available channel is lower.

Figure 3.38, which shows the new call blocking rate versus the channel utilisation, gives a better representation of the system performance. The curves are now a lot closer, but the new call blocking rate for stationary MSs is still higher than for the moving ones for the same level of channel utilisation.

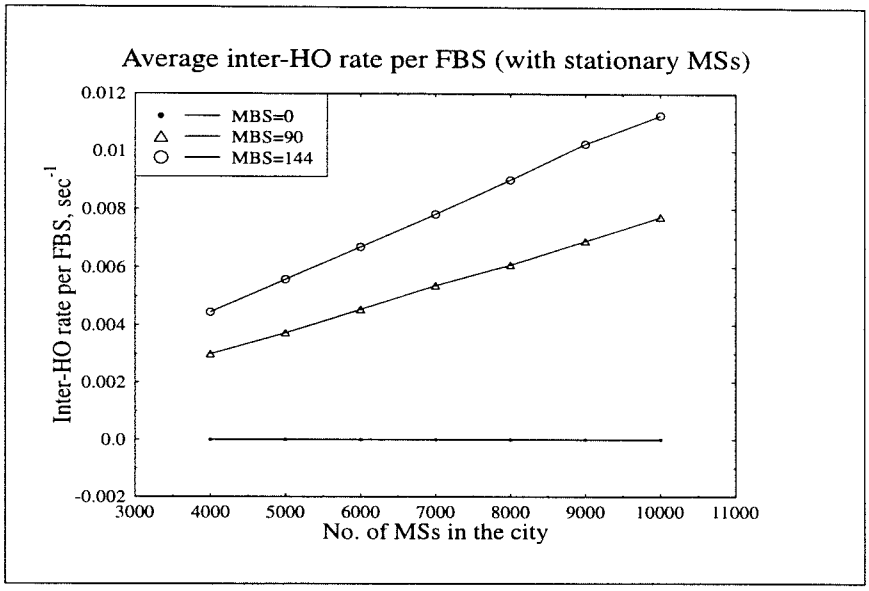

Figure 3.34: Average inter-HO rate invoked per FBS (with stationary MSs)

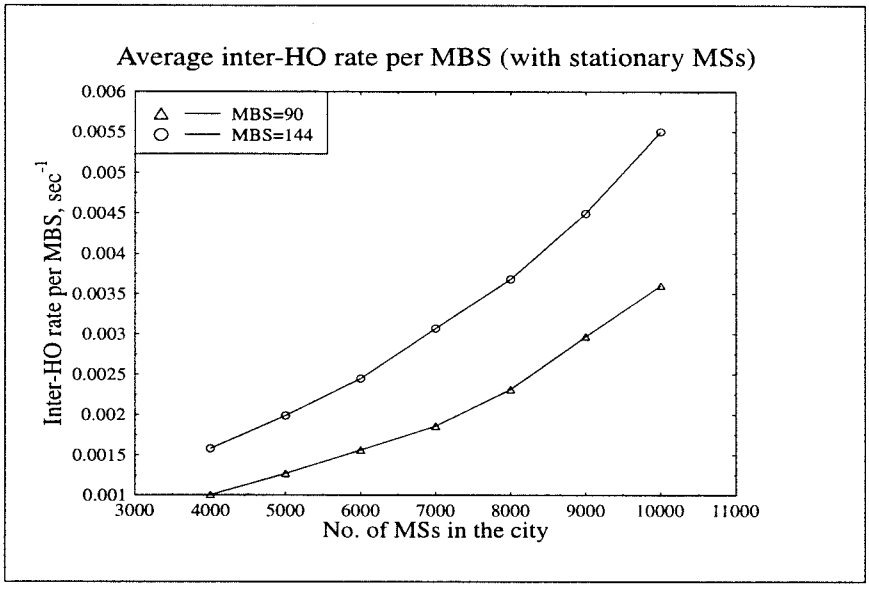

Figure 3.35: Average inter-HO rate invoked per MBS (with stationary MSs)

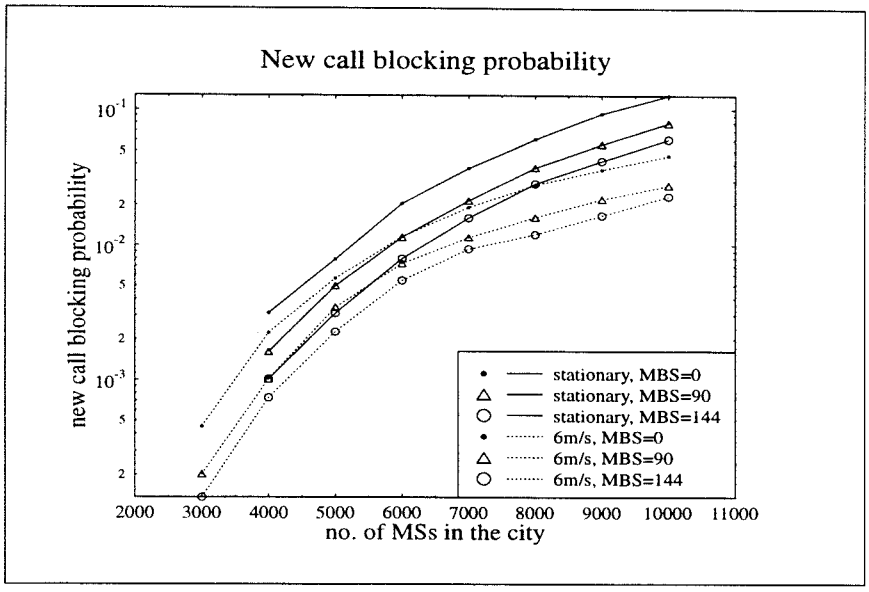

Figure 3.36: Comparison in new call blocking probability between moving MSs and stationary MSs for different MS population

However, we must also examine the forced termination probability which is shown in Figure 3.37 and 3.39 in order to judge the system's grade of service (GOS). The forced termination probability is significantly lower when the MSs are stationary, and it is zero if MBSs are not employed. Notice also that the forced termination probability actually increases with increasing number of employed MBSs, which is the opposite to the system where the MSs' mobility is high. This is because the MBSs themselves are responsible for the dropped calls.

3.3.3 Conclusions

In the system where the MS mobility is high and handovers occur frequently, the introduction of MBSs can be used as additional servers and it can reduce *both* the new call blocking probability and the forced termination probability. However, a system with low MS mobility and low handover activities may not welcome the increasing forced termination probability accompanied with the employment of MBSs.

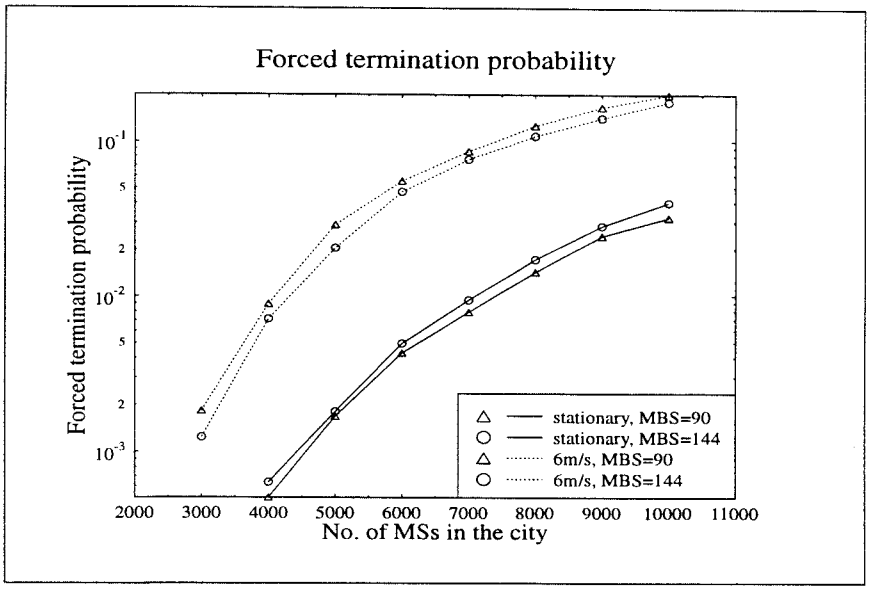

Figure 3.37: Comparison in forced termination probability between moving MSs and stationary MSs for different MS population

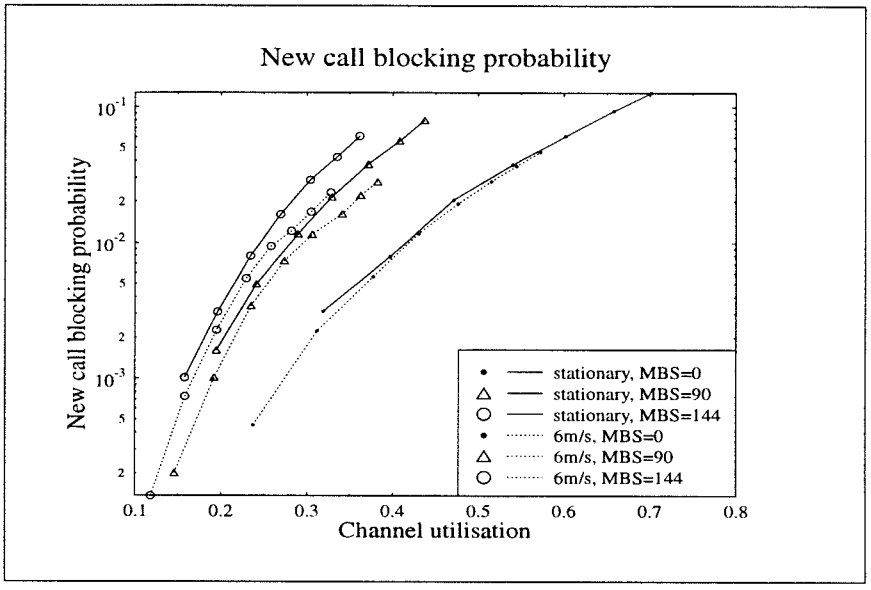

Figure 3.38: Comparison in new call blocking probability between moving MSs and stationary MSs for different channel utilisation

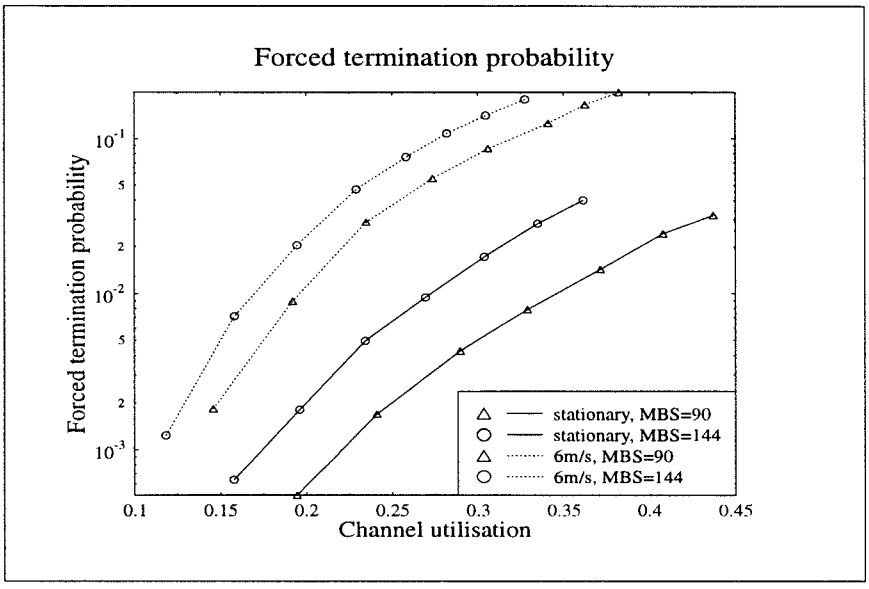

Figure 3.39: Comparison in forced termination probability between moving MSs and stationary MSs for different channel utilisation

Chapter 4

MBS System with Dynamic Channel Assignment (DCA) Scheme and Power Control

After the preliminary study on the moving base station (MBS) system in the last chapter, we will now study a dynamic channel assignment scheme that can be adopted by the fixed base stations (FBSs) and the MBSs. It was shown that an unconstrained dynamic channel assignment (DCA) scheme will be outperformed by a FCA scheme at high teletraffic load [23, 24, 26, 28, 73, 14, 33]. This is because a BS in an unconstrained DCA scheme will assign the first channel that has an acceptable signal-to-interference ratio (SIR), without considering the usage of that channel in its vicinity. Consequently, radio channels are reused at distances greater than the minimum reuse distance, resulting in lower channel utilisation.

A number of algorithms have been proposed to address this problem. The one our MBS system adopts is called *Borrowing with Channel Ordering (BCO)*, proposed by Elnoubi [27]. However, his proposed switching strategies are not implemented here to avoid additional complexity. In addition to the adoption of a DCA scheme, power control is also employed by this system to reduce interference and thereby increase system capacity.

The available spectrum is divided into four groups, forming four channel sets. Each FBS in our four-cell cluster is assigned with a nominal channel set in the same manner as the FCA scheme. However, channel borrowing is allowed

between the FBSs. In addition, the MBSs do *not* require an additional channel set. They borrow channels from the FBSs. Consequently, both the FBSs and the MBSs must be able to transmit and receive all channels available to the system.

In the last chapter, we described how the mobiles access the network by scanning for any on-air broadcast control channels (BCCHs) from nearby BSs and measuring their respective received power levels. This method of accessing the network is the same as in the GSM system. Hereafter we refer to this scheme as the standard access scheme. This scheme, however, requires the MBSs and the FBSs to broadcast on their BCCHs at all times. As the MBSs change their positions all the time, they have to use different BCCHs, and some of them may have to stop broadcasting in order to avoid causing unacceptable cochannel interferences to each other. Consequently the number of MBSs accessible to the mobiles for new call set up is reduced.

The power escalation access (PEA) scheme is proposed to solve this problem. The PEA scheme uses the request-and-reply method, allowing the mobiles to initiate new call requests to nearby FBSs or MBSs without the need to camp on to their BCCHs first. Therefore the MBSs are no longer required to broadcast continuously on their BCCHs. Consequently all MBSs are available for new call setup. Both schemes are studied for a system that has a total of 16 traffic channels (TCHs), i.e. each channel set has four TCHs.

4.1 Standard Access Scheme

In this scheme, all FBSs and MBSs broadcast on their BCCHs at all times with maximum transmission power of Tx_{max}. Each channel set in this scheme is arranged to have one FBS BCCH, one MBS BCCH and four TCHs. We will now describe how the FBSs and the MBSs decide which BCCHs they should use.

4.1.1 Broadcast Mechanism

Each FBS is assigned with a nominal channel set, and it always broadcasts using the FBS BCCH of that channel set. The MBSs, on the other hand, must first identify their nearest FBSs, and then broadcast on the MBS BCCHs of

the nominal channel sets of these FBSs. Figure 4.1 shows four diagonal tiers of zones. Each zone is cross shaped with the centre of the zone at a FBS site. A zone is identified as the area where the FBS at the centre provides the strongest radio coverage.

When a MBS enters a new zone, its home channel set changes to the nominal channel set of the FBS of the new zone. The network will inform this MBS whether it is allowed to broadcast on the MBS BCCH of its new home channel set. Only one MBS is allowed to broadcast at any one time per zone. If there is another MBS already using the MBS BCCH of that zone, the newly entered MBS cannot broadcast until the former MBS leaves the zone. This restriction only applies to the use of the MBS BCCH, the MBSs can still continue to communicate with their connected MSs via the previously assigned TCHs.

4.1.2 Traffic Channel Assignment Strategy

For calls in progress, their uplink and the downlink transmission power are adjusted so that the received power is always at the wanted level or below. The wanted received power level, Rx_{opt}, is set at 10dB above the minimum received threshold, Rx_{min}. The maximum transmitter power, which is the same for both the BS and the MS, is 1 mW. When the transmitter reaches its maximum power, the radio link continues until the received power drops below Rx_{min}. Then an inter-HO procedure will take place. If a new BS is found, the MS will be informed of its new channel and transmission power. If the inter-HO procedure fails, the call is dropped.

In addition to the received power level check, the uplink and the downlink SIRs are also measured. If both SIRs pass the system specifications, the MS may continue the call on the same channel. Otherwise, the serving BS executes an intra-HO procedure. If a new channel is found, the same BS continues to serve the call and the uplink and the downlink transmission power remains the same. If the intra-HO attempt fails, then the MS must initiate an inter-HO.

When a MS searches for connection to a BS, it first scans all the FBS BCCHs and the MBS BCCHs. The BS (FBS or MBS) that provides the strongest BCCH and acceptable SIR is requested for connection first. This BS then searches for a vacant traffic channel (TCH) to serve this MS. If a TCH is found, the connection is established. Otherwise the MS requests the next

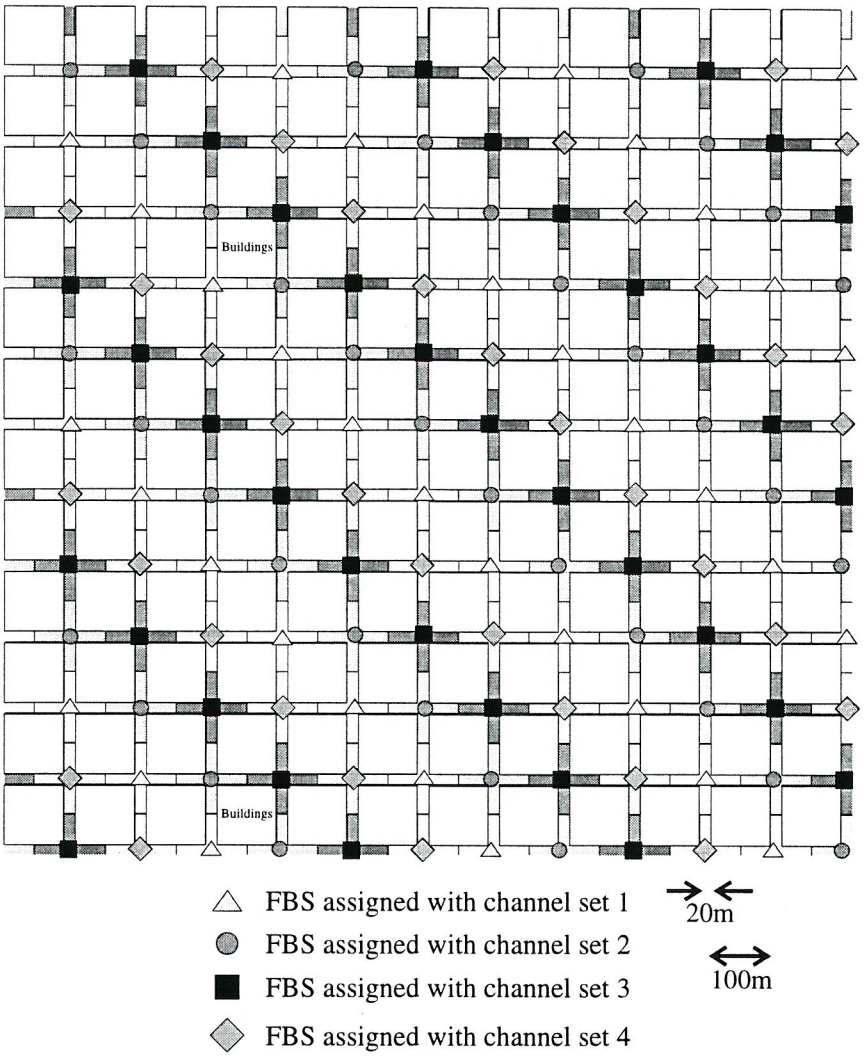

Figure 4.1: The 144 zones in the city.

strongest BS. If none of the BSs are suitable for connection, a new call will be blocked or a call in progress will be dropped as a result.

Although both the FBSs and the MBSs use the same channel borrowing scheme, the order in which they search channels for assignment is different. Figure 4.2 shows the channel tables displayed by the simulator. The larger table on the left hand side of this picture is the channel table for the FBSs, and the smaller one on the right hand side is for the MBSs. Each one of the small four by four tables represents a BS. Each row of these small tables represents a channel set. There are four channel sets in this system, and they are colour coded blue, green, red and brown. Each channel set has four TCHs, and they are represented by the columns of these tables. Consequently, a total of 16 TCHs are available to this system.

A FBS starts its channel search from the leftmost channel (leftmost column) of its nominal channel set (row). If this channel is already occupied, or its uplink or downlink SIR is below threshold, the next channel (next column) is examined. If none of the channels in its nominal channel set is suitable for connection, the FBS *borrows* a channel from other channel sets (other rows). The non-nominal channel set that belongs to the furthest BS and therefore less likely to cause cochannel interference is examined first. Channels from the non-nominal channel sets are searched in the reverse order, i.e., starting from the rightmost channel. This encourages the leftmost channels to be reused at minimum reuse distance, while the rightmost channels are used for borrowing. Unlike the Hybrid Channel Assignment (HCA) scheme, channels are not divided explicitly into borrow-able and non-borrow-able [25]. If no channel can be found for connection, this FBS cannot serve the MS.

The MBSs do not have a pre-allocated nominal channel set, and therefore they always borrow channels from the FBSs. Consequently, they always search the rightmost channels for connection first. A MBS always examines its home channel set last because that channel set is assigned nominally to the FBS residing in the same zone and therefore is most likely to cause cochannel interference.

4.1.3 FBS Statistics

There are three types of users: new call users who originate the call within the coverage of the FBS in question, HO users who were previously handed

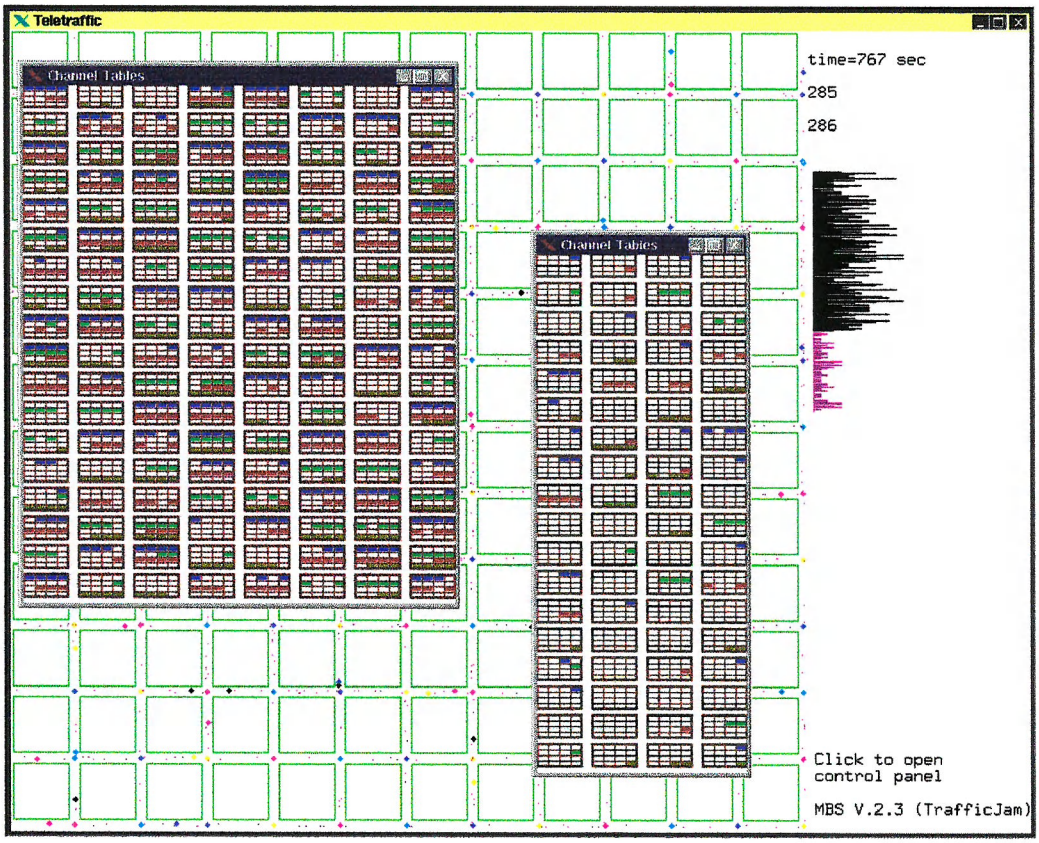

Figure 4.2: Visual representation of the channel assignment strategy

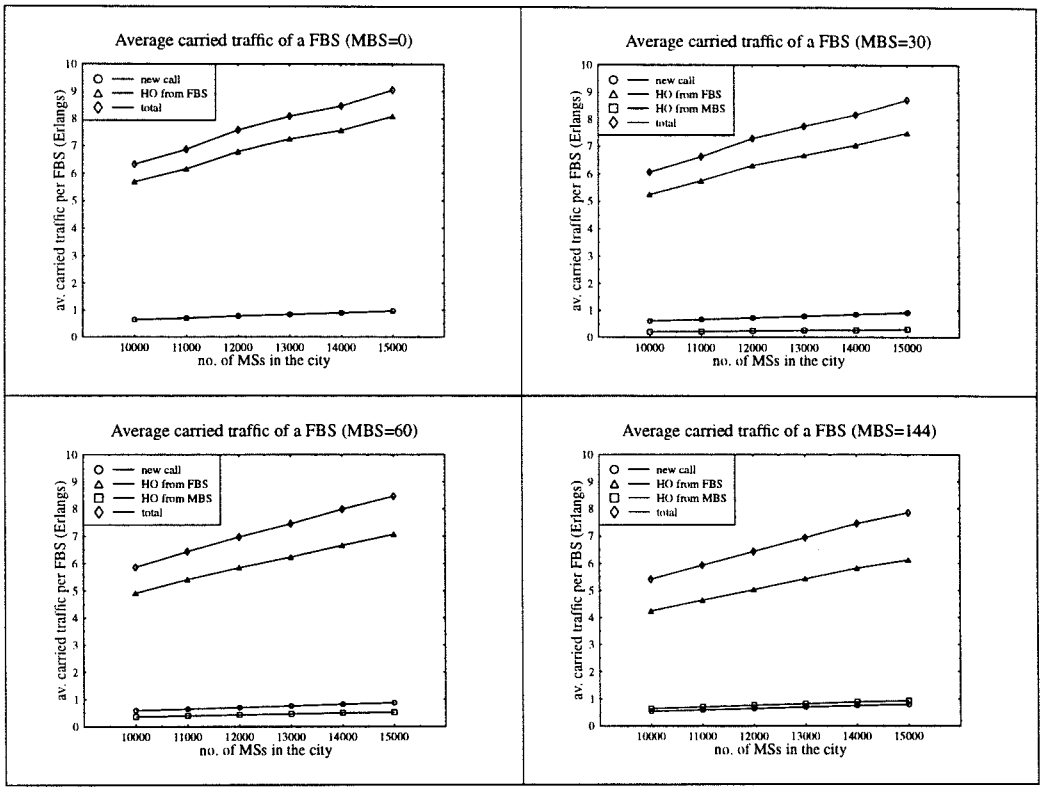

Figure 4.3: Average carried traffic per FBS for new call users, users handed over from another FBS and users handed over from a MBS

over from an adjacent FBS, and HO users who were previously handed over from a nearby MBS. Figure 4.3 shows the traffic generated by these three types of users and carried by a FBS. As each connected user occupies one channel, the carried traffic also represents the average number of that type of user presented to the FBS. As we increase the density of MSs, the carried traffic of all three types of users increase. HO traffic from adjacent FBSs dominates the overall traffic. As we employ more MBSs, the overall carried traffic per FBS decreases. This is because more traffic is diverted and carried by the MBSs.

Figure 4.4 shows the number of intra-HOs invoked by a FBS per second. An intra-HO is invoked if the uplink or the downlink SIR drops below the threshold. Figure 4.4 shows that the intra-HOs due to uplink SIR failure occur more often than those due to downlink SIR failure. The intra-HO

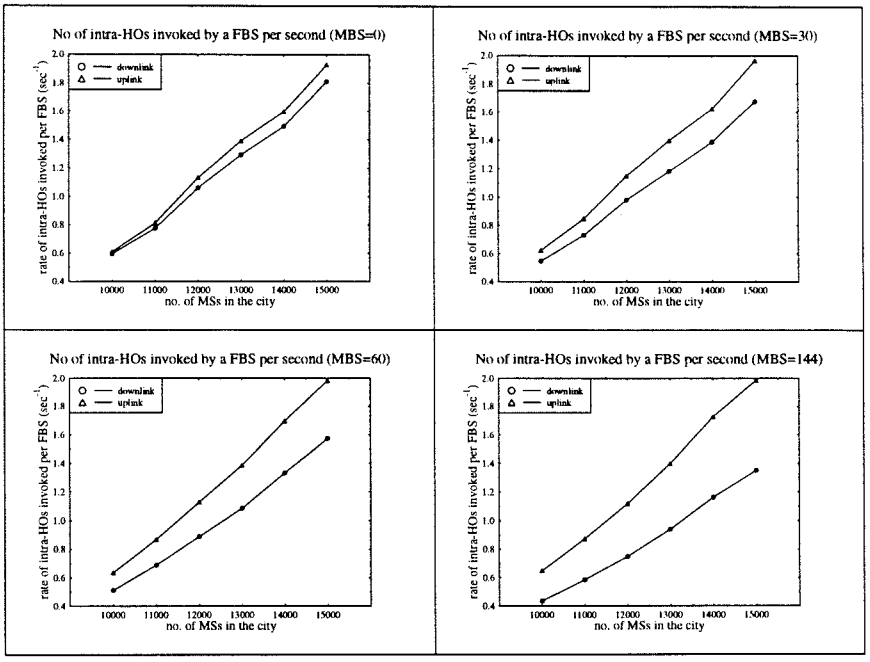

Figure 4.4: Rate of intra-HOs invoked by s FBS

request rate increases as the density of MSs increases. When we employ more MBSs, the intra-HO request rate due to downlink SIR failure decreases. However, the intra-HO request rate due to uplink SIR failure remains roughly the same regardless of the number of MBSs employed. Employment of MBSs seems to improve the downlink quality. Figure 4.5 shows the rate of intra-HOs that successfully occurred at a FBS. Simulation results demonstrate that intra-HO is usually successful. Unsuccessful intra-HO resulting in an inter-HO rarely occurs. In fact, only a very few of many simulation runs record such event, and the highest reported probability of intra-HO failure is 7×10^{-7}.

An inter-HO is evoked if the uplink or the downlink signal level falls below the threshold, or if an intra-HO fails to maintain the SIRs at an acceptable level. The last case has been shown by the simulation to be negligible. Note also that although the uplink pathloss is the same as the downlink pathloss in the case of LOS, it is not true for the OOS situation. Figure 4.6 shows the rate of inter-HOs requested by a FBS. The inter-HO request rate is proportional to the number of users connected to the FBS, i.e. the FBS's carried traffic.

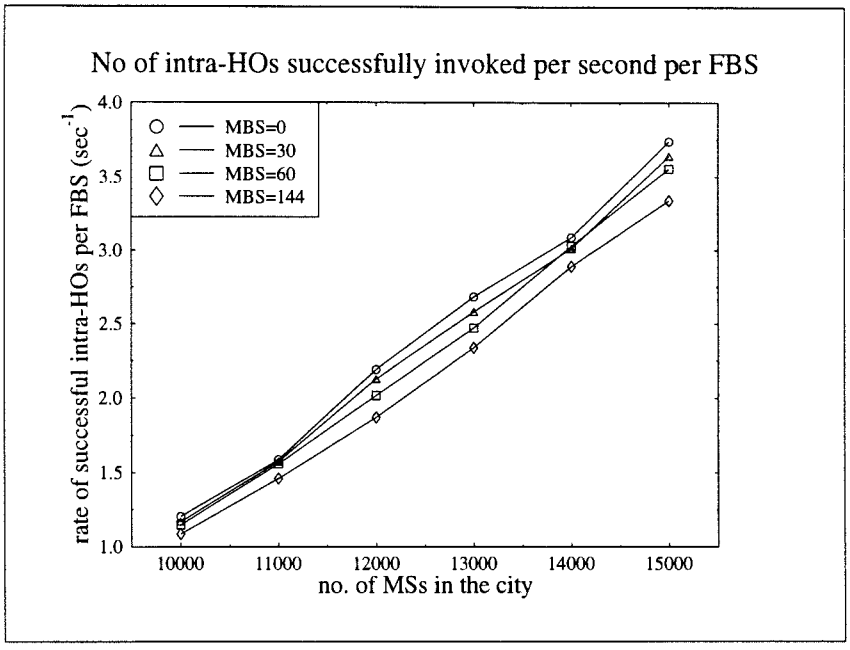

Figure 4.5: Rate of successful intra-HOs per FBS

Thus the inter-HO request rate increases with increasing MS density, and decreases with increasing number of MBSs employed. Figure 4.7 shows the rate of inter-HOs successfully transferred to a FBS.

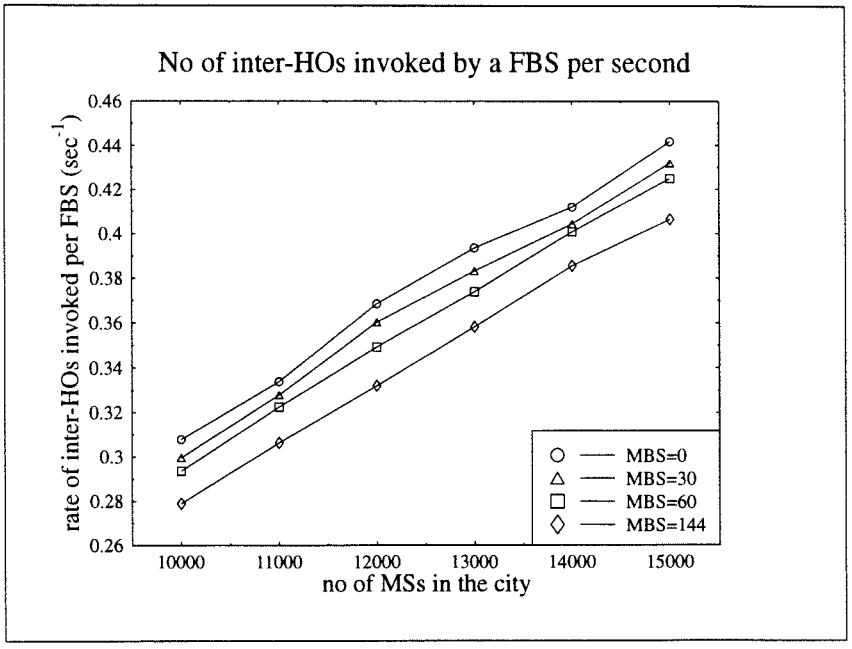

Figure 4.6: Inter-HO request rate per FBS

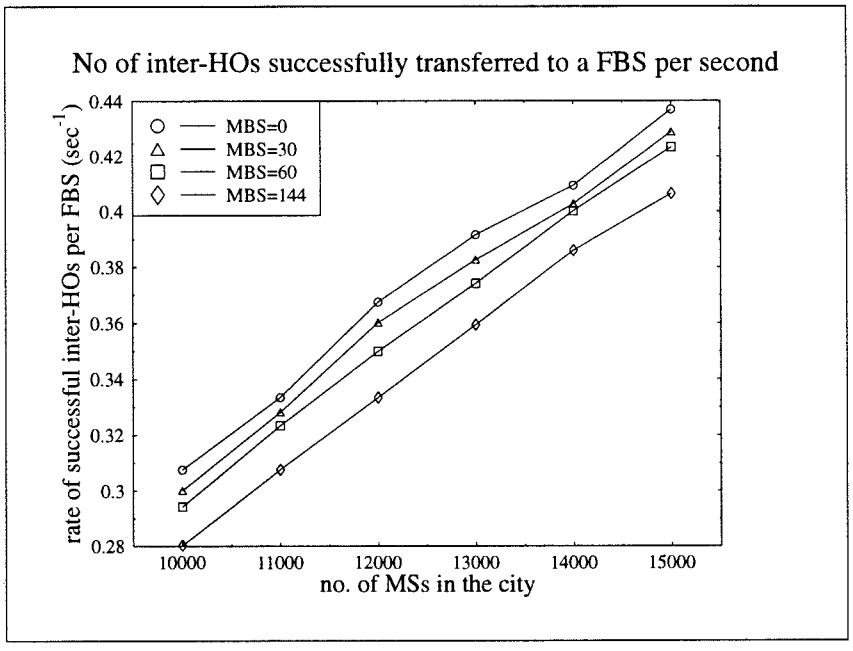

Figure 4.7: Rate of successful inter-HOs per FBS

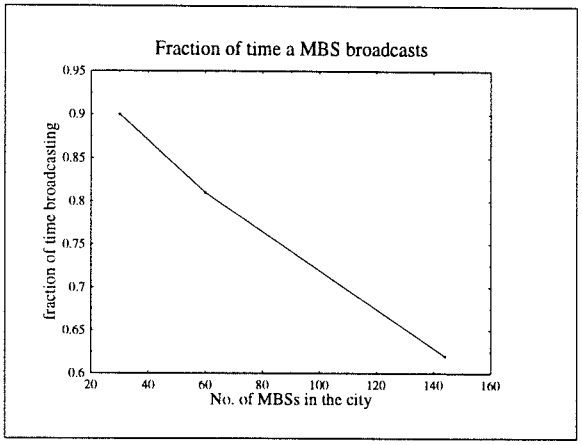

Figure 4.8: Fraction of time a MBS broadcasts

4.1.4 MBS Statistics

Since only one MBS is allowed to broadcast per zone, the fraction of time a MBS broadcasts is inversely proportional to the MBS density. Figure 4.8 shows that even when the number of MBSs employed is as low as 30, a MBS still has a 10% chance of not being allowed to broadcast. When the number of MBSs increases to one MBS per zone (i.e. 144 MBSs), the MBSs are broadcasting only just over 60% of their times. This indicates that these roaming MBSs are unevenly spaced and explains their lower carried traffic when compared with the FBS carried traffic. The MBS carried traffic is shown in Figure 4.9. Traffic carried by a FBS is approximately four to five times that carried by a MBS. As the number of MBSs increases the carried traffic per MBS decreases. When we divide the carried traffic into new call traffic, HO traffic from FBS and HO traffic from MBS, it gives a similar pattern to that obtained for the FBS. The majority of the traffic comes from the HO traffic handed over from a FBS.

Figure 4.10 shows the average connection time between a MBS and a MS. Again we divide the users into new call users, HO users from another MBS and HO users from a FBS. The longest connection time with a MBS is from new call users, approximately 21 sec, followed by HO users from MBS and HO users from FBS. This order is the opposite to the FBS statistics. The longest connection time with a FBS is from HO users from FBSs, approximately 18.5 sec, followed by HO users from MBSs and new call users. However, the

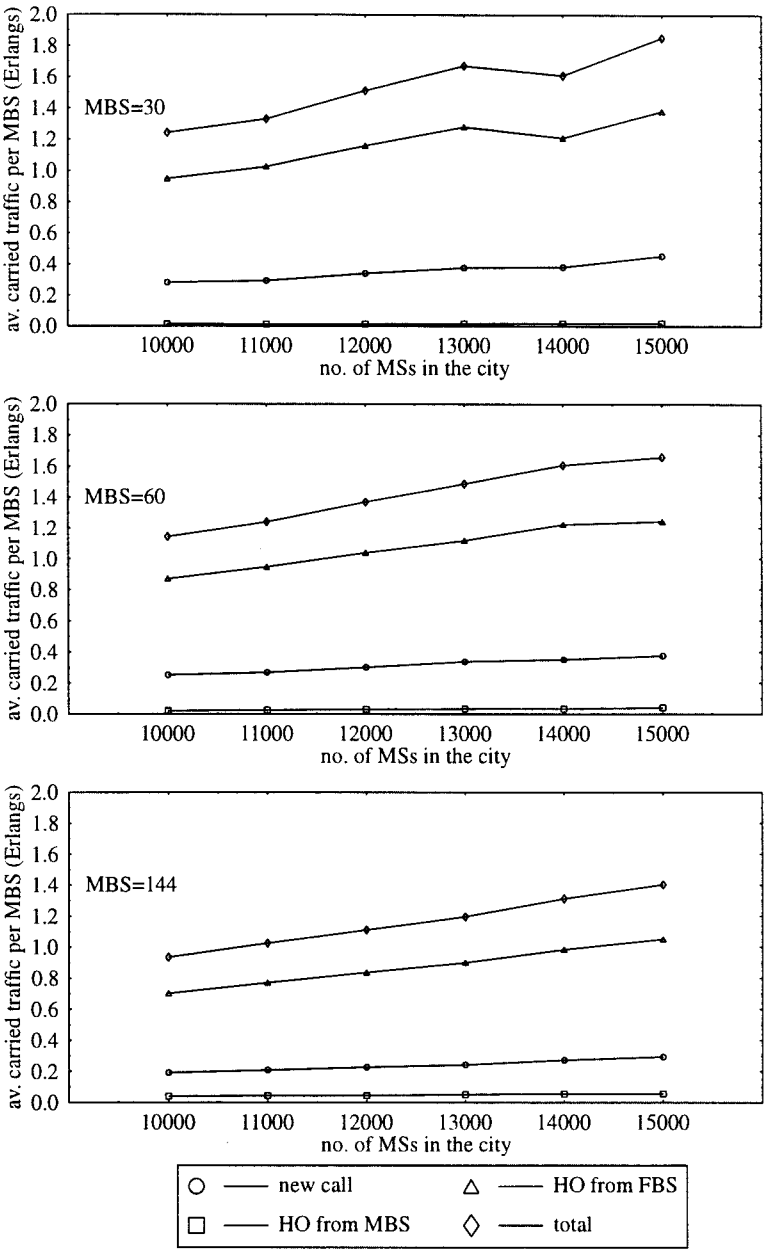

Figure 4.9: Average traffic carried by a MBS for new call users, users handed over from a FBS and users handed over from another MBS

majority of the carried traffic come from users who were previously handed over from a FBS for both cases. Consequently, the overall mean connection time for a MBS is approximately 15 sec which is lower than that for a FBS which is between 16 to 18 sec. A HO between two MBSs is rare especially when the number of MBSs employed is low. Hence there are fewer data samples collected for users who were handed over from one MBS to another MBS, resulting in a less smooth curve as seen in Figure 4.10.

The rate of intra-HOs invoked by a MBS is shown in Figure 4.11. It is lower than that for a FBS. This is because MBSs carry less traffic than FBSs. The number of intra-HOs evoked due to insufficient downlink SIRs is higher than due to insufficient uplink SIRs. This is the opposite to the FBS case. As the number of MBSs employed increases, the rate of intra-HOs evoked due to insufficient downlink SIR reduces while the rate of intra-HOs due to insufficient uplink SIR remains the same. Figure 4.12 shows the rate of intra-HOs that successfully occur at a MBS. The probability that a MBS fails its intra-HO is minute.

Figure 4.13 and Figure 4.14 shows the rate of inter-HOs invoked by a MBS and the rate of inter-HOs successfully transferred to a MBS, respectively. The number of inter-HO activities that took place at a MBS is lower than FBS, because MBS carries less traffic than FBS.

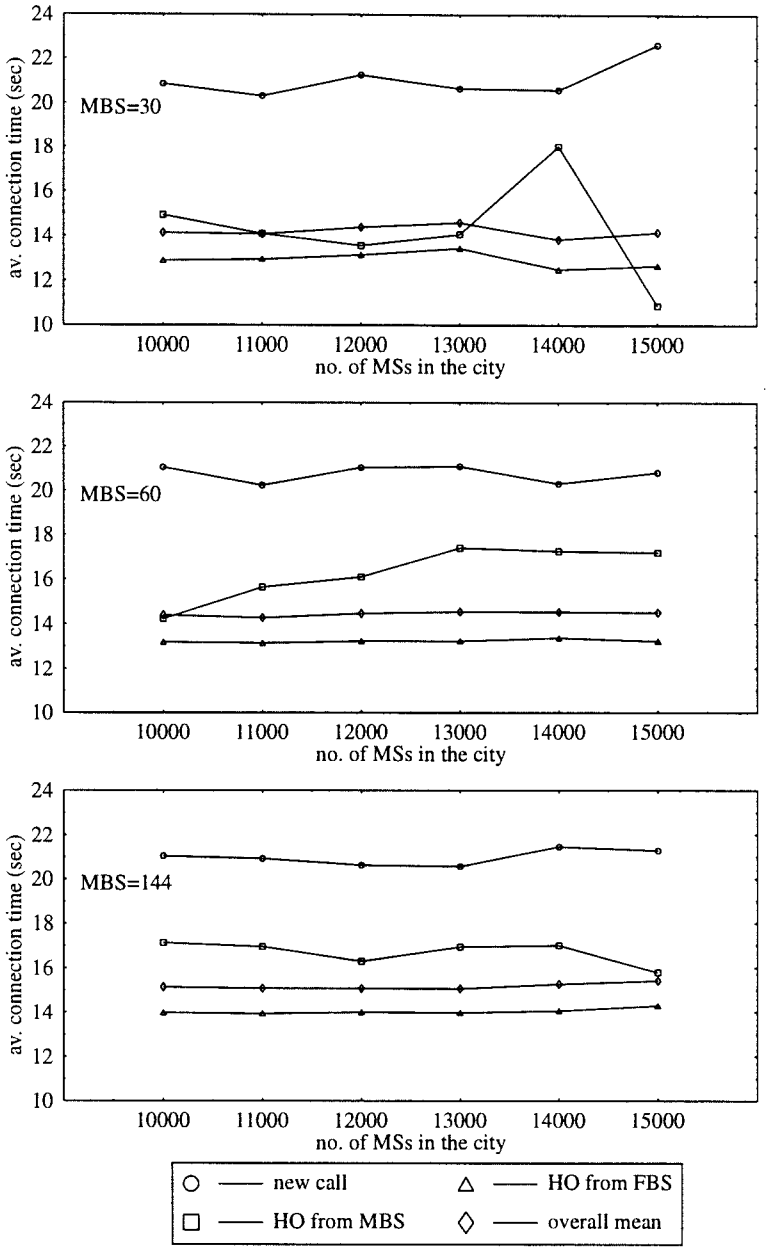

Figure 4.10: Average connection time with a MBS for new call users, users handed over from a FBS and users handed over from another MBS

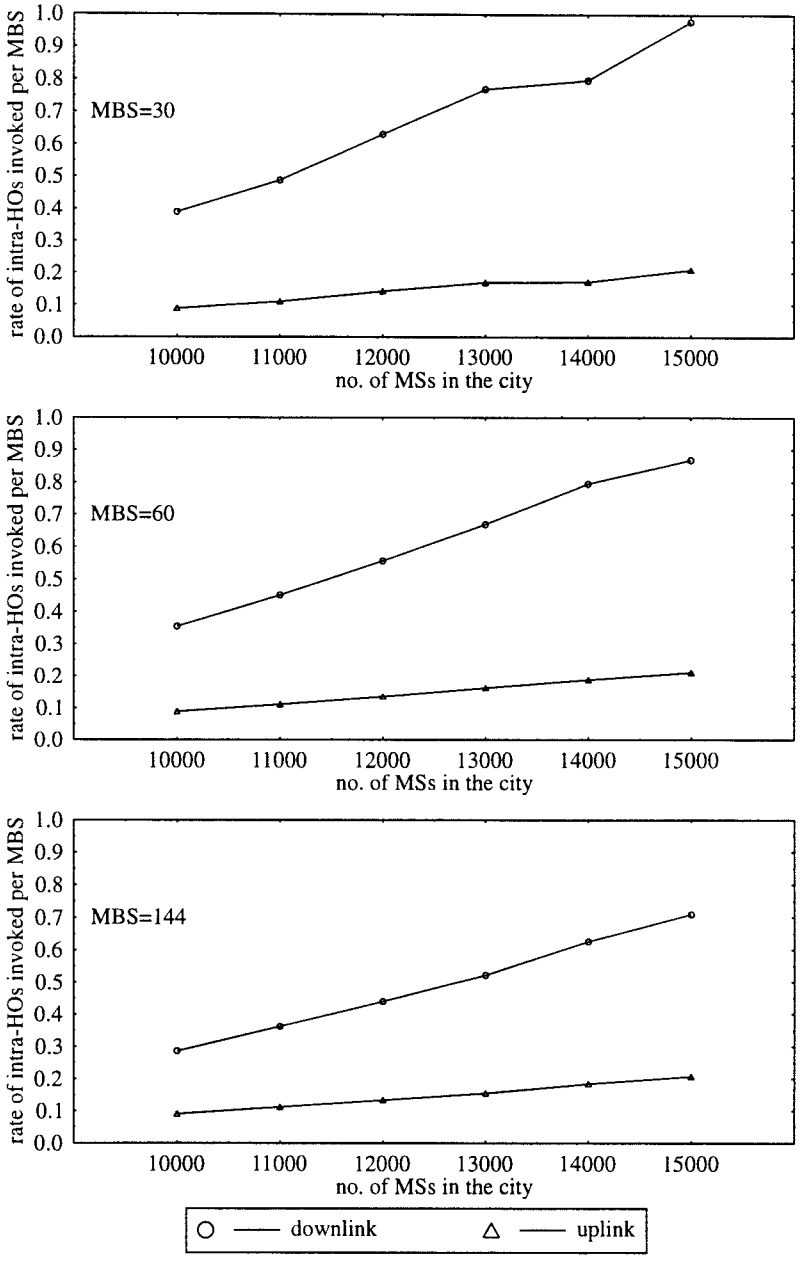

Figure 4.11: Number of intra-HOs invoked by a MBS per second

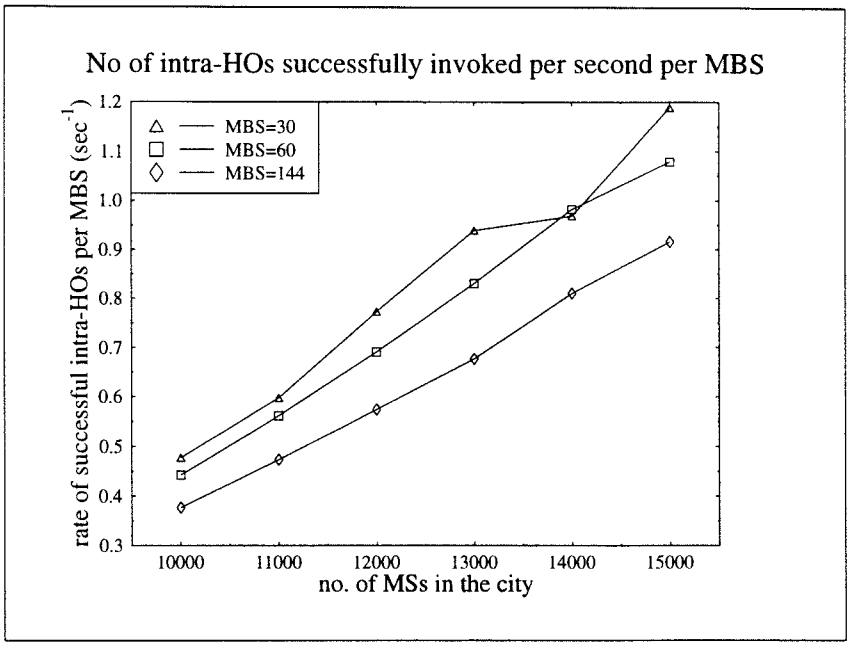

Figure 4.12: Rate of successful intra-HOs per MBS

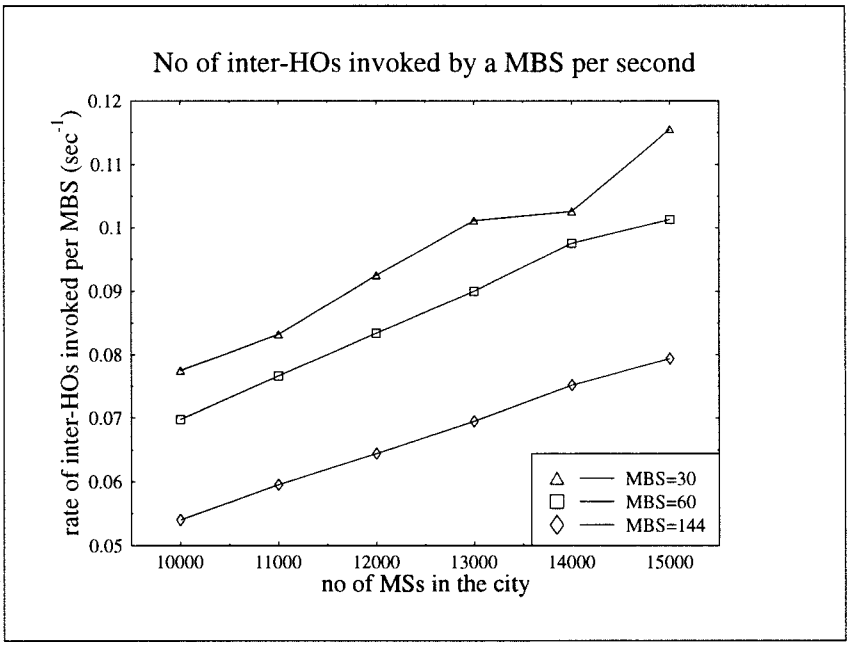

Figure 4.13: Rate of inter-HOs invoked by a MBS

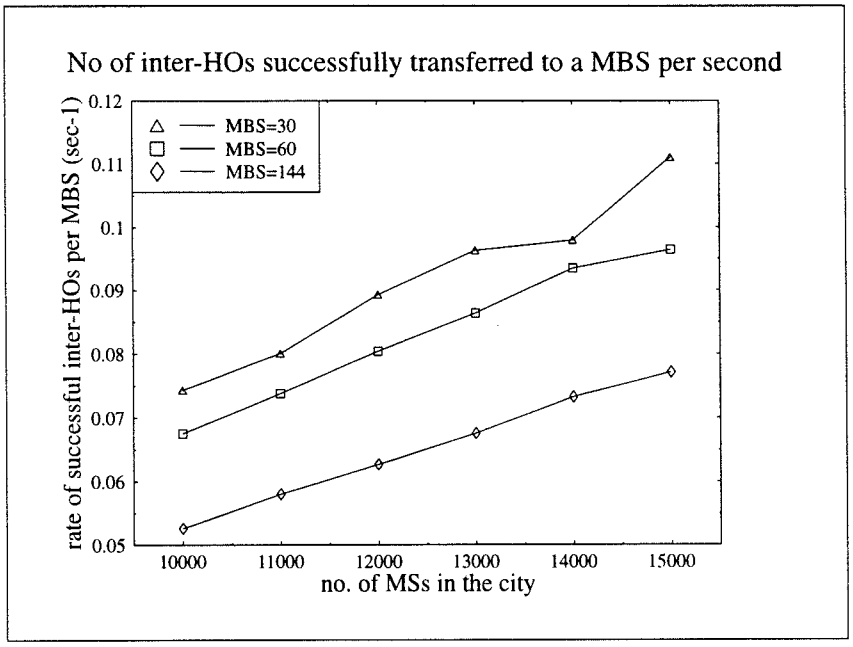

Figure 4.14: Rate of successful inter-HOs per MBS

4.1.5 Mobile User Statistics

Figures 4.15 and 4.16 show the average number of intra-HOs and inter-HOs a mobile user experiences per call. As we increase the user density, the cochannel interference experienced by users increases. More intra-HOs are evoked to ensure that links have an acceptable SIR. When we employ more MBSs, we increase the carried traffic resulting a higher cochannel interference level and thus a higher number of intra-HOs occur. The number of inter-HOs per call, on the other hand, decreases as we increase the user density. This is because of the dramatic increase in the forced termination probability, P_F, at the high level of offered traffic. As we employ more MBSs, the forced termination probability decreases. Hence the number of inter-HOs per call increases. The mean call duration is 120 sec. As the MSs are travelling at 6 m/s, they cover 720m per call. The FBSs are 120m apart, and consequently we would expect the average number of inter-HOs per call to be around six. The number of intra-HOs per call is far more than the number of inter-HOs.

Figure 4.17 shows the forced termination probability versus the number of MSs in the city. The forced termination probability increases exponentially with user density. The employment of MBSs significantly decreases the forced termination probability. A similar result is seen for the new call blocking probability shown in Figure 4.18. The forced termination probability is higher than the new call blocking probability. There are various techniques that can be employed to trade the new call blocking probability for the forced termination probability, such as the use of guard channels [12, 14], deployment of overlaying macrocell [7, 8] and queueing of HO requests [13, 60, 15]. However, these techniques have already been extensively studied by other researchers. Our objective is to study the employment of MBSs.

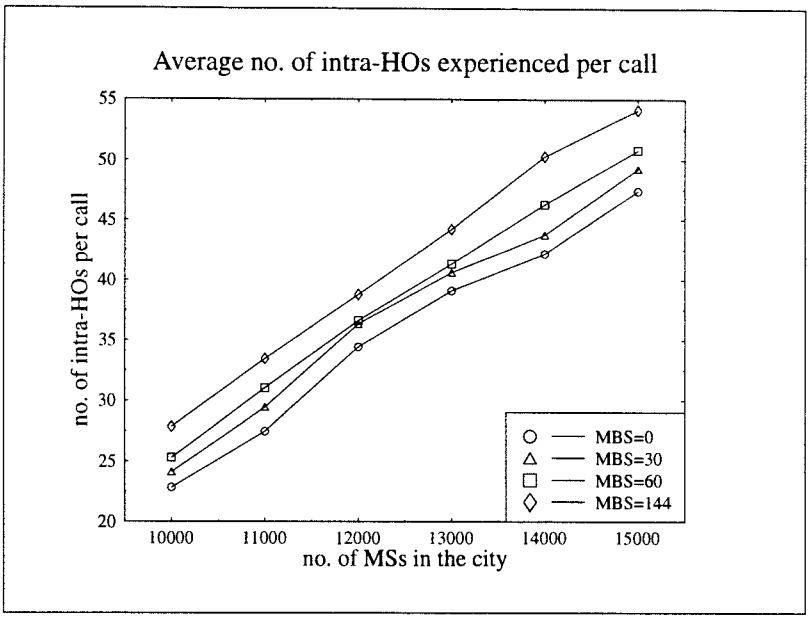

Figure 4.15: Average number of intra-HOs experienced by a mobile user per call

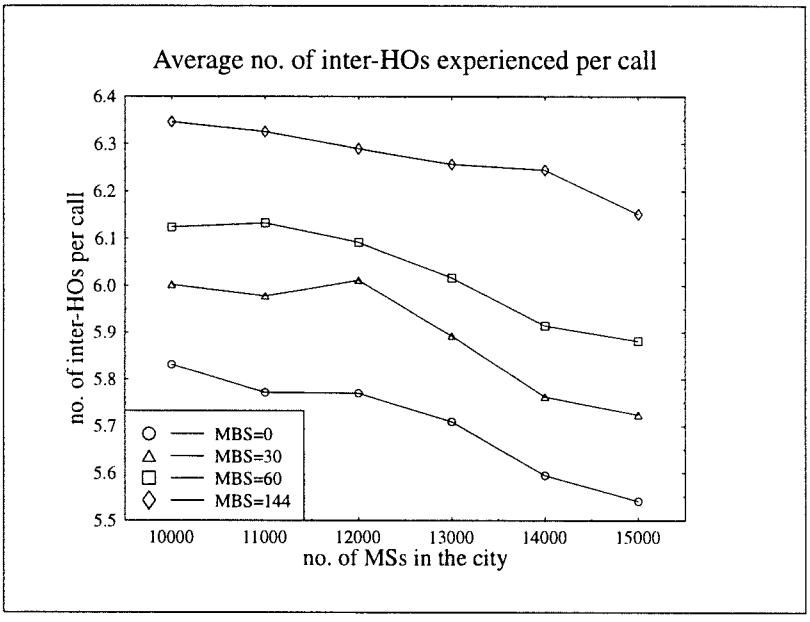

Figure 4.16: Average number of inter-HOs experienced by a mobile user per call

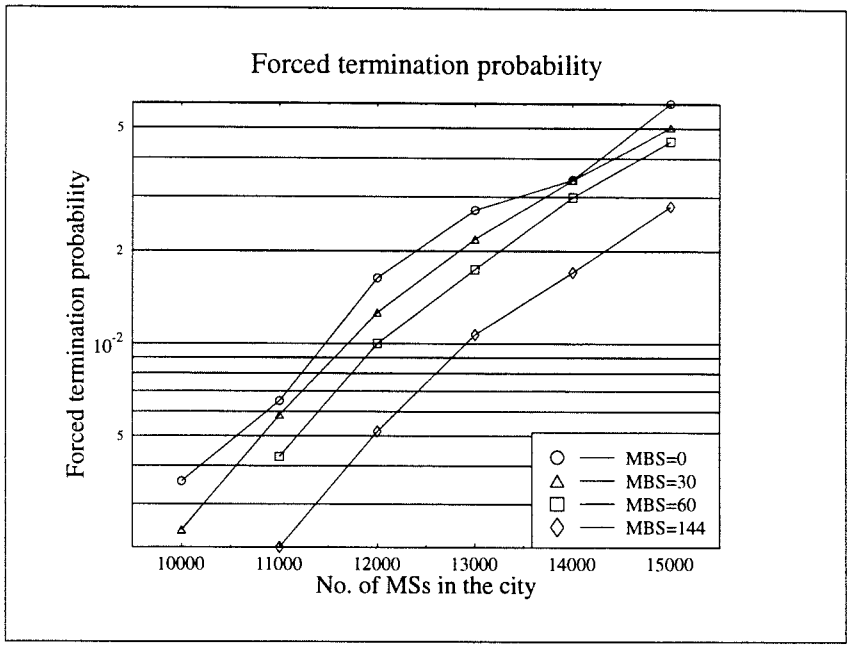

Figure 4.17: Forced termination probability, P_F

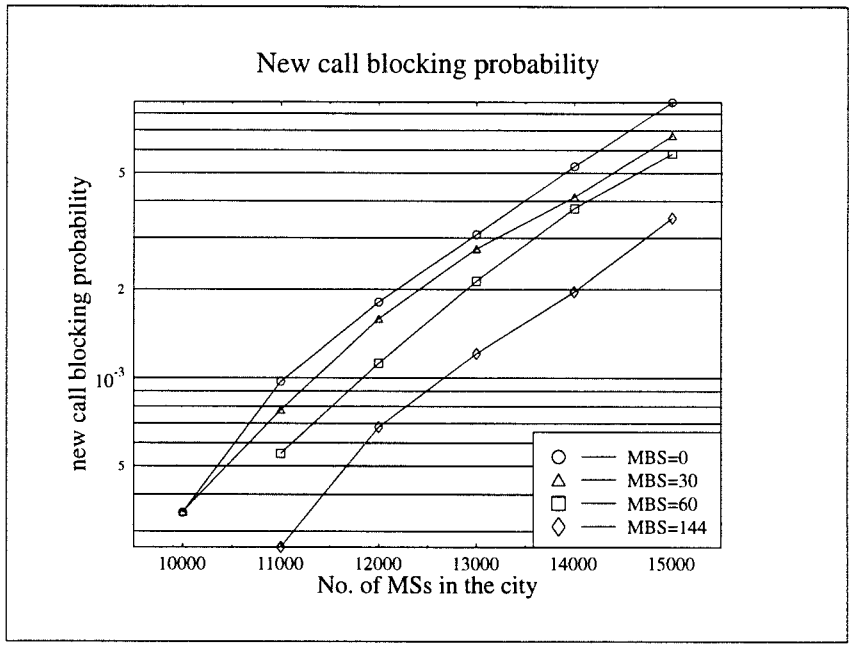

Figure 4.18: New call blocking probability, P_B

4.1.6 Non-uniform Teletraffic Demand

We have showed that the employment of MBSs improves both the blocking and dropping probabilities. However, the simulation results also showed that the amount of teletraffic carried by a MBS is less than a FBS. This is because the separation between the MBSs varies as the MBSs roam in the city. On the other hand, the FBSs are pre-planned to be placed uniformly as the teletraffic demand is uniformly distributed. Thus if we replace the MBSs with the FBSs of the same number, we would expect a better performance. However, in practice, the teletraffic level is usually non-uniform and varies with time. Since the teletraffic distribution is unknown and variable, the pre-planning of FBS sites becomes tenuous. There is an advantage in employing MBSs. In this section, we will study the performance of the MBSs in situations where the teletraffic level is non-uniform.

Figure 4.19 shows the same city we used in our previous simulations. However, this time we will create a vehicular traffic jam in the central shaded area. Vehicles entering this region will reduce their speed from 6 m/s to 1 m/s. Consequently, the density of MSs in this shaded region is increased by six fold. Relevant statistics are collected for both the congested region and the non-congested region.

Figures 4.20 and 4.21 show the probability density function (PDF) of the uplink SIR when the MS resides in the congested and non-congested areas, respectively. Both figures show that the shape of the PDF envelop is more affected by the number of MBSs than by the MS population. The probability that an uplink TCH has a high SIR level is greater when the number of MBSs employed is larger. This is because the average distance between a MS and its serving BS is shortened. The figures also show that the uplink TCH SIR is better in the congested area than in the non-congested area.

The situation is perhaps clearer in Figure 4.22, where we express the quality of an uplink TCH in terms of the fraction of time the uplink SIR is greater than 30dB. In both areas, the uplink quality is improved when more MBSs are employed. However, it is unexpected that the uplink quality is higher for higher MS population. Furthermore, in the congested area, the uplink SIR is greater than 30dB for between 65 to 95 percent of the time. On the other hand, it is only so between 24 to 42 percent of the time for the TCHs in the non-congested area. The improvement in the uplink SIR at high MS density

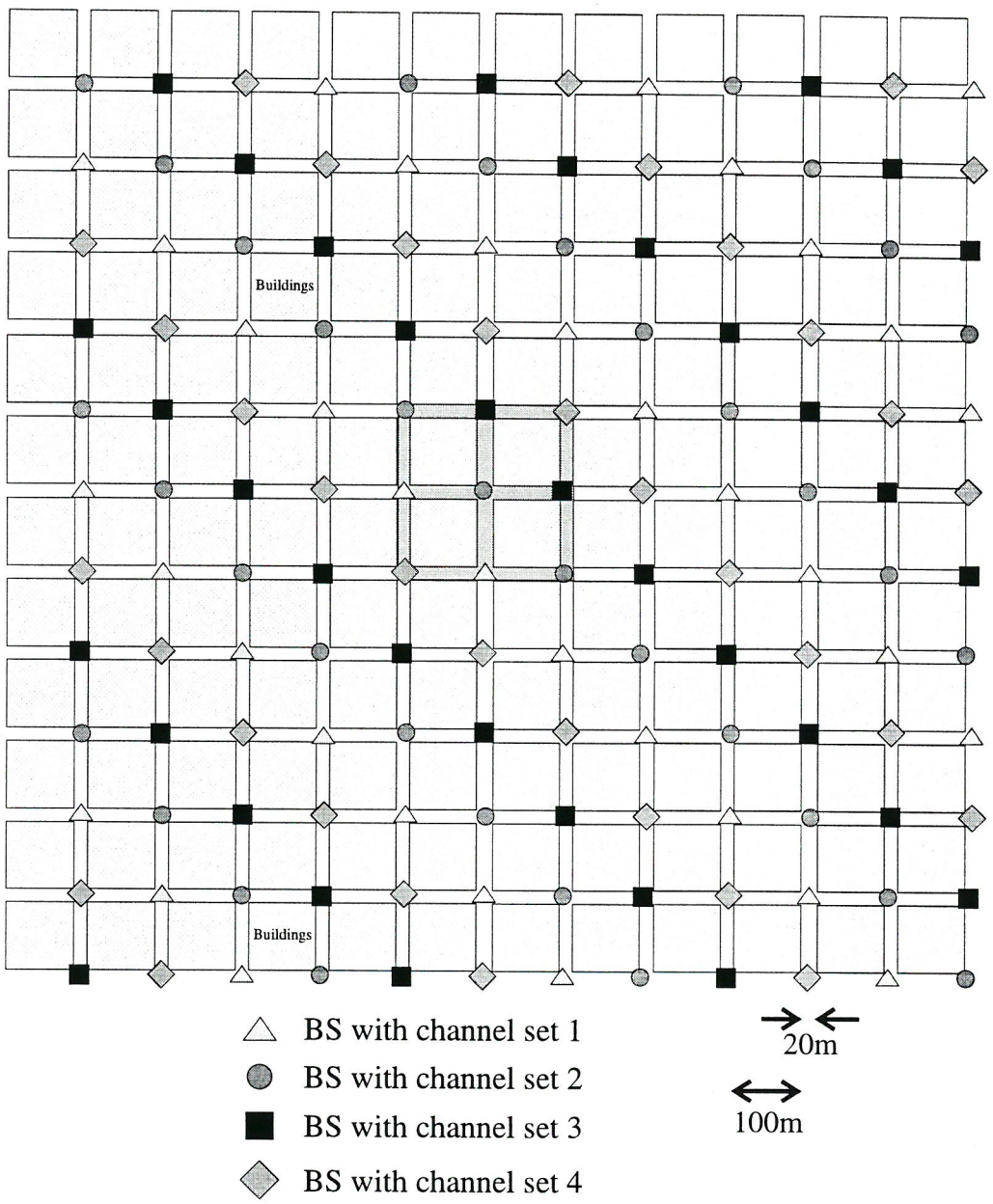

Figure 4.19: A diagram showing the congested region (shaded area)

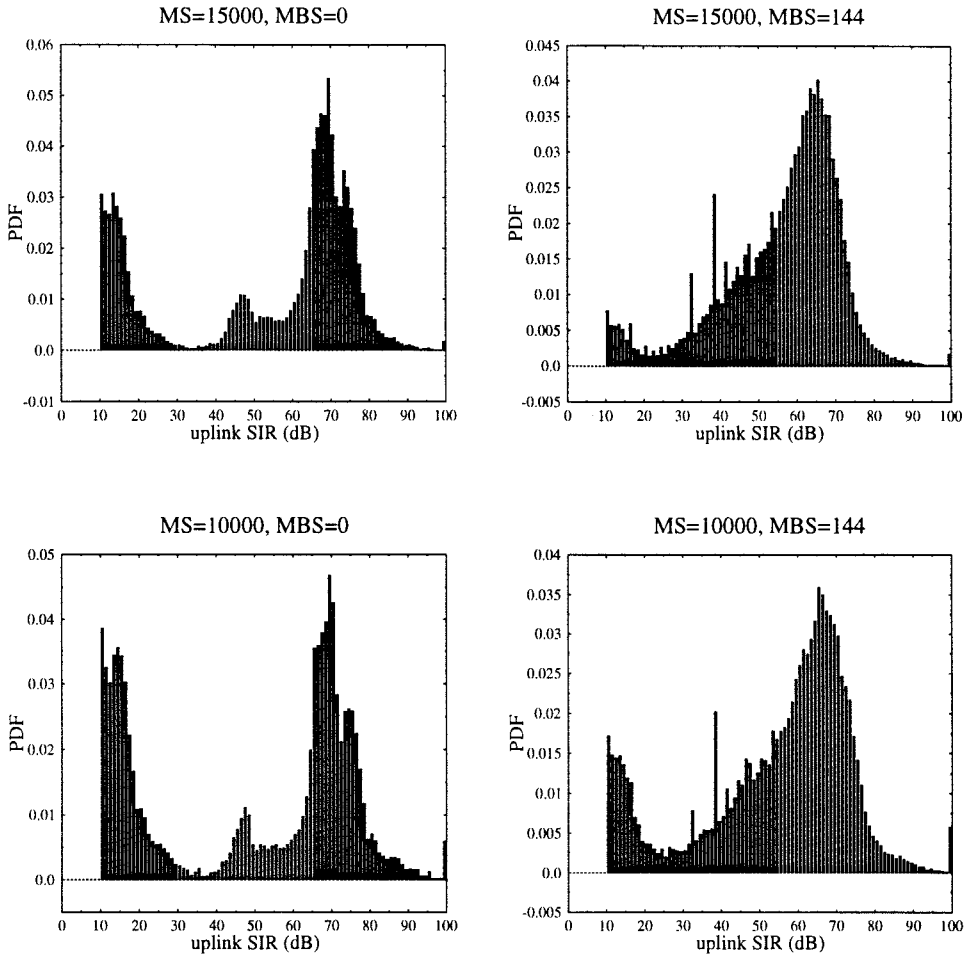

Figure 4.20: Probability density function of the uplink SIR for MSs residing in the congested area

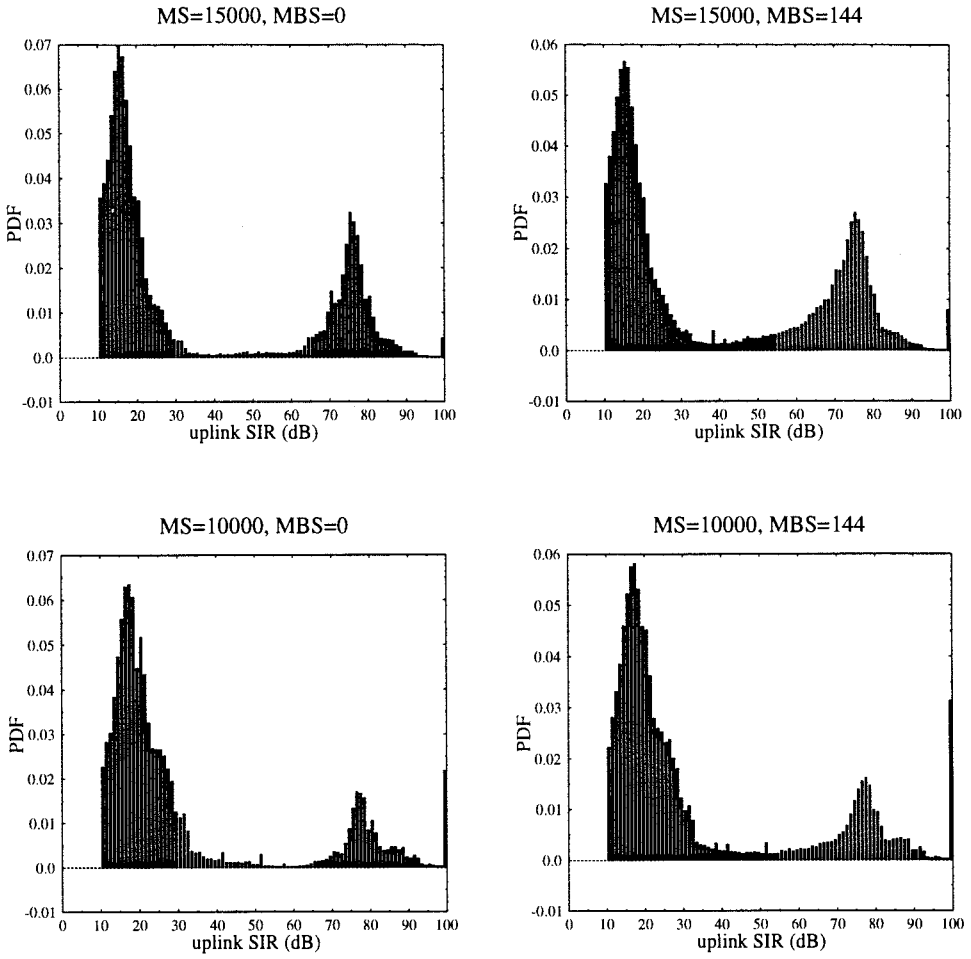

Figure 4.21: Probability density function of the uplink SIR for MSs residing in the non-congested area

is explained when we examine the level of intra-HO activities.

Figure 4.23 shows the average number of intra-HOs per call when MSs reside in either the congested or the non-congested areas. In the congested area, there is as high as 90 intra-HOs evoked per call. As the MS density is increased, the number of intra-HOs per call in the non-congested area increases, while that in the congested area is almost constant. This indicates that for the range of MS density considered, the system is almost saturated in the congested area, while there is still available capacity in the non-congested area.

When the MS density is low and there is a low level of offered traffic, the BSs assign TCHs from their own nominal channel set. This means the radio channels are reused at least a minimal reuse distance away. As the offered traffic increases, the level of cochannel interference increases. However, as long as the channels are assigned from the nominal channel set, the SIRs are still above the threshold. As the offered traffic increases, the fraction of time a channel experiences low but acceptable SIR increases. However, if we increase the offered traffic further, channel borrowing occurs and this frequently violates the minimal reuse distance condition. In this situation, a radio channel used at one BS site can suddenly experience unacceptable SIR due to a new assignment of a radio channel at a nearby BS site. Consequently, frequent intra-HOs are needed to maintain the link quality. In this case, the radio links either have high SIRs, or SIRs below the acceptable level when intra-HOs are required. This explains the higher SIRs obtained at higher MS densities.

To prove our theory, we re-simulate at a lower range of MS density. Figure 4.24 shows the uplink quality for the new range of MS density. At low offered traffic, the uplink quality decreases with increasing MS density as we expect. The curve then begins to rise when we increase the MS density further, which is what we observed in Figure 4.22. Figure 4.25 shows the carried traffic per FBS in congested and non-congested areas. As each channel set has four pairs of TCHs, channel borrowing occurs when the carried traffic reaches four Erlangs. This happen when the MS population reaches 2000 and 9000 for the congested and non-congested area respectively. They coincide with the minimums of the curves in Figure 4.24. The number of intra-HOs per call for the new extended range of MS population is shown in Figure 4.26. These same characteristics were observed when we examined the downlink

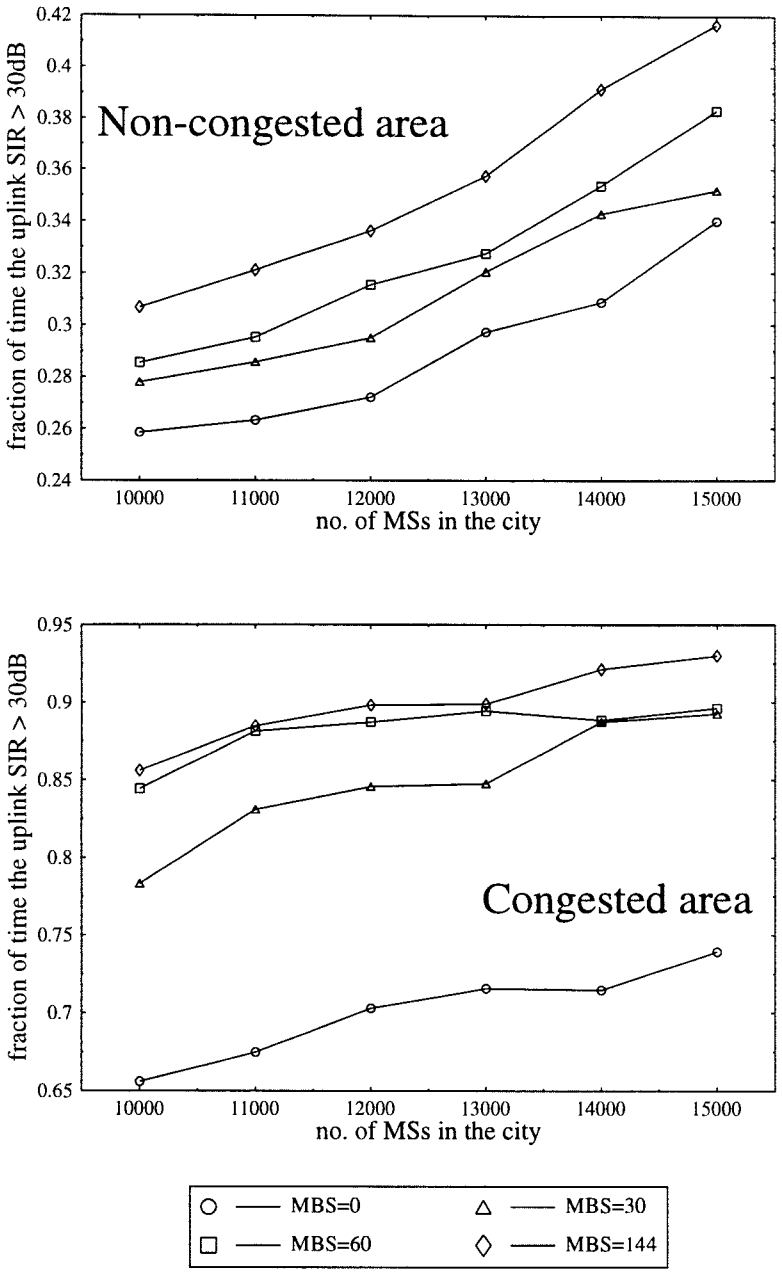

Figure 4.22: Fraction of time the uplink SIR is greater than 30dB while the mobile user resides in the congested and the non-congested areas

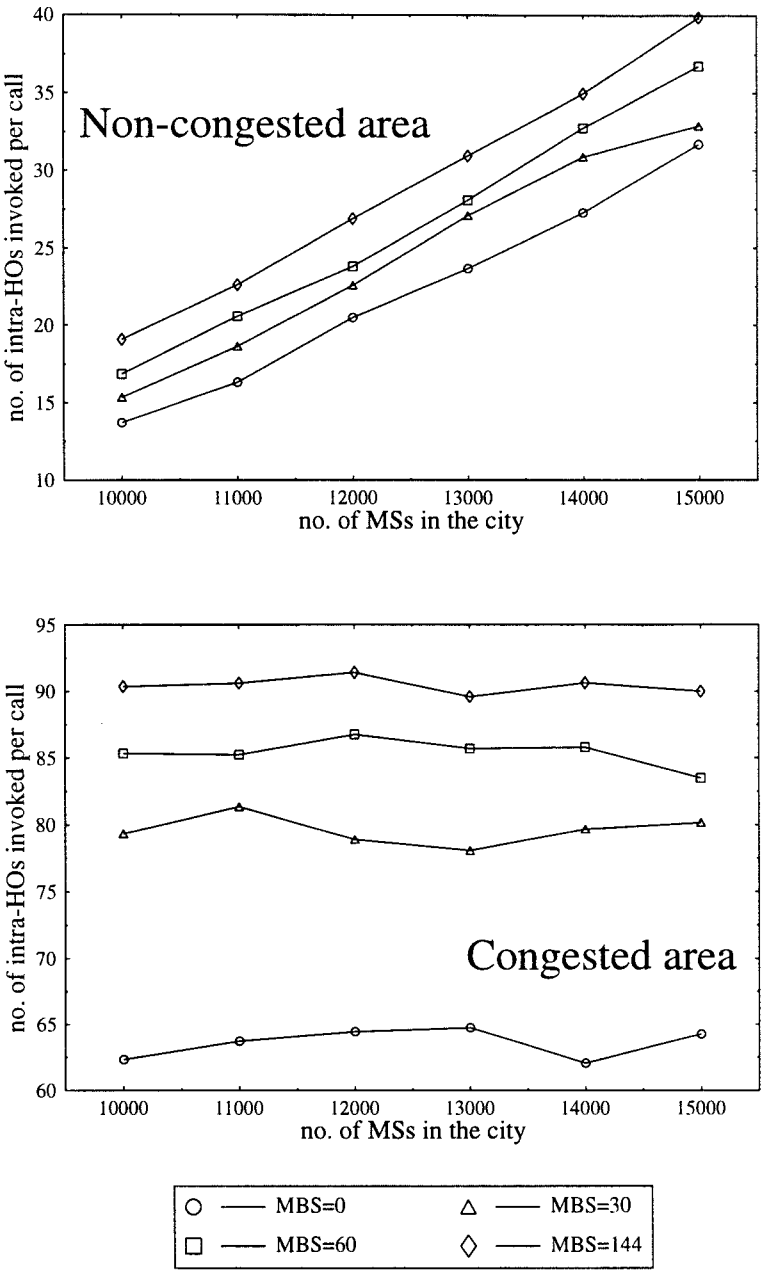

Figure 4.23: Average number of intra-HOs a MS experienced per call while residing in the congested and the non-congested areas

quality.

Another important issue is the average transmission power required from the handsets. This determines the life of the battery, and the compactness of the handset. Figure 4.27 shows the average transmission power of the MS. In our propagation model, pathloss is the only form of signal deterioration, and it directly governs the level of transmission power required. When more MBSs are employed, the average transmission power drops. This is because the average distance between a MS and its serving BS is reduced. The average transmission power when the MS resides in the non-congested area is higher than when it resides in the congested area. This is because the eight FBSs located near the edge of the congested area are 10 metres away from the edge as they lie in the middle of the intersections of the 20 metre wide road, as shown in Figure 4.19. Therefore the average distance between one of these FBSs and their MSs that reside inside the congested area is slightly shorter than those FBSs in the non-congested area. As pathloss increases exponentially with distance the transmission power also increases exponentially with distance. When a MS just enters the congested region while it is connected to one of the FBSs, it only needs to transmit at extremely low power. Consequently, the statistical mean of the transmission power for the congested area is significantly reduced. The smallest transmitted power is 1.75×10^{-3}mW when the MS is 1 metre away from its serving BS.

Figure 4.28 shows the number of inter-HOs invoked per call when the MS resides in the congested and non-congested areas. MSs residing in the non-congested area travel six times as fast as those residing in the congested area. Consequently there is a higher number of inter-HOs per call in the non-congested area. The number of inter-HOs per call increases when the number of MBSs employed is increased.

The two most important parameters in judging the grade of service (GOS) are the new call blocking probability and the forced termination probability. Figure 4.29 shows that the new call blocking probability is reduced when MBSs are employed. The rate of blocking is higher in the congested area than in the non-congested area as expected. A similar result is seen for the forced termination probability shown in Figure 4.30.

The number of MBSs employed is 0, 30, 60 and 144. Increasing the MBS from 60 to 144 does not significantly decrease the new call blocking nor the forced termination probabilities. This is mainly because of the access

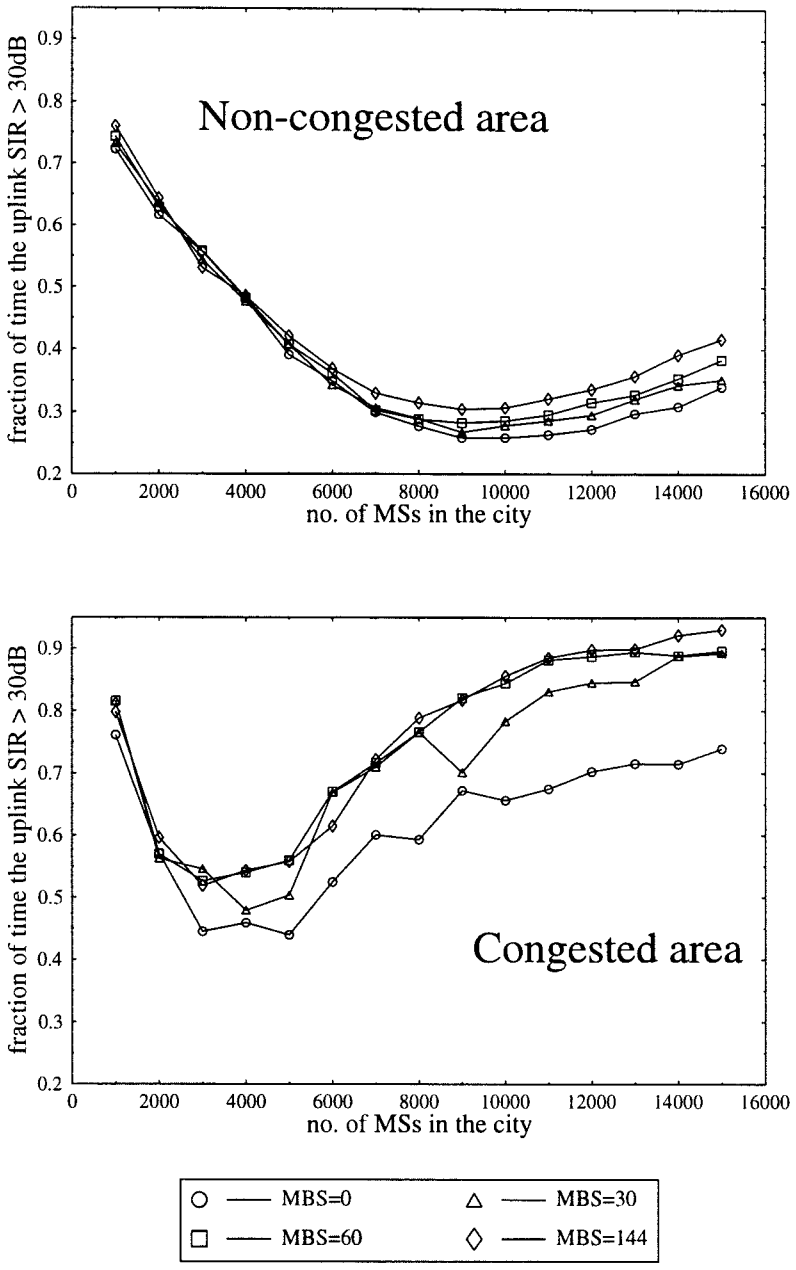

Figure 4.24: Fraction of time the uplink SIR is greater than 30dB while the mobile user resides in the congested and the non-congested areas

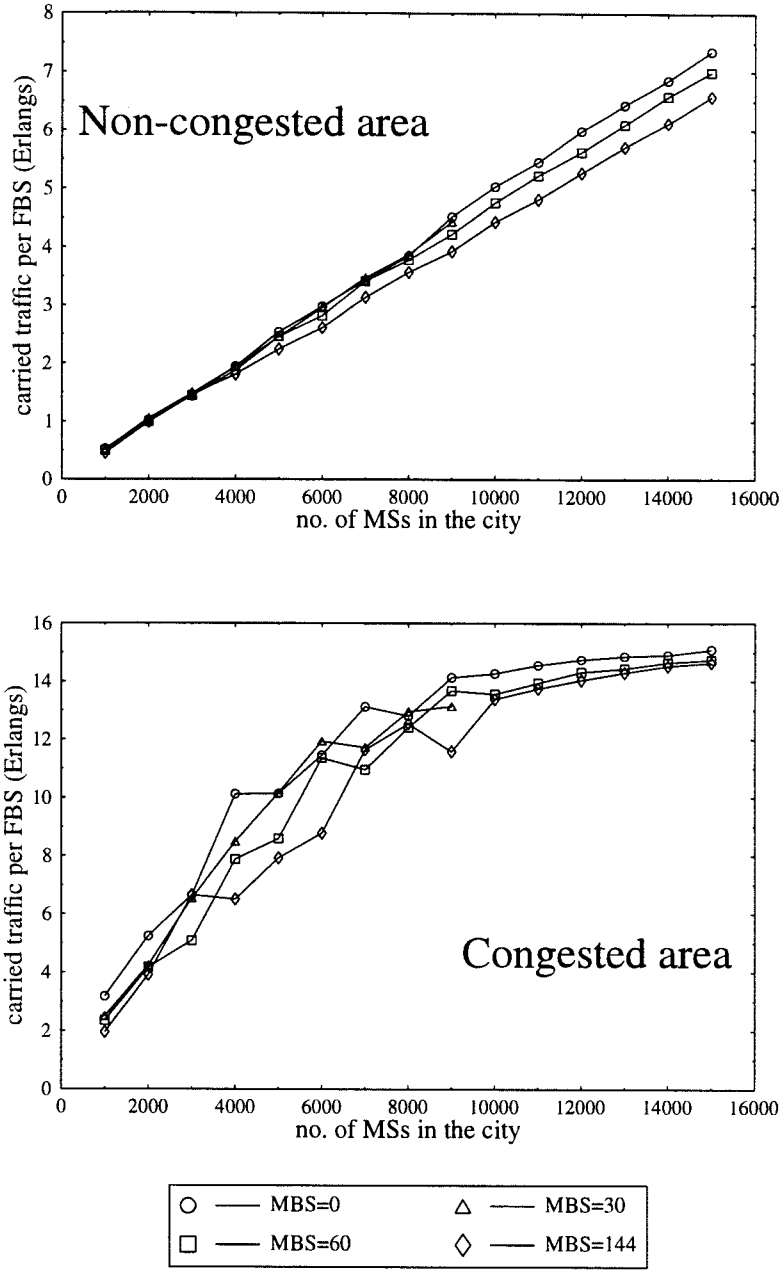

Figure 4.25: Average traffic carried by a FBS in the congested and non-congested areas

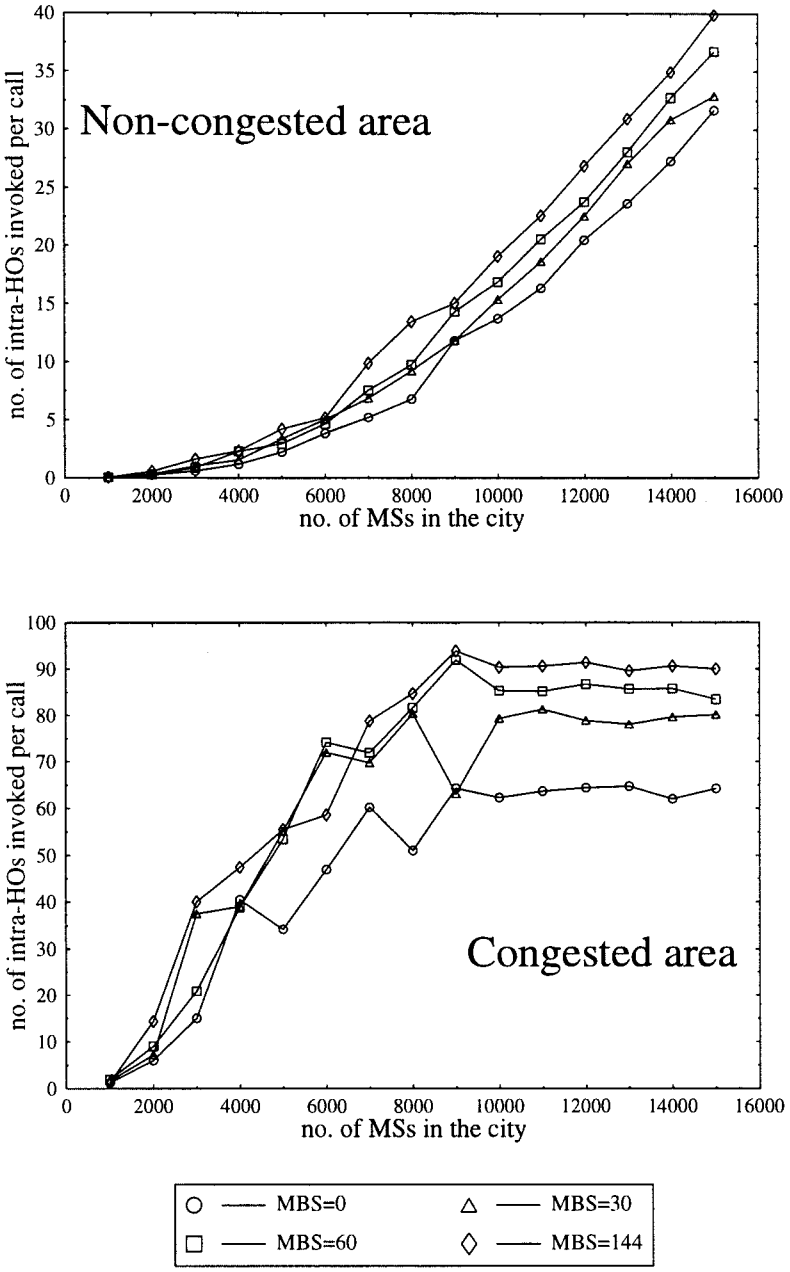

Figure 4.26: Average number of intra-HOs a MS experienced per call while residing in the congested and the non-congested areas

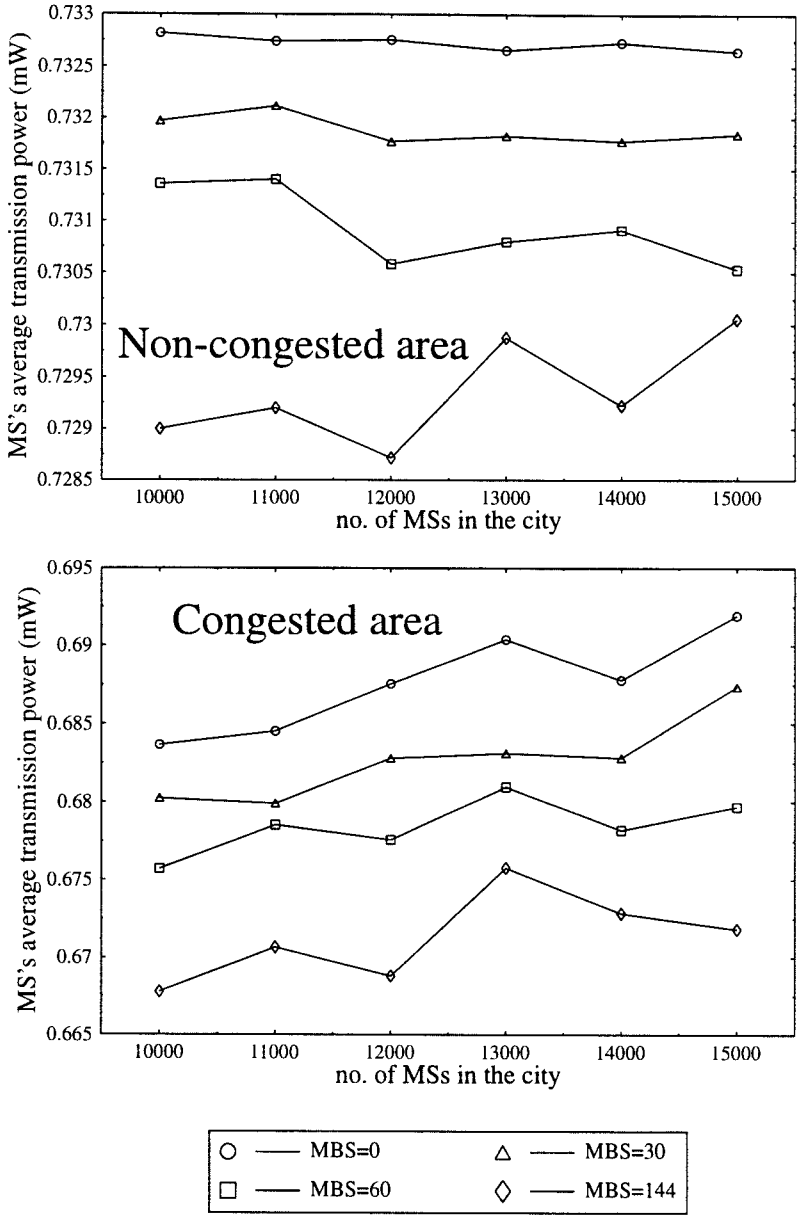

Figure 4.27: Mobile users' average transmission power (mW) while residing in the congested and the non-congested areas

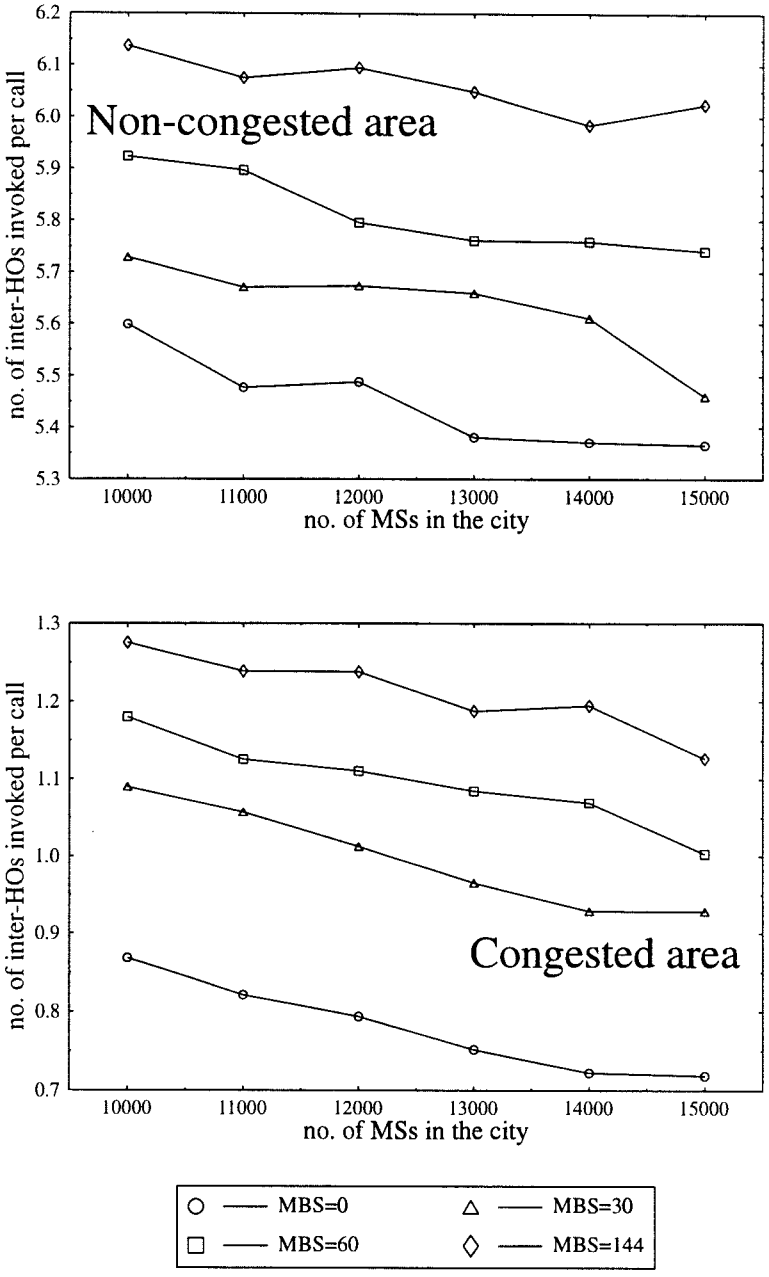

Figure 4.28: Average number of inter-HOs a MS experienced per call while residing in the congested and the non-congested areas

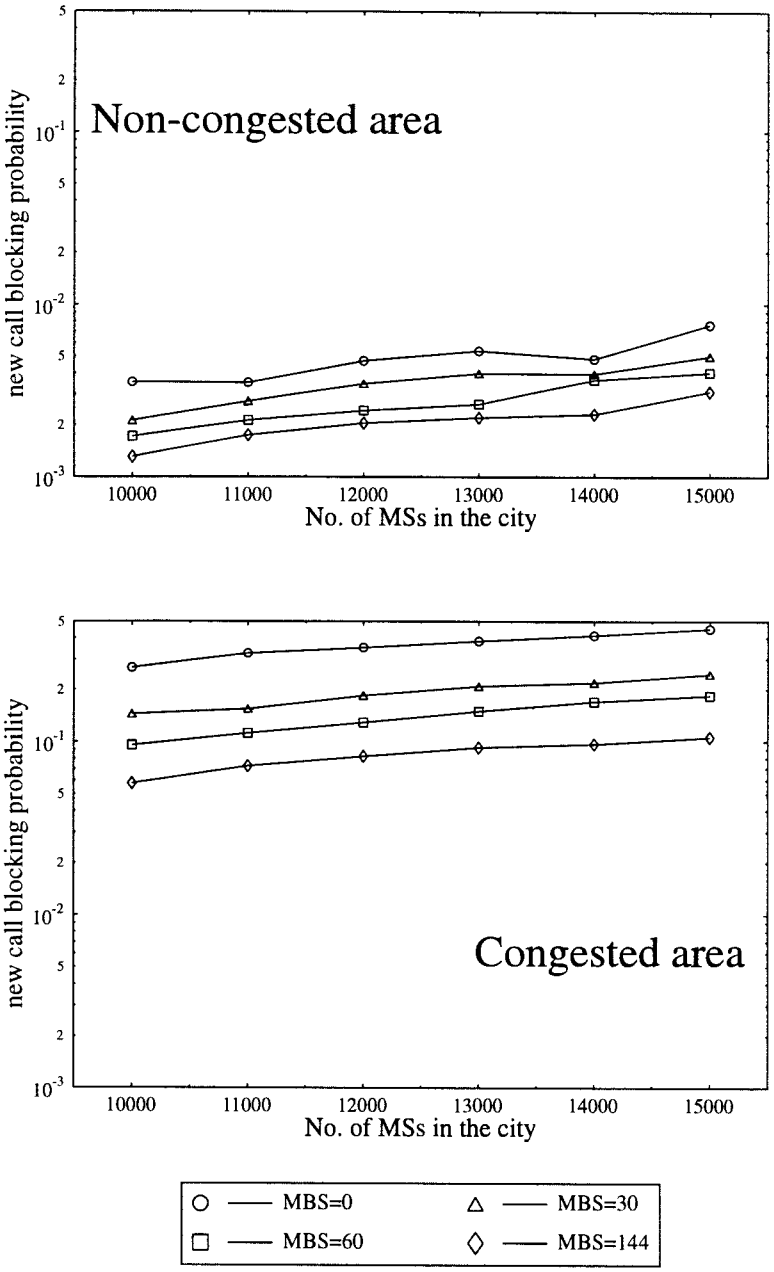

Figure 4.29: New call blocking probability for the mobile users in the congested and the non-congested areas

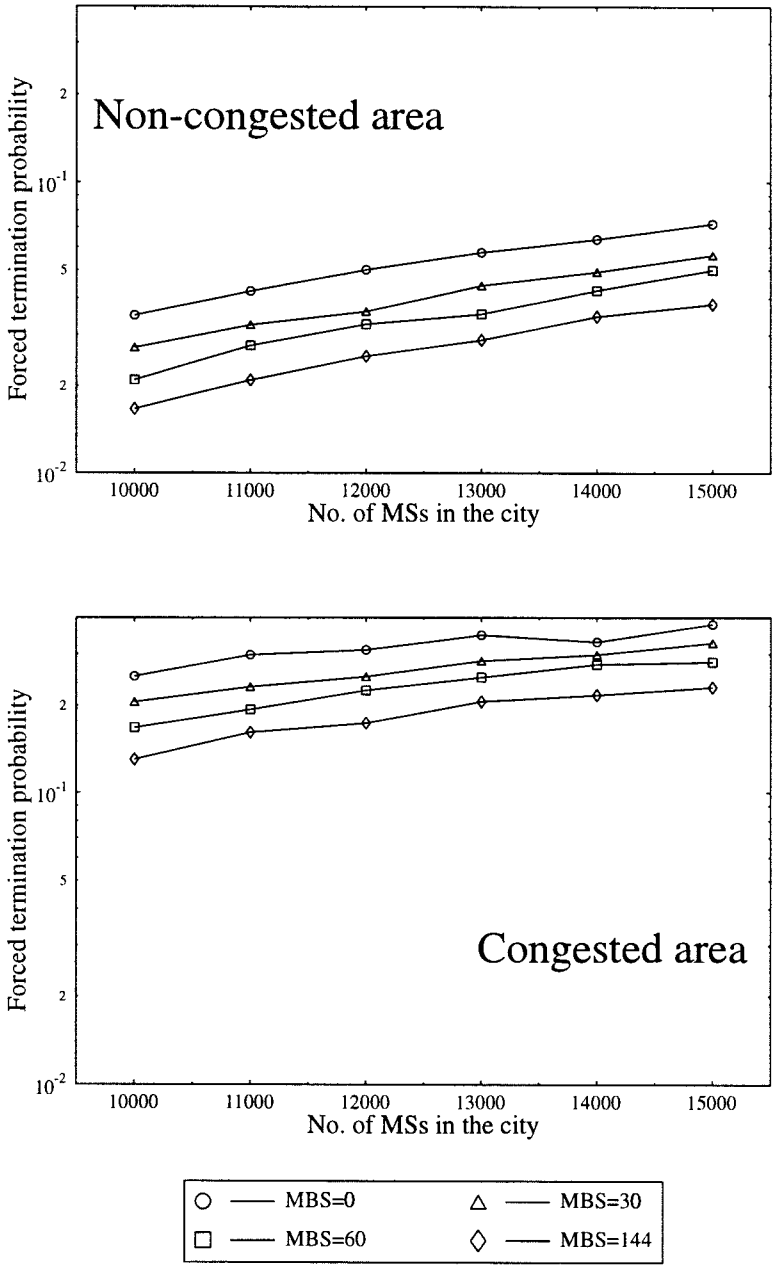

Figure 4.30: Forced termination probability for mobile users in the congested and the non-congested areas

scheme employed. The limitation imposed by the BCCH management forces the number of MBSs allowed to broadcast per zone to be one. This means any new call initiated in any zone can only request at most one FBS and one MBS for a connection. This opposes the original idea of employing MBSs; that is more BSs are available to serve in area where demand is high.

The current scheme allows a connection to be sustained until the radio link quality becomes unacceptable. However, since both the MBSs and the MSs are mobile, there are situations where a MBS becomes closer to the MS than the MS's current serving BS. In such a situation, an inter-HO would mean a reduction in transmission power. Thus both the MS in question and other cochannel MSs would benefit. In the next section, we will study another access scheme which addresses these problems.

4.2 Power Escalation Access (PEA) Scheme

In the last section, we encountered the problems that occur when BCCHs are required in the network access procedure. We will now study an access scheme which does not require the use of BCCHs. When a MS requests a connection, it transmits a request signal on a dedicated random access channel (RACH) on the uplink. If any nearby BS receives this signal, it will reply via the dedicated access grant channel (AGCH) on the downlink. All BSs must listen to the RACH at all times. Both the RACH and the AGCH are collision type channels. The MS first transmits the request signal at some predefined minimal power level. If it does not receive any reply at timeout, it increments its transmission power. Hence we call this procedure power escalation access (PEA). When the MS reaches the maximal transmission power and still receives no reply, the new call is blocked and the request is terminated. This way the BS located nearest to the MS would receive the request signal first. If this BS cannot find an adequate channel to serve this MS, a request is made to other BSs in ascending order of their associated path losses. All BSs in the vicinity are eligible for connection.

In GSM, a BCCH physical channel contains a BCCH logical channel, as well as a frequency correction channel (FCCH), a synchronisation channel (SCH) and others. It is the FCCH and the SCH that a BCCH physical channel is required to broadcast at constant power at all times in order to allow the mobiles to camp on the network. Here we assume that only the FBSs broadcast the FCCH and the SCH, and both the MBSs and the MSs synchronise to the FBSs in their regions. With the PEA scheme, the BCCHs do not take part in the network access mechanism, therefore they are not included in our simulation model. In addition we do not simulate the collision condition on the RACH and the AGCH.

When a mobile makes a new call, all BSs that have vacant channels measure the uplink path losses between this mobile and them. The mobile will then examine these BSs in ascending order of their reported uplink path losses. For each BS examined, the transmission power on the uplink and the downlink must first be adjusted to achieve the wanted received signal power levels. Then the examined BS searches for a TCH that can provide acceptable uplink and downlink SIRs. If a TCH is successfully found, a connection is established. Otherwise another BS will be examined. If none of the BSs

are adequate to serve this MS, the new call is blocked.

The TCH assignment strategies for the FBSs and the MBSs remain the same. Although the MBSs in this scheme do not broadcast, they are still required to identify their residing zones as they roam the city. This is because the TCH assignment strategy for the MBS requires the channel set used by the FBS residing in the same zone as the MBS to be known. Consequently the MBS can search TCHs from the furthest nominal channel set first, and those from the nominal channel set of the nearest FBS last. This procedure encourages the TCHs to be reused at the minimal reuse distance.

4.2.1 Channel Re-arrangement Facility

In addition to the alteration in the network access mechanism, we also include the channel re-arrangement facility in this scheme. All BSs are required to monitor all known uplink TCHs at all times. When the received power level of a given uplink TCH exceeds the pre-defined optimal received level, $\mathrm{Rx}_{\mathrm{opt}}$, it indicates that the uplink pathloss between the transmitting MS and the measuring BS is less than the uplink pathloss between the transmitting MS and its serving BS. In this case, the MS is handed over to the new BS and thereby lower transmission power is required. Consequently lower levels of cochannel interference will be experienced by other MSs. We denote this type of inter-HOs as level-2 inter-HOs. We refer the inter-HOs that are invoked inevitably when the MSs leave their cells as level-1 inter-HOs.

The number of level-2 inter-HOs can be controlled by adjusting a hysteresis threshold factor, δ. Level-2 inter-HO is deployed when the BS receives an uplink TCH whose power level exceeds $\mathrm{Rx}_{\mathrm{opt}} \times \delta$. We set δ to be 2.

For calls in progress, their uplink and downlink pathlosses are measured. If either of them are too high, then level-1 inter-HO is immediately triggered to seek an alternative BS. Failing to do so will result in a dropped call. If both the uplink and the downlink pathlosses are acceptable, the MS applies power control to its uplink so that the serving BS will receive this uplink TCH with a power less or equal to $\mathrm{Rx}_{\mathrm{opt}}$, but greater than $\mathrm{Rx}_{\mathrm{min}}$. All other BSs with vacant channels are instructed to measure this uplink TCH. Any BS whose received power is greater than $\mathrm{Rx}_{\mathrm{opt}} \times \delta$ is an eligible candidate for the level-2 inter-HO procedure. If no BS is suitable for level-2 inter-HO, the MS continues with its current serving BS. In this case, power control is

applied on the downlink, and the uplink and downlink SIRs are measured. If both of them are acceptable, then the MS continues on the same TCH. Otherwise, the intra-HO procedure begins to seek another vacant TCH on the current serving BS. If an adequate TCH is not found, the level-1 inter-HO procedure searches for another BS.

For the level-2 inter-HO procedure, the MS and its current serving BS must temporarily stop transmission on the current uplink and downlink TCH until the level-2 inter-HO procedure completes. Otherwise the correct uplink and downlink SIRs of the new link can not be measured. The BSs are examined in ascending order of their associated pathlosses. For each examined BS, its associated downlink pathloss is measured. If the downlink pathloss is acceptable, a temporary link is established between the MS and this BS. Power control is applied to this link. This BS will then find an adequate vacant TCH for connection. If it succeeds, the MS will disconnect from its old serving BS and re-connect to this BS via the new TCH. If it fails, the next BS will be examined. If the level-2 inter-HO procedure does not find a more suitable BS, the MS resumes transmission with its old serving BS.

4.2.2 Simulation Results

Same as in the standard access scheme, a vehicular traffic jam is created at the centre of the city. Simulation results are collected for both the congested and non-congested areas. Figure 4.31 shows the total traffic carried by all FBSs that reside inside the congested area, and the total traffic carried by all FBSs that reside in the non-congested area. Figure 4.32 shows the corresponding curves for the MBSs.

The total carried traffic in the non-congested area is greater than the congested area because the non-congested area is approximately 21 times bigger than the congested area, and there are 9 FBSs inside the congested area comparing to 135 FBSs residing in the non-congested area. Thus the carried traffic per unit area or per FBS is actually higher in the congested area than the non-congested area. The total traffic carried by the MBSs, on the other hand, is roughly the same whether they reside in the congested or non-congested areas. This is because the MBSs are distributed according to the teletraffic demand. The density of the MBSs in the congested area is six times that in the non-congested area, just the same as the MS density.

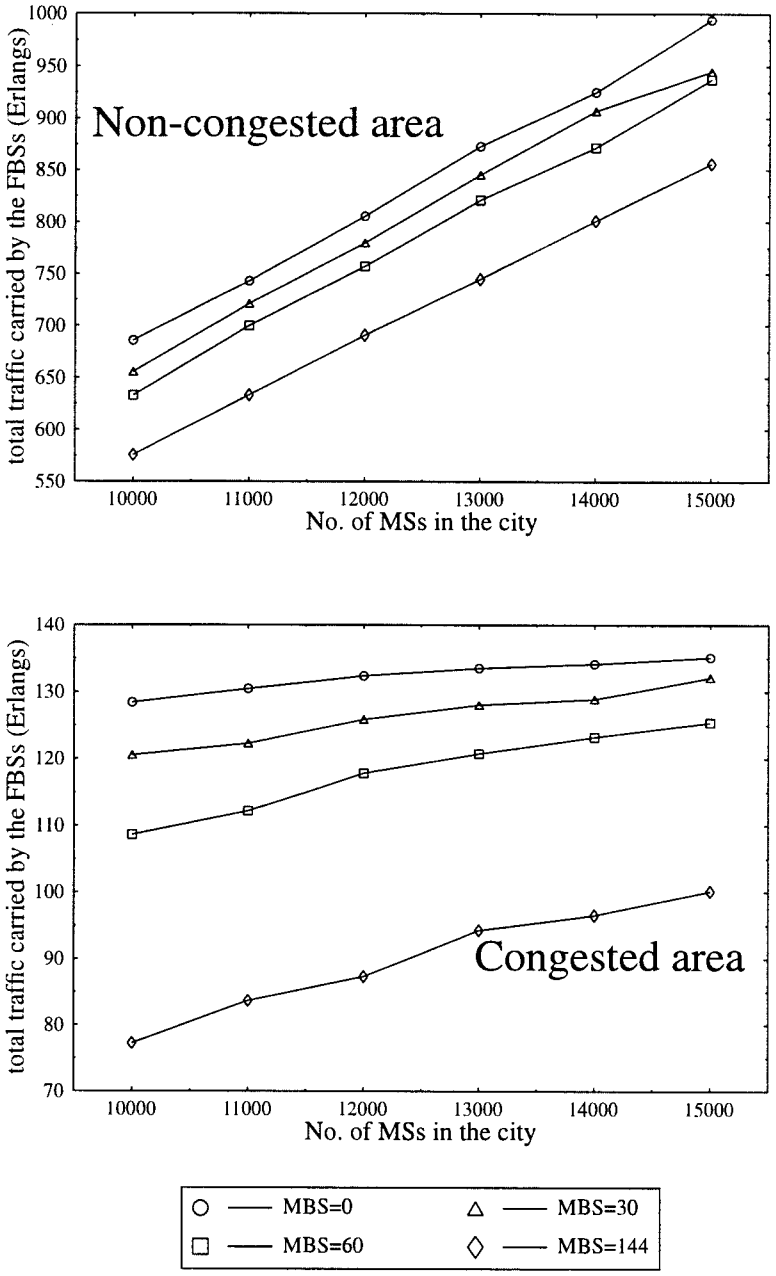

Figure 4.31: Traffic carried by the FBSs in the congested area and traffic carried by the FBSs in the non-congested area (Erlangs)

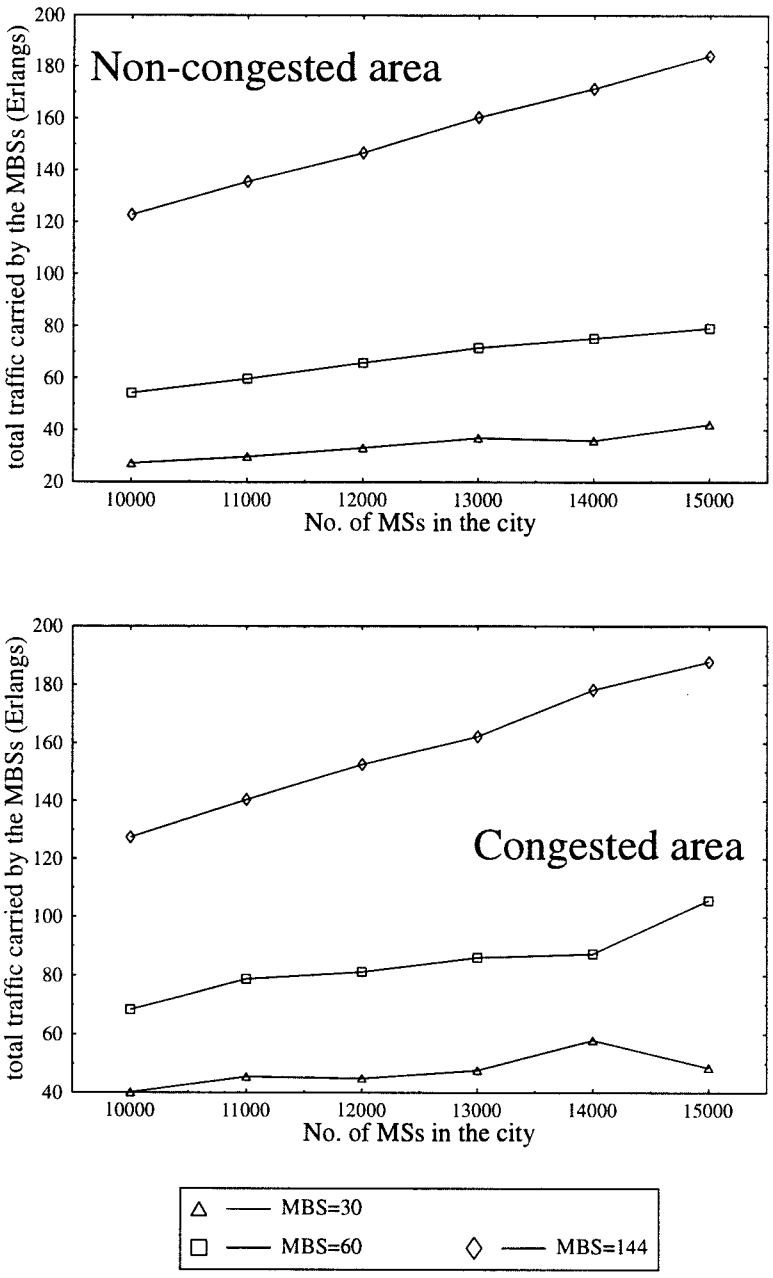

Figure 4.32: Traffic carried by the MBSs in the congested area and traffic carried by the MBSs in the non-congested area (Erlangs)

Let us concentrate on the results for the congested area. Given the non-congested area is 21 times bigger than congested area and vehicular density inside the congested area is six times that in the non-congested area, we can calculate the average number of MBSs inside the congested area for a given overall number of MBSs employed. When the total number of MBSs employed is 30, 60 and 144, the average number of MBSs reside in the congested area is 6.7, 13.3 and 32 respectively. The total number of FBSs inside the congested area is 9. Figure 4.33 shows that the carried traffic per MBS is always less than the carried traffic per FBS. It also shows that the carried traffic per FBS or per MBS decreases when the number of MBSs employed increases. Although the results show that the MBSs are less effective than the FBSs in carrying traffic on the per BS basis, the overall carried traffic does increase because the MBSs out-number the FBSs in the area where the teletraffic demand is high. Referring back to Figure 4.31 and 4.32, in the congested area, when the total number of MBSs employed is 144, the overall traffic carried by the MBSs exceeds the overall traffic carried by the FBSs.

Figure 4.34 shows the number of intra-HOs per call. It is very similar to the one we obtained for the standard access scheme. Figure 4.35 shows the number of level-1 inter-HOs per call. They are slightly less than in the standard access scheme. This is because some of the calls are prematurely handed over by the level-2 inter-HO mechanism before the MS reaches the border of its serving cell.

Figure 4.36 shows the number of level-2 inter-HOs per call. The number of level-2 inter-HOs is less than the level-1 inter-HOs in the non-congested area, while the opposite is true for the congested area. In both areas, the number of level-2 inter-HOs is significantly increased when the number of MBSs employed is increased. The total number of inter-HOs is comparable to the standard access scheme when no MBSs are employed. However, it is significantly greater than the standard access scheme when more MBSs are employed because of the increase in the level-2 inter-HOs.

Figure 4.37 and 4.38 shows the new call blocking probability and the forced termination probability, respectively. The PEA scheme is shown in solid lines, and the standard access scheme is shown in dotted lines. All four graphs show that the PEA scheme out-performs the standard access scheme. The differences are most noticeable when the number of MBSs employed is high. This is because the standard access scheme only allows one MBS broadcasting

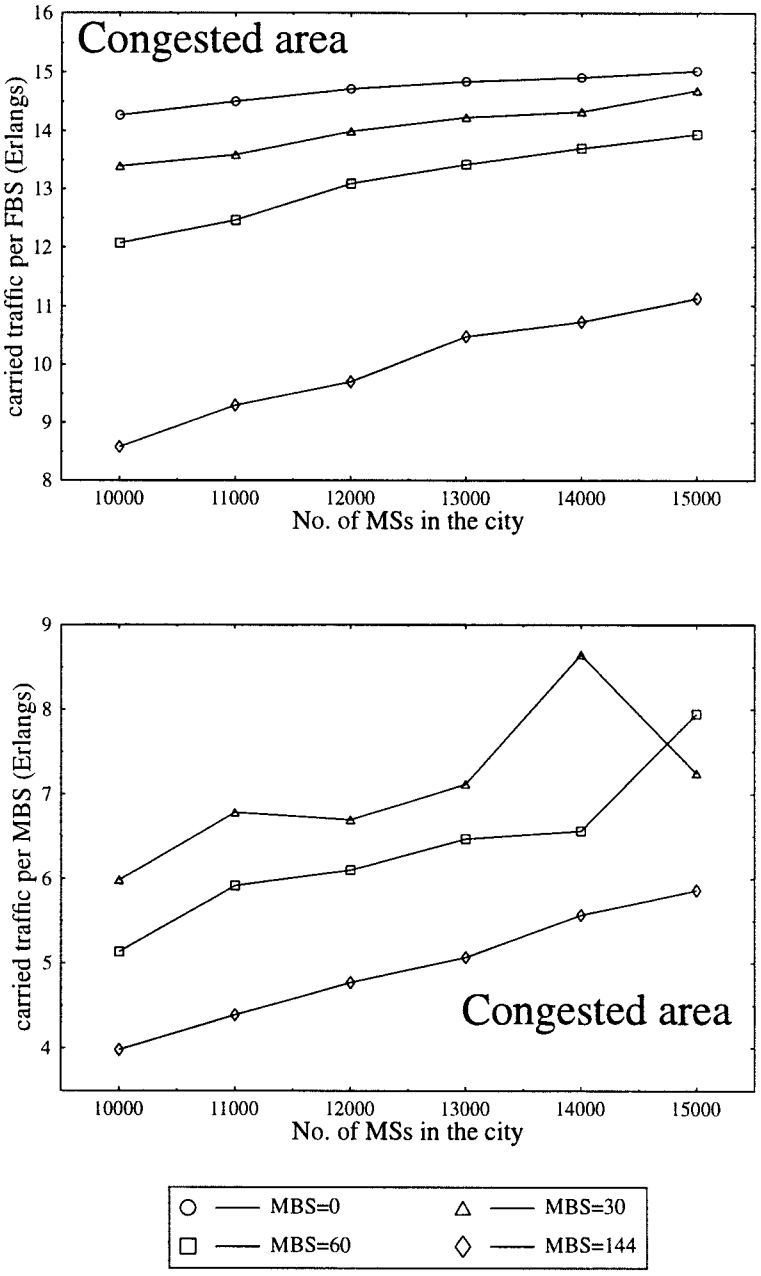

Figure 4.33: Carried traffic per FBS and carried traffic per MBS in the congested area (Erlangs)

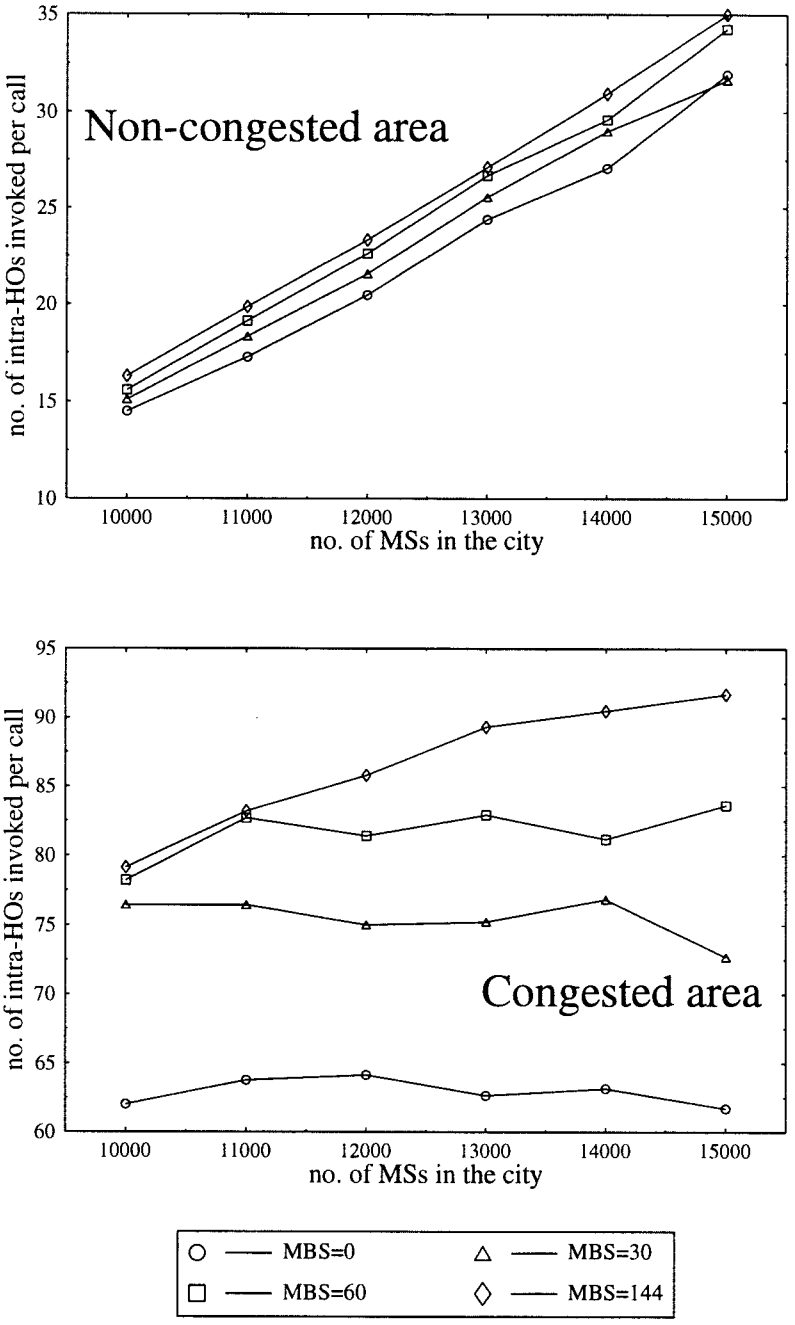

Figure 4.34: Average number of intra-HOs per call

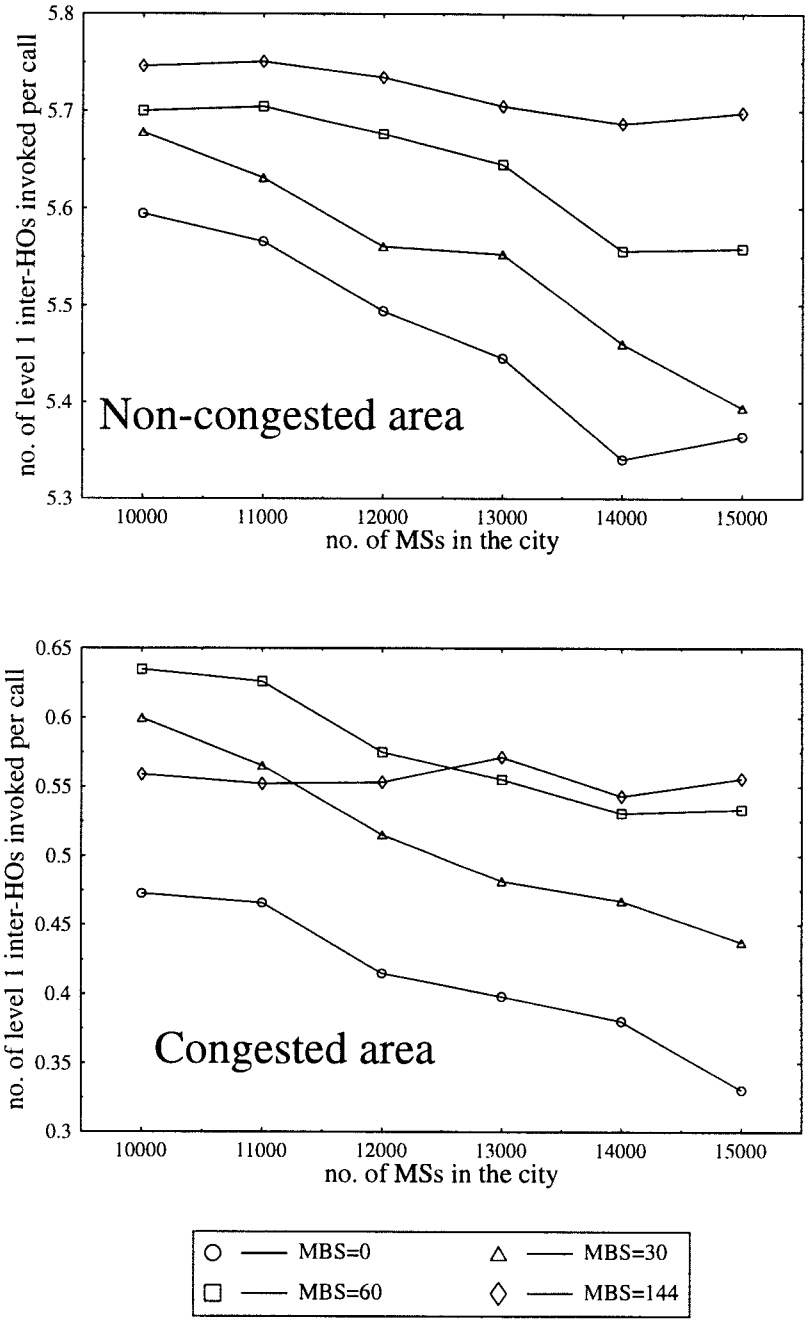

Figure 4.35: Average number of level-1 inter-HOs per call

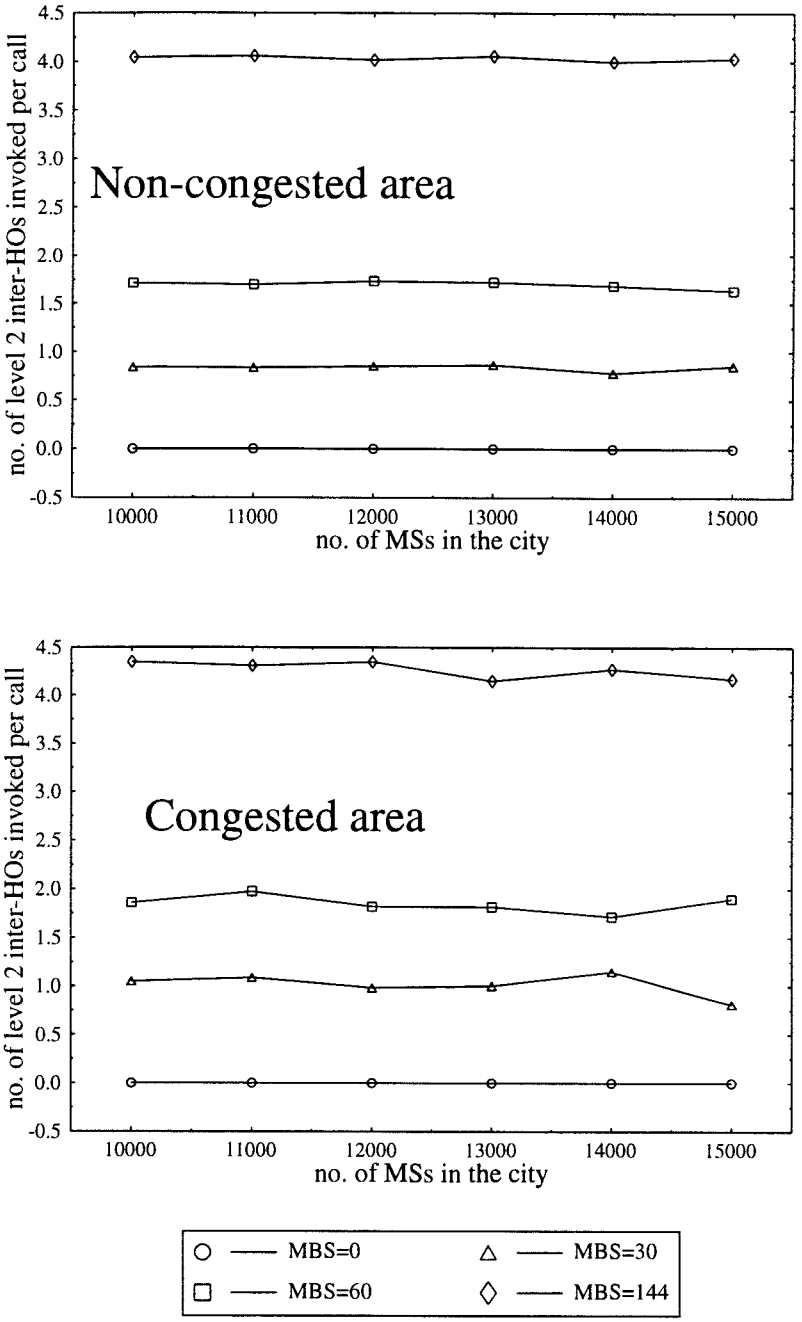

Figure 4.36: Average number of level-2 inter-HOs per call

per zone. On the other hand, the PEA scheme allows the MSs to request connection to any BSs in the vicinity. Since the MBSs can effectively move to areas of high teletraffic demand, both the new call blocking probability and the forced termination probability can be significantly reduced.

4.3 Conclusions

We have studied the MBS system with both FCA scheme and DCA scheme. FCA scheme is spectrally inefficient when applied to the MBS system. The mobile nature of the MBS needs to work with a DCA scheme. Under FCA scheme, we studied the MBS system performances when the MSs are stationary and when the MSs are travelling at the constant speed of 6m/s. When the MSs travel at the same speed as the MBSs, both the new call blocking probability and the forced termination probability are reduced as the number of MBSs employed increases. When the MSs are stationary, the increase in the number of MBSs employed improves the new call blocking probability but worsens the forced termination probability. Notice that the forced termination probability is zero if MBSs are not employed. We conclude that the mobility of the MBSs must be comparable to the MSs. Otherwise, the increase in forced termination probability will significant degrade the quality of the service.

With the DCA scheme, we studied the standard access scheme and the PEA scheme. The standard access scheme is less effective than the PEA scheme. Although the MBSs can successfully move to area of high teletraffic demand, the standard access scheme limits the number of MBSs that can serve new connections. Both schemes can successfully employ MBSs to decrease the new call blocking probability and the forced termination probability. The increase in inter-HO rate is small when the MBSs have the same mobility as the MSs. However, further research needs to be done to find an effective means of transferring the data between the MBSs and the fixed network. The cost of the additional MBSs and the complexity of the system must also be taken into account. Nonetheless, the concept of MBS offers an alternative solution to the unpredictable variation of teletraffic demand.

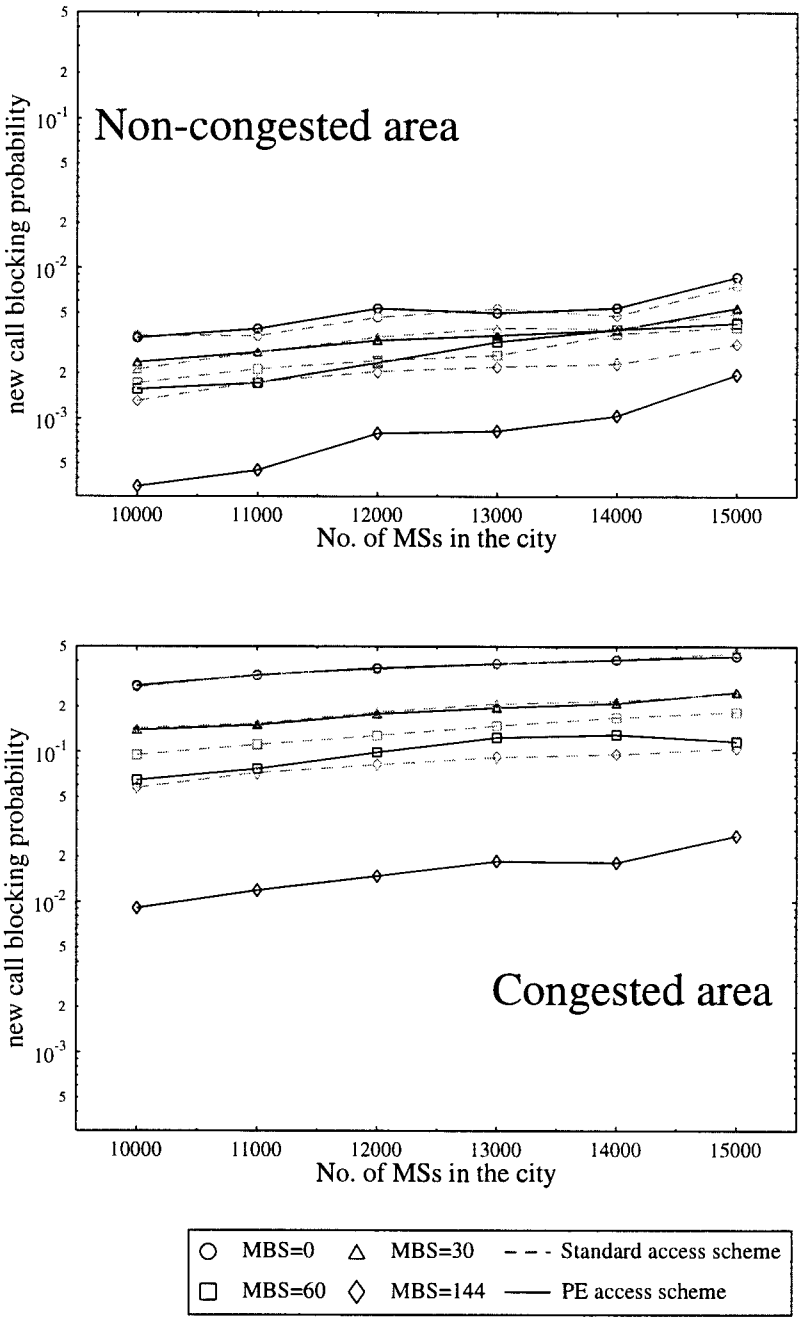

Figure 4.37: New call blocking probability

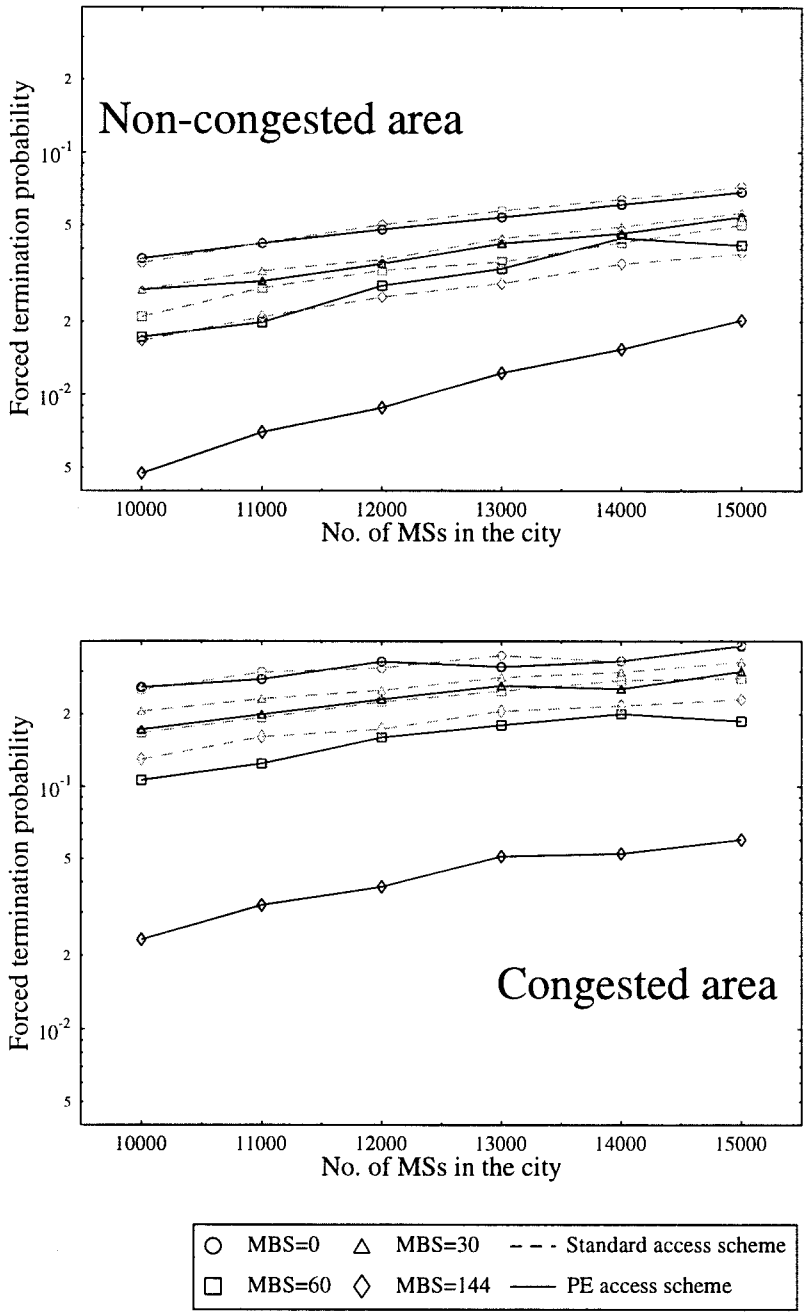

Figure 4.38: Forced termination probability

Chapter 5

Conclusions and Suggestions for Further Work

5.1 Summary and Conclusions

This thesis is concerned with the evaluation of the teletraffic performance of a rectilinear street microcellular network. The teletraffic performance of the system is judged by the new call blocking probability, P_B, and the forced termination probability, P_F. The city used in the simulations consists of square cross-sectional buildings, each of 100 m length. The buildings are separated by 20 m wide roads. All users are assumed to be travelling on vehicles at constant speed. They are arranged to have a probability of 0.8 to continue travelling straight at road junctions, and a probability of 0.1 of either turning left or right. Each user offers teletraffic of 0.1 Erlangs. The teletraffic performance of the system is studied for different levels of offered traffic by varying the number of users present in the city. To avoid edge effects, the simulation considers the city to wrap around from the East-most edge to the West-most edge, and from the North-most edge to the South-most edge. Consequently the density of users in the city is constant. The fixed base-stations (FBSs) are placed at each road intersection spaced 120 m apart.

Two handover (HO) priority schemes, namely the HO guard channel scheme and the HO queueing scheme are examined. These schemes are applied

to a system that adopts a fixed channel assignment (FCA) strategy. Both schemes achieve reductions in P_F by enduring higher P_B. The HO guard channel scheme achieves this by reserving a number of channels exclusively for HO calls. Systems that have 8, 16 and 24 channels per FBS, respectively, are studied. To simulate urban road traffic conditions, the users are arranged to travel at a constant speed of 6 m/s.

We compare the reductions in the P_F against the increases in the P_B when the number of HO guard channels is increased from 0 to 1. For a system that has eight channels per FBS, the P_B is increased from 2% to 5.8%, and the P_F is merely reduced from 16.7% to 14.2%. For a system that has 16 channels per FBS, the P_B is increased from 2% to 4.9%, and the P_F is reduced from 16.3% to 14.1%. For a system that has 24 channels per FBS, the P_B is increased from 2% to 4.5%, and the P_F is reduced from 16.2% to 14%.

The poor trade-off between the P_B and the P_F indicates that the HO guard channel scheme is not suitable for our microcellular system where the HO rates are high. With further investigations, we found that a beneficial trade-off can be achieved by this scheme when the users travelling speed is reduced to below 0.1 m/s and the number of channels per FBS is 16. This indicates that there is an advantage in applying the HO guard channel scheme when the HO activities are low and there are many channels per FBS, for example, in the case of macrocellular FBSs. This agrees with the conclusions drawn from references [7, 60].

The HO queueing scheme reduces the P_F by allowing blocked HO requests to be queued, while blocked new call requests are immediately cleared. When a mobile moves near to the border of its serving cell, the received signal strength from the adjacent FBS becomes stronger. When the received level of this signal exceeds that from the serving FBS by some threshold, a HO request is made to the adjacent FBS. If this FBS does not have any vacant channels, the HO request is placed in a queue. A queued HO call is forced to terminate when the mobile moves out of its current FBS's coverage area. The time a HO request spends in the queue depends on the travelling speed of the mobile, and the received signal strength hysteresis set by the system that controls when to request the HO.

A system that has eight channels per FBS is examined. All mobiles travel at the same speed. To study the teletraffic performance of the system for both high and low HO rates, two sets of data are collected, one for mobile speed

of 6 m/s and the other for mobile speed of 1 m/s. For the system where the mobile speed is 6 m/s, the introduction of the HO queueing scheme reduces the P_F from 8.3% to 4.5%, but increases the P_B from 1.1% to 1.7%. Comparing with the results from the HO guard channel scheme for the same system configuration, the HO queueing scheme offers a more beneficial trade-off between the P_B and the P_F. However, the maximum achievable reduction in the P_F by this scheme is restricted by the size of the overlapped radio coverage between the two adjacent FBSs. Although the P_F is reduced from 8.3% to 4.5%, it is still too high for a practical system.

However, when the mobile speed is reduced to 1 m/s, the HO queueing scheme can reduce the P_F from 2.1% to 0.48% while increasing the P_B from 1.6% to 1.9%. In this case, the HO queueing scheme successfully improves the service quality. Like the HO guard channel scheme, the HO queueing scheme is effective only when applied to systems where the HO rates are low [15]. Although both these schemes have proven to be successful in macrocellular networks where the handover (HO) rates are low, they are not effective in microcellular networks.

Due to the high level of HO activities in our microcellular network, the fluctuations of the teletraffic load at the microcellular base stations are high and rapid. To cope with this problem, the microcellular network must adopt a dynamic channel assignment (DCA) strategy. The solution to the problem of dropped calls lies in the flexibility of its channel assignment strategy. A HO priority scheme on its own does not solve the problem.

Next we propose two base station (BS) selection algorithms, namely the BS load equalisation (BSLE) and the re-arrangement upon blocking (RAUB) algorithms. These algorithms exploit the overlapped radio coverage between cells. Results from the directed retry method are used as benchmarks for these two algorithms. The BSLE system regularly checks the number of available channels of all FBSs in the vicinity of the mobile, and informs the mobile to change its FBS when another FBS has more capacity. The RAUB system, on the other hand, only rearranges the FBS and mobile connections when another call would otherwise be lost.

The studied system has eight channels per FBS, and the mobile speed is fixed at 6 m/s. The levels of HO traffic generated by these two algorithms are monitored, as well as their levels of channel utilisation, new call blocking probabilities and forced termination probabilities.

Results show that the BSLE algorithm generates more handovers than both the RAUB and the directed retry algorithms. Mobiles in the BSLE system, on average, experience an average of 6.8 handovers during their calls, whereas mobiles in the RAUB system or the directed retry system only experience an average of 5.8 handovers. Consequently, the BSLE system generates more handover control signalling than the other two systems.

Both the BSLE and the RAUB systems can achieve higher channel utilisation levels than the directed retry system for the same level of new call blocking probability. At 2% new call blocking rate, the levels of the channel utilisation for the directed retry, the BSLE and the RAUB systems are 0.38, 0.5 and 0.64, respectively. At 0.38 channel utilisation level, the forced termination probabilities for the directed retry, the BSLE and the RAUB systems are 4.5%, 0.45% and 0.3%, respectively. Both the BSLE and the RAUB algorithms achieve better new call blocking probabilities and forced termination probabilities than realised by the directed retry method. However, in order to achieve a substantial gain in the system performance, new concepts are needed at the system level. To this end, we propose a system of moving BSs (MBSs).

Our preliminary study of the MBS system assumes both the fixed BSs (FBSs) and the MBSs employ a fixed channel allocation (FCA) scheme. This arrangement on examination is impractical as the channels used by the MBSs are not reused. A more sophisticated system is next considered, that adopts a dynamic channel allocation (DCA) strategy as well as power control. Furthermore, two network access schemes are studied, namely the standard access scheme and the power escalation access (PEA) scheme. With the standard access scheme, the mobiles detect nearby FBSs and MBSs by scanning for their broadcast control channels (BCCHs), a similar arrangement to that used in the GSM system. The BCCH acts as a beacon signal and needs to be transmitted at full power at all times. The drawback of this method is that when two cochannel MBSs are close to each other, one of them needs to turn off its BCCH. MBSs that are not broadcasting on their BCCHs are not accessible to the mobiles for new call setup.

The PEA scheme solves this problem by allowing the mobiles to access the network by transmitting an access request in ascending power levels until a reply is received from a nearby FBS or MBS. This eliminates the requirement of the MBSs broadcasting continuously on the BCCHs. Consequently, there

will be more MBSs to serve more new calls on congested roads where higher teletraffic demand is expected. A city consisting of 12 by 12 building blocks with 144 FBSs, located at each road intersection, is studied. The system has a total of 16 channels (four radio carriers, each with four time slots). Both the FBSs and the MBSs adopt a DCA strategy, and have access to all of these 16 channels. The effect of road traffic congestion is also studied. This is done by reducing the speed of mobiles in the congested area from 6 m/s to 1 m/s. The roads around the central four building blocks are the congestion areas of the city.

The standard access scheme is first investigated under a non-congested uniform road traffic condition. When there are 15000 mobiles present in the city and no MBS is deployed, the new call blocking probability and the forced termination probability are 8.7×10^{-3} and 6.0×10^{-2}, respectively. When there are 144 MBSs deployed, the same number as the FBSs, the new call blocking probability drops to 3.5×10^{-3} and the forced termination probability is decreased to 2.8×10^{-2}. The MBSs improve the service quality using the spare system capacity. However, the majority of the teletraffic is carried by the FBSs. When there are 144 MBSs deployed, the teletraffic carried by a FBS is 5.8 times of that carried by a MBS.

Next a non-uniform road traffic condition is studied for the standard access scheme. A congestion area is arranged in the central part of the city while the rest of the city has the same road traffic conditions as before. When there are 15000 mobiles present in the city and no MBS is deployed, the new call blocking probabilities, P_B, and the forced termination probabilities, P_F, are 45% and 38%, respectively, for the congested zone. For the the non-congested zone, the P_B and the P_F are 0.76% and 7.2%, respectively. When 144 MBSs are deployed, the P_B and the P_F are reduced to 11% and 23%, respectively, for the congested zone. For the non-congested zone, the P_B and the P_F are reduced to 0.31% and 3.8%, respectively.

Due to the above-mentioned drawback of the standard access scheme, the reductions of the P_B and the P_F in the congested zone are less than satisfactory. Under the same system configurations, the PEA scheme is able to achieve greater reductions in the P_B and the P_F for both the congested and the non-congested zones. In the congested zone, the system adopting the PEA scheme decreases the P_B from 43% to 2.7% when 144 MBSs are deployed, while the P_F is reduced from 38% to 6%. In the non-congested

zone, the P_B is reduced from 0.87% to 0.2%, while the P_F is reduced from 6.8% to 2%. This shows that with the adoption of the PEA scheme, the MBSs that are caught in road traffic congestion can effectively improve the service qualities to the mobiles in their vicinities.

This thesis is solely dedicated to the study of a street microcellular network. As mobile telephony continues to grow, the deployment of smaller cells is inevitable because it is the most efficient way to gain system capacity. Two of the key problems of microcell deployment are the rapid HO rates and containing the infrastructure cost. Both issues have been addressed in this thesis. We hope our findings will make a significant contribution to future microcellular systems. In particular, the role of moving base stations may turn out to be highly significant in containing the infrastructure costs in microcellular networks.

5.2 Suggestions for Further Work

An attractive feature of the MBS system is its lack of fixed infrastructure. The MBSs require no site acquisition, have no fixed locations. Their presence does not require network re-planning for the existing FBSs. However, in order to realise the MBS system, a method to download the data from the MBSs back to the fixed network is required. A repeater system can be one solution to this problem. Data can be relayed from one MBS to another until the collection node (e.g. a FBS) is reached. Each packet of data needs to find its way to the destination. The routes taken by successive packets can be quite different as the MBSs that make up the relay path change their positions.

Alternatively, microwave links operating in a different frequency band from the mobiles and with steerable antennas can be used. Collection points can be to radio ports mounted on the walls of buildings that could relay the signals onwards. The MBSs could be arranged to download their data when they have LOS contacts with these radio ports. However, the introduction of radio ports does mean the deployment of some fixed infrastructure.

Bibliography

[1] W. C. Y. Lee, *Mobile communications design fundamentals.* John Wiley & Sons, Inc., 2nd ed., 1993.

[2] Y. Ko and R. Steele, "Packet transmissions over a combined digital cellular mobile radio-LAN system," *IEE Colloquium (Digest)*, pp. 3. 1–3. 5, 1986.

[3] J. C.-I. Chuang, "Operation and performance of a self-organising frequency assignment method for TDMA portable radio," *GLOBECOM '90 IEEE Global Telecommunications Conference and Exhibition*, pp. 1548–1552, 1990.

[4] W. C. Jakes, Jr., *Microwave mobile communications.* New York : Wiley, 1974.

[5] R. C. V. Macario, ed., *Modern personal radio systems.* The Institution of Electrical Engineers, London, United Kingdom, 1996.

[6] W. Webb, J. Williams, and R. Steele, "Microcellular teletraffic levels," *IEE Conference Publication*, pp. 125–130, Dec. 1993.

[7] R. Steele and M. Nofal, "Tele-traffic performance of microcellular personal communication networks," *IEE Proceedings, Part I: Communications, Speech and Vision*, vol. 139, pp. 448–461, Aug. 1992.

[8] D. Giancristofaro, M. Ruggieri, and F. Santucci, "Queueing of handover requests in microcell network architectures," *IEEE Vehicular Technology Conference*, vol. 3, pp. 1846–1849, June 1994.

[9] S. A. El-Dolil, W.-C. Wong, and R. Steele, "Teletraffic performance of highway microcells with overlay macrocell," *IEEE Journal on Selected Areas in Communications*, vol. 7, pp. 71–78, Jan. 1989.

[10] R. Steele, "Cellular environment of lightweight handheld portables," *IEEE Communications Magazine*, vol. 27, pp. 20–29, July 1989.

[11] R. Steele, J. Williams, D. Chandler, S. Dehghan, and A. Collard, "Teletraffic performance of GSM900/DCS1800 in street microcells," *IEEE Communications Magazine*, pp. 102–108, Mar. 1995.

[12] R. Steele, M. Nofal, and S. Eldolil, "Adaptive algorithm for variable teletraffic demand in highway microcells," *Electronics Letters*, vol. 26, pp. 988–990, 5th July 1990.

[13] G. Lyberopoulos, J. Markoulidakis, and M. Anagnostou, "Impact of evolutionary cell architectures on handover in future mobile telecommunication systems," *Proceedings of the 1994 IEEE 44th Vehicular Technology Conference. Part 1 (of 3), Stockholm, Swed, (Conf. code 21444)*, vol. 1, pp. 120–124, Jun 8-10 1994.

[14] S. Tekinay and B. Jabbari, "Handover and channel assignment in mobile cellular networks," *IEEE Communications Magazine*, vol. 29, pp. 42–46, Nov. 1991.

[15] S. Tekinay and B. Jabbari, "A measurement-based prioritization scheme for handovers in mobile cellular networks," *IEEE Journal on Selected Areas in Communications*, vol. 10, pp. 1343–1350, Oct. 1992.

[16] N. Mitrou, G. Lyberopoulos, and A. Panagopoulou, "Voice and data integration in the air-interface of a microcellular mobile communication system," *IEEE Transactions on Vehicular Technology*, vol. 42, pp. 1–13, Feb. 1993.

[17] J. E. Padgett, C. G. Gunther, and T. Hattori, "Overview of wireless personal communications," *IEEE Communications Magazine*, vol. 33, pp. 28–41, Jan. 1995.

[18] R. Steele, J. Whitehead, and W. Wong, "System aspects of cellular radio," *IEEE Communications Magazine*, vol. 33, pp. 80–86, Jan. 1995.

[19] R. Steele and J. Williams, "Third generation PCN and the intelligent multimode portable," *Electronics & Communication Engineering Journal*, vol. 5, pp. 147–156, June 1993.

[20] J. Wang, "Microcellular CDMA mobile communications," *International Conference on Communication Technology Proceedings, ICCT*, vol. 2, pp. 1123–1125, 1996.

[21] T. Buot, "Channel allocation algorithm for TDMA with multiclass users," *IEEE Vehicular Technology Conference*, vol. 2, pp. 953–957, 1996.

[22] K. Okada and F. Kubota, "On dynamic channel assignment in cellular mobile radio systems," *Proceedings - IEEE International Symposium on Circuits and Systems*, vol. 2, pp. 938–941, 1991.

[23] D. C. Cox and D. O. Reudink, "Dynamic channel assignment in two-dimensional large-scale mobile radio systems," *The Bell System Technical Journal*, vol. 51, pp. 1611–1629, Sept. 1972.

[24] D. C. Cox and D. O. Reudink, "Increasing channel occupancy in large-scale mobile radio systems: Dynamic channel reassignment," *IEEE Transactions on Vehicular Technology*, vol. 22, pp. 218–222, Nov. 1973.

[25] T. J. Kahwa and N. D. Georganas, "Hybrid channel assignment scheme in large-scale, cellular-structured mobile communication systems," *IEEE Transactions on Communications*, vol. 26, pp. 432–438, Apr. 1978.

[26] J. S. Engel and M. M. Peritsky, "Statistically-optimum dynamic server assignment in systems with interfering servers," *IEEE Transactions on Vehicular Technology*, vol. 22, pp. 203–209, Nov. 1973.

[27] S. M. Elnoubi, R. Singh, and S. C. Gupta, "A new frequency channel assignment algorithm in high capacity mobile communication systems," *IEEE Transactions on Vehicular Technology*, vol. 31, pp. 125–131, Aug. 1982.

[28] M. Zhang and T.-S. P. Yum, "Comparisons of channel assignment strategies in cellular mobile telephone systems," *IEEE Transactions on Vehicular Technology*, vol. 38, pp. 211–215, Nov. 1989.

[29] M. Zhang and T.-S. P. Yum, "The nonuniform compact pattern allocation algorithm for cellular mobile systems," *IEEE Transactions on Vehicular Technology*, vol. 40, pp. 387–391, May 1991.

[30] H. Jiang and S. S. Rappaport, "CBWL: a new channel assignment and sharing method for cellular communication systems," *IEEE Transactions on Vehicular Technology*, vol. 43, pp. 313–322, May 1994.

[31] S. Kuek and W. Wong, "Ordered dynamic channel assignment scheme with reassignment in highway microcells," *Proceedings - IEEE International Symposium on Circuits and Systems*, vol. 2, pp. 954–957, 1991.

[32] Y. Furuya and Y. Akaiwa, "Channel segregation, a distributed adaptive channel allocation scheme for mobile communication systems," *IEICE Transactions*, vol. E74, pp. 1531–1537, June 1991.

[33] Y. Akaiwa and H. Andoh, "Channel segregation - a self-organized dynamic channel allocation method: application to TDMA/FDMA microcellular system," *IEEE Journal on Selected Areas in Communications*, vol. 11, pp. 949–954, Aug. 1993.

[34] T.-P. Chu and S. S. Rappaport, "Overlapping coverage and channel rearrangement in microcellular communication systems," *IEEE Global Telecommunications Conference*, vol. 3, pp. 1674–1678, 1994.

[35] J. Karlsson and B. Eklundh, "Cellular mobile telephone system with load sharing - an enhancement of directed retry," *IEEE Transactions on Communications*, vol. 37, pp. 530–535, May 1989.

[36] M. Yacoub and K. Cattermole, "Alternative routing strategies for adjacent cells in mobile radio systems," *IEE Proceedings: Communications*, vol. 142, pp. 115–120, Apr. 1995.

[37] M. Yacoub and K. Cattermole, "Novel technique for efficient channel utilization in a mobil radio system.," *IEEE Global Telecommunications Conference and Exhibition Part 3 (of 3), San Diego, CA, USA, 02-05 Dec 1990, (Conf. code 15019) GLOBECOM '90*, vol. 3, pp. 1559–1563, 1990.

[38] G. L. Choudhury and S. S. Rappaport, "Cellular communication schemes using generalised fixed channel assignment and collision type

request channels," *IEEE Transactions on Vehicular Technology*, vol. 31, pp. 53–65, May 1982.

[39] T.-P. Chu and S. S. Rappaport, "Overlapping coverage and channel rearrangement in microcellular communication systems," *IEE Proceedings: Communications*, vol. 142, pp. 323–332, Oct. 1995.

[40] M. Au, R. Steele, and M. Nofal, "Teletraffic performance of different base station selection algorithms in street microcells," *1995/6 Research Journal, Department of Electronics and Computer Science, University of Southampton*, 1996.

[41] A. Gamst, "Application of graph theoretical methods to GSM radio network planning," *Proceedings - IEEE International Symposium on Circuits and Systems*, vol. 2, pp. 942–945, 1991.

[42] H. Takanashi and S. Rappaport, "Dynamic base station selection for personal communication systems with distributed control schemes," *IEEE Vehicular Technology Conference*, vol. 3, pp. 1787–1791, 1997.

[43] R. Steele, ed., *Mobile Radio Communications.* John Wiley and IEEE Press, 1992.

[44] S. Nanda and D. J. Goodman, *Third Generation Wireless Information Networks.* Kluwer Academic Publishers, 1992.

[45] C.-L.I, L. Greenstein, and R.D.Gitlin, "A microcell/macrocell cellular architecture for low and high mobility wireless users," *GLOBECOM '91 Conf. Record*, pp. 1006–1011, Dec. 1991.

[46] C. C. Lee and R. Steele, "CDMA for city street microcells," *Electronics Division Colloquium on "Spread spectrum techniques for radio communication systems". Organised by Professional Group E8 (Radiocommunication systems)*, Tuesday, 27 April 1993.

[47] B. W. Unger, D. J. Goetz, and S. W. Maryka, "Simulation of SS7 common channel signaling," *IEEE Communications Magazine*, vol. 32, pp. 52–62, Mar. 1994.

[48] V. S. Frost and B. Melamed, "Traffic modelling for telecommunications," *IEEE Communications Magazine*, vol. 32, pp. 70–81, Mar. 1994.

[49] M. Gibbard, G. Morrison, A. Sesay, and M. Fattonche, "Broadband TDMA over the indoor radio channel," *Electronics letters*, vol. 30, Feb. 1994.

[50] R. C. Bernhardt, "Time-slot management in digital portable radio systems," *IEEE Transactions on Vehicular Technology*, vol. 40, pp. 261–272, Feb. 1991.

[51] R. Bernhardt, "Automatic time-slot reassignment in a frequency reuse TDMA portable radio system," *IEEE Transactions on Vehicular Technology*, vol. 41, pp. 296–304, Aug. 1992.

[52] K. Nagata, "Control functions and their implementation in mobile communications," *Proceedings - IEEE International Symposium on Circuits and Systems*, vol. 2, pp. 962–965, 1991.

[53] A. S. Acampora and M. Naghshineh, "Control and quality-of-service provisioning in high-speed microcellular networks," *IEEE Personal Communications*, vol. 1, no. 2, pp. 36–43, 1994.

[54] R. Steele, "Speech codecs for personal communications," *IEEE Communications Magazine*, vol. 31, pp. 76–83, Nov. 1993.

[55] R. Steele, "Evolution of personal communications," *IEEE Personal Communications, 2nd Quarter*, vol. 1, no. 2, pp. 6–11, 1994.

[56] R. Steele, "Therapy of percy comms: a dialogue on PCS issues," *International Journal of Wireless Information Networks*, vol. 2, pp. 123–132, July 1995.

[57] "The highway code." Prepared by the Department of Transport and the Central office of Information, HMSO publication, 1978.

[58] E. Kreyszig, *Advanced Engineering Mathematics.* John Wiley & Sons, Inc., 6 ed., 1988.

[59] W. H. Press, S. A. Teukolsky, W. T. Vetterling, and B. P. Flannery, *Numerical Recipes in C.* Cambridge University Press, 2 ed., 1992.

[60] D. Hong and S. S. Rappaport, "Traffic model and performance analysis for cellular mobile radio telephone systems with prioritised and

non-prioritised hand-off procedures," *IEEE Transactions on Vehicular Technology*, vol. 35, pp. 77–92, Aug. 1986.

[61] B. Eklundh, "Channel utilisation and blocking probability in a cellular mobile telephone system with directed retry," *IEEE Transactions on Communications*, vol. COM-34, pp. 329–337, Apr. 1986.

[62] R.B. Cooper, *Introduction to Queueing Theory.* New York : Elsevier North Holland, 2 ed., 1981.

[63] D. Gross and C. M. Harris, *Fundamentals of queueing theory.* John Wiley & Sons, Inc., 2nd ed., 1985.

[64] M. Au and R. Steele, "Teletraffic performance of a city street microcellular system using equalized base station loading for TDMA/FCA," *Electronics Letters*, vol. 30, pp. 1649–1650, Sept. 1994.

[65] W. T. Webb, "Sizing up the microcell for mobile radio-communications," *Electronics & Communication Engineering Journal*, vol. 5, pp. 133–140, June 1993.

[66] P. Harley, "Short distance attenuation measurements at 900 MHz and 1.8 GHz using low antenna heights for microcells," *IEEE Journal on Selected Areas in Communications*, vol. 7, pp. 5–11, Jan. 1989.

[67] R. J. Bultitude and G. K. Bedal, "Propagation characteristics on microcellular urban mobile radio channels at 910 MHz.," *IEEE Journal on Selected Areas in Communications*, vol. 7, pp. 31–39, Jan. 1989.

[68] A. J. Rustako, Jr., N. Amitay, G. Owens, and R. Roman, "Radio propagation measurements at microwave frequencies for microcellular mobile and personal communications," *IEEE Int. Conf. on Communications, ICC 89*, pp. 482–486, June 1989.

[69] V. Erceg, S. Ghassemzadeh, M. Taylor, D. Li, and D. L. Schilling, "Urban/suburban out-of-sight propagation modeling," *IEEE Communications Magazine*, vol. 30, pp. 56–61, June 1992.

[70] J.-E. Berg, R. Bownds, and F. Lotse, "Path loss and fading models for microcells at 900MHz," *IEEE Vehicular Technology Conference 42nd*, vol. 1-2, pp. 666–671, May 1992.

[71] J. B. Andersen, T. S. Rappaport, and S. Yoshida, "Propagation measurements and models for wireless communications channels," *IEEE Communications Magazine*, vol. 33, pp. 42–49, Jan. 1995.

[72] L. B. Milstein, D. L. Schilling, R. L. Pickholtz, V. Erceg, M. Kullback, E. G. Kanterakis, D. S. Fishman, W. H. Biederman, and D. C. Salerno, "On the feasibility of a CDMA overlay for personal communications networks," *IEEE Journal on Selected Areas in Communications*, vol. 10, pp. 655–668, May 1992.

[73] H. Jiang and S. S. Rappaport, "CBWL: A new channel assignment and sharing method for cellular communications systems," *IEEE Vehicular Technology Conference 93'*, pp. 189–193, 1993.